UC San Diego

UC San Diego Electronic Theses and Dissertations

Title

Mesencephalic Astrocyte–derived Neurotrophic Factor is an ER-resident Chaperone that Protects Against Reductive Stress in the Heart

Permalink

https://escholarship.org/uc/item/5q18p0bc

Author

Arrieta, Adrian

Publication Date

2020

Peer reviewed|Thesis/dissertation

eScholarship.org Powered by the California Digital Library
University of California

UNIVERSITY OF CALIFORNIA SAN DIEGO

SAN DIEGO STATE UNIVERSITY

Mesencephalic Astrocyte–derived Neurotrophic Factor is an ER-resident Chaperone that Protects Against Reductive Stress in the Heart

A dissertation submitted in partial satisfaction of the requirements for the degree

Doctor of Philosophy

in

Biology

by

Adrian Arrieta

Committee in charge:

San Diego State University

Professor Christopher C. Glembotski, Chair
Professor Sanford I. Bernstein
Professor Mark A. Sussman

University of California San Diego

Professor Randolph Y. Hampton
Professor Farah Sheikh

2020

©
Adrian Arrieta, 2020
All rights reserved.

The Dissertation of Adrian Arrieta is approved, and it is acceptable in quality and form for publication on microfilm and electronically:

_____

_____

_____

_____

_____
Chair

University of California San Diego

San Diego State University

2020

DEDICATION

To my mother (my #1 fan),

who is, without a doubt, the strongest person I have ever met.

To my sister (my scientific patron),

who is, without a doubt, the most courageous person I have ever met.

They provide me with boundless love, support, strength, and courage.

EPIGRAPH

“Find a mentor in your field and do everything they do.”

-Unknown

“Do everything I say, and you’ll be a great success.”

-Christopher C. Glembotski, Ph. D

“You can start writing your dissertation from the day you first walk into the lab.”

-Christopher C. Glembotski, Ph. D

My dream is to become a scientist that studies the molecular mechanisms of heart disease; having Dr. Christopher C. Glembotski as my mentor is what made that dream come true. From him, I learned everything that a scientist needs to know to be successful— how to identify and ask the important questions in biology, how to design experiments to answer those questions, and how to interpret the results and draw conclusions from those experiments. But most importantly, it is from him that I learned that the pen(cil) is the most powerful tool in the scientist’s toolbox. It is the pen(cil) with which scientists ultimately tell their tales.

“Someone needs to tell those tales. When the battles are fought and won and lost, when the pirates find their treasures and the dragons eat their foes for breakfast with a nice cup of Lapsang Souchong (smoked black tea), someone needs to tell their bits of overlapping narrative. There's magic in that. It's in the listener, and for each and every ear it will be different, and it will affect them in ways they can never predict. From the mundane to the profound. You may tell a tale that takes up residence in someone's soul, becomes their blood and self and purpose. That tale will move them and drive them and who knows what they might do because of it, because of your words. That is your role, your gift.”

-*The Night Circus,* Erin Morgenstern

TABLE OF CONTENTS

LIST OF ABBREVIATIONS AND NOMENCLATURE

AAV9	adeno-associated virus serotype 9
ANOVA	analysis of variance
ATF6	activating transcription factor 6 alpha
DTT	dithiothreitol
ER	endoplasmic reticulum
GRP78	78 kilodalton glucose-regulated protein, Hspa5
GRP94	94 kilodalton glucose-regulated protein, Hsp90b1
HSP	heat shock protein
HMGB1	High mobility group box 1 protein
I/R	ischemia/reperfusion
LV	left ventricle
LVDP	left ventricular developed pressure
MANF	mesencephalic astrocyte derived neurotrophic factor
MTT	Methylthialazole Tetrazolium
NEM	N-ethyl maleimide
PARP	Poly (ADP-ribose) polymerase
PDI	protein disulfide isomerase
sHSP	small heat shock protein
SEM	standard error of mean
sI	simulated ischemia
sI/R	simulated ischemia/reperfusion
TG	thapsigargin
TTC	2,3,5-triphenyl tetrazolium chloride
UPR	unfolded protein response

LIST OF FIGURES

Chapter 1 Figures

Chapter 2 Figures

Chapter 3 Figures

Chapter 4 Figures

LIST OF TABLES

Chapter 2

Chapter 4

ACKNOWLEDGMENTS

I first thank Dr. Christopher C. Glembotski, whom when I first met, completely unraveled what little understanding I had about what it meant to be a scientist, and in its place planted the seed of inspiration that would grow into the dream of becoming a successful independent scientist. And it is in the lab that he created that that seed had room to grow.

I thank Drs. Erik A. Blackwood and Winston T. Stauffer who made critical contributions to the animal work presented in this dissertation. But more importantly they were there to have those difficult scientific conversations with me and raise the hard but important questions. It is because of them that I am able to tell the tale presented in this dissertation.

I thank Donna J. Thuerauf, M.S. who taught me how to play i.e. molecular cloning. She changed my thinking of molecular cloning as something impossible to something full of limitless possibilities.

I thank Dr. Shirin Doroudgar, my in-lab mentor who taught how to design and execute experiments, and that “the experiment can always be better”. To me she is the shining example of what it means to be a fearless scientist.

I thank Kayleigh Marsh, who took a chance on me as her mentor in her studies on the function of peroxisomes in the heart and is an amazing fellow scientist in her own right.

I would like to thank my dissertation committee, Drs. Mark A. Sussman and Sanford I Bernstein from SDSU, and Drs. Farah Sheikh and Randolph Y. Hampton from UCSD for their critical feedback and unrelenting enthusiasm about the work presented here.

Chapter 2, in full, is a reproduction of the material as it appears in *Journal of Biological Chemistry*, 2020. Arrieta A, Blackwood E.A., Stauffer W.T., Santo Domingo M, Bilal A.S., Thuerauf D.J., Pentoney A.N., Aivati C, Sarakki A.V., Doroudgar S., Glembotski C.C. Mesencephalic astrocyte-derived neurotrophic factor is an ER-resident chaperone that protects

against reductive stress in the heart. *J Biol Chem.* (2020); 295(22):7566-7583. The dissertation author was the primary author and investigator for this publication.

Chapter 3, in full, is a reproduction of the material as it appears in *Journal of Biological Chemistry*, 2020. Arrieta A, Blackwood E.A., Stauffer W.T., Santo Domingo M, Bilal A.S., Thuerauf D.J., Pentoney A.N., Aivati C, Sarakki A.V., Doroudgar S., Glembotski C.C. Mesencephalic astrocyte-derived neurotrophic factor is an ER-resident chaperone that protects against reductive stress in the heart. *J Biol Chem.* (2020); 295(22):7566-7583. The dissertation author was the primary author and investigator for this publication.

A portion of Chapter 4 is a reproduction of the material as it appears in *Journal of Biological Chemistry*, 2020. Arrieta A, Blackwood E.A., Stauffer W.T., Santo Domingo M, Bilal A.S., Thuerauf D.J., Pentoney A.N., Aivati C, Sarakki A.V., Doroudgar S., Glembotski C.C. Mesencephalic astrocyte-derived neurotrophic factor is an ER-resident chaperone that protects against reductive stress in the heart. *J Biol Chem.* (2020); 295(22):7566-7583. The dissertation author was the primary author and investigator for this publication.

CURRICULUM VITAE

A. Education and Training

Bachelor of Science, Molecular Toxicology (2011)
Department of Nutritional Sciences and Toxicology, University of California Berkeley, CA

Master of Science, Molecular Biology (2015)
Department of Biology, Cell and Molecular Biology Program Area, San Diego State University, San Diego, CA
Advisor: Dr. Christopher C. Glembotski, Ph.D., Professor of Biology and Director of the SDSU Heart Institute

Doctor of Philosophy, Biology (2020)
Department of Biology, San Diego State University, San Diego, CA
Department of Biology, University of California San Diego, San Diego, CA
Advisor: Dr. Christopher C. Glembotski, Ph.D., Professor of Biology and Director of the SDSU Heart Institute

B. Positions and Honors

Positions and Employment

06/2011-06/2012	Undergraduate Researcher; Evolution of phosphoregulatory networks University of California Berkeley; Dr. Liam Holt
03/2013-07/2013	Jr. Research Specialist; Engineering of genetic systems for rapid evolution. University of California Irvine; Dr. Chang C. Liu
08/2013-03/2015	Teaching Assistant; Microbiology (Biol 350), undergraduate laboratory course, San Diego State University
01/2016-05/2016	Teaching Assistant; Molecular Basis of Heart Disease (Biol 575), undergraduate lecture course, San Diego State University
08/2013-07/2015	Graduate Student (MS); Cell and Molecular Biology San Diego State University; Dr. Chris Glembotski
08/2015-12/2020	Graduate Student (Ph.D); Cell and Molecular Biology San Diego State University/UC San Diego; Dr. Chris Glembotski

Other Experience and Professional Memberships

08/2014-present	Member– American Heart Association
03/2017-03/2018	Member– International Society for Heart Research
09/2015	Presenter– ER Stress Club; La Jolla, CA
06/2016	Presenter– Gordon Research Seminar (GRS) on Cardiac Regulatory Mechanisms: “Innovative Answer to Classic Cardiac Questions”, Gordon Research Conference; New London, NH
06/2016	Presenter– Gordon Research Conference (GRC) on Cardiac Regulatory Mechanisms; New London, NH
07/2016	Presenter– The Council on Basic Cardiovascular Sciences Conference, American Heart Association; Phoenix, AZ

09/2016	Presenter– Alternative Muscle Club Symposium; La Jolla, CA
11/2016	Presenter– American Heart Association Conference; New Orleans, LA
05/2017	Presenter– International Society for Heart Research Conference; New Orleans, LA
07/2017	Presenter– The Council on Basic Cardiovascular Sciences Conference, American Heart Association; Portland, OR **(Abstract score top 10 percentile; selected as the best of BCVS)**
11/2017	Presenter – American Heart Association Conference; Anaheim, CA
04/2018	Cold Spring Harbor Laboratory Meeting on Proteostasis in Health and Disease, 2018
06/2018	Presenter– Gordon Research Seminar (GRS) on Cardiac Regulatory Mechanisms: "Pioneering Developments in Basic and Translational Cardiovascular Research", Gordon Research Conferences; New London, NH
06/2018	Presenter– Gordon Research Conference (GRC) on Cardiac Regulatory Mechanisms: "From Cardiac Mechanisms to Novel Therapeutic Approaches"; New London, NH
06/2018	Presenter– The Council on Basic Cardiovascular Sciences Conference, American Heart Association; San Antonio, TX
07/2019	Attendee– The Council on Basic Cardiovascular Sciences Conference, American Heart Association; Boston, Massachusetts

Honors

08/2015-12/2020	Rees-Stealy Research Fellowship, Rees-Stealy Research Foundation
06/2017-06/2019	National Heart, Lung, and Blood Institute, National Institutes of Health; Research Supplements to Promote Diversity in Health-Related Research. Grant Number: R01 HL127439 02S1 Awarded 06/2017-06/2019
02/2015-07/2016	National Heart, Lung, and Blood Institute, National Institutes of Health; Research Supplements to Promote Diversity in Health-Related Research. Grant Number: 2 P01 HL085577-07; Awarded 02/20/2015 - 7/31/2016
06/2016	Exemplary Participation Award, Gordon Research Conference (GRC) on Cardiac Regulatory Mechanisms; New London, NH
09/2016	Young Investigator Award, Alternative Muscle Club, San Diego 2016

C. Contributions to science

1. Mesencephalic astrocyte–derived neurotrophic factor is an ER-resident chaperone that protects against reductive stress in the heart

We have previously demonstrated that ischemia/reperfusion (I/R) impairs endoplasmic reticulum (ER)-based protein folding in the heart and thereby activates an unfolded protein response (UPR) sensor and effector, activated transcription factor 6α (ATF6). ATF6 then induces mesencephalic astrocyte–derived neurotrophic factor (MANF), an ER-resident protein with no known structural homologs and unclear ER function. To determine MANF's function in the heart in vivo, here we developed a cardiomyocyte-specific MANF-knockdown mouse model. The MANF knockdown increased cardiac damage after I/R, which was reversed by AAV9-mediated ectopic MANF expression. Mechanistically, MANF knockdown in cultured neonatal rat ventricular myocytes (NRVMs) impaired protein folding

in the ER and cardiomyocyte viability during simulated I/R. However, this was not due to MANF-mediated protection from reactive oxygen species generated during reperfusion. Since I/R impairs oxygen-dependent ER protein disulfide formation and such impairment can be caused by reductive stress in the ER, we examined the effects of the reductive ER stressor dithiothreitol (DTT). MANF knockdown in NRVMs increased cell death from DTT-mediated reductive ER stress, but not from non-reductive ER stresses caused by thapsigargin-mediated ER Ca^{+2} depletion or tunicamycin-mediated inhibition of ER protein glycosylation. In vitro, recombinant MANF exhibited chaperone activity that was dependent on its conserved cysteine residues. Moreover, in cells, MANF bound to a model ER protein exhibiting improper disulfide bond formation during reductive ER stress, but did not bind to this protein during non-reductive ER stress. We conclude that MANF is an ER chaperone that enhances protein folding and myocyte viability during reductive ER stress.

Arrieta A, Blackwood E.A., Stauffer W.T., Santo Domingo M, Bilal A.S., Thuerauf D.J., Pentoney A.N., Aivati C, Sarakki A.V., Doroudgar S., Glembotski C.C. Mesencephalic astrocyte-derived neurotrophic factor is an ER-resident chaperone that protects against reductive stress in the heart. *J Biol Chem.* (2020); 295(22):7566-7583.

2. An Orthogonal DNA Replication System in Yeast.An extranuclear replication system, consisting of an orthogonal DNA plasmid-DNA polymerase pair, was developed in Saccharomyces cerevisiae. Engineered error-prone DNA polymerases showed complete mutational targeting in vivo: per-base mutation rates on the plasmid were increased substantially and remained stable with no increase in genomic rates. Orthogonal replication serves as a platform for in vivo continuous evolution and as a system whose replicative properties can be manipulated independently of the host's.

Ravikumar, A., **Arrieta, A**., and Liu, C.C. (2014). An Orthogonal DNA Replication System in Yeast. *Nat. Chem. Biol.*, 10, 175-177 (2014).

D. All Current and Pending Publications

Full list of published work in Pubmed: 10 peer-reviewed papers
https://pubmed.ncbi.nlm.nih.gov/?term=Arrieta%2C+Adrian&sort=date

Ravikumar, A., **Arrieta, A**., and Liu, C.C. (2014). An Orthogonal DNA Replication System in Yeast. *Nat. Chem. Biol.*, 10, 175-177 (2014).

Arrieta, A., Blackwood, E.A. and Glembotski, C.C. ER Protein Quality Control and the Unfolded Protein Response in the Heart. *Curr. Top Microbiol Immunol.* 2018; 414:193-213.

Blackwood, E.A., Hofmann, C., Santo Domingo, M., Bilal, A.S., Sarakki, A., Stauffer, W., **Arrieta, A.**, Thuerauf, D.J., Kolkhorst, F., Muller, O.J., Jakobi, T., Dieterich, C., Katus, H.A., Doroudgar, S., and Glembotski, C.C. ATF6 regulates cardiac hypertrophy by transcriptional induction of the mTORC1 activator, Rheb. *Circ Res*. 2019; 124(1):79-93.

Arrieta, A. The Pursuit of Success and HapP(h.D)ness. *Circ. Res.* 2019;124(1):21-22

Glembotski, C.C., **Arrieta, A.**, and Blackwood, E.A. Unfolding the roles of mitochondria as therapeutic targets of heart disease. *J Am Coll Cardiol*. 2019; 73(14):1807-1810.

Arrieta, A., Blackwood, E.A., Stauffer, W.T., and Glembotski, C.C. Integrating ER and mitochondrial proteostasis in the healthy and diseased heart. *Front Cardiovasc Med.* 2020; 6:193.

Stauffer, W.T., **Arrieta, A.**, Blackwood, E.A., and Glembotski, C.C. Sledgehammer to scalpel: broad challenges to the heart and other tissues yield specific cellular responses via transcriptional regulation of the ER-stress master regulator ATF6. *Int Journ of Mol Sci*. 2020; 21(3).

Blackwood, E.A., Bilal, A.S., Stauffer, W.T., **Arrieta, A.**, and Glembotski, C.C. Designing novel therapies to mend broken hearts: ATF6 and cardiac proteostasis. *Cells.* 2020; 9(3).

Glembotski, C.C., **Arrieta, A.**, Blackwood, E.A., and Stauffer, W.T. ATF6 as a nodal regulator of proteostasis in the heart. *Front Physiol.* 2020; 11:267.

Arrieta A., Blackwood E.A., Stauffer W.T., Santo Domingo M, Bilal A.S., Thuerauf D.J., Pentoney A.N., Aivati C, Sarakki A.V., Doroudgar S., Glembotski C.C. Mesencephalic astrocyte-derived neurotrophic factor is an ER-resident chaperone that protects against reductive stress in the heart. *J Biol Chem.* (2020); 295(22):7566-7583.
Selected as a JBC editor's pick, top 2% of all manuscripts reviewed and accepted by JBC.

Marsh, K.M., **Arrieta, A.,** Blackwood, E.A, MacDonnell, L.F., Thuerauf, D.J. and Glembotski, C.C. ATF6 maladaptively regulates peroxisome function during simulated ischemia/reperfusion by transcriptional induction of the plasmalogen synthesis enzyme, FAR1. *Manuscript in preparation for submission to the American Journal of Physiology: Heart and Circulatory Physiology.* (2020)

E. Research Support

Ongoing Research Support

Rees-Stealy Research Foundation 08/2015-12/2020
SDSU Heart Institute/RSRF Graduate Fellowships

Recently Completed Research Support

R01 HL127439 02S1 (**PI: Glembotski, CC; Arrieta, A**) 08/08/2016 – 06/30/2017
Supplement Award, NHLBI

3P01HL085577-07S1 (**PI: Sussman, MA; Glembotski, CC; Arrieta, A**) 02/20/2015 – 07/31/2015

ABSTRACT OF THE DISSERTATION

Mesencephalic astrocyte–derived neurotrophic factor is an ER-resident chaperone that protects against reductive stress in the heart

by

Adrian Arrieta

Doctor of Philosophy in Biology

University of California San Diego 2020

San Diego State University 2020

Professor Christopher C. Glembotski, Chair

Heart disease, in its many different forms, is the leading cause of death worldwide for which there is no cure. The lethality of heart failure stems both from its limited capacity to withstand injury, its inherent inability to regenerate upon injury. In order to develop effective therapies that mitigate the extent of injury, novel disease mechanisms must be discerned that will pave the way for development of new therapies. We have previously demonstrated that ischemia/reperfusion (I/R) impairs endoplasmic reticulum (ER)-based protein folding in the heart and thereby activates an unfolded protein response sensor and effector, activated transcription factor 6 (ATF6). ATF6 then induces mesencephalic astrocyte-derived neurotrophic factor (MANF), an ER-resident protein with no known structural homologs and unclear ER function. To determine

MANF's function in the heart in vivo, here we developed a cardiomyocyte-specific MANF-knockdown mouse model. MANF knockdown increased cardiac damage after I/R, which was reversed by adeno-associated virus serotype 9 (AAV9)-mediated ectopic MANF expression. Mechanistically, MANF knockdown in cultured neonatal rat ventricular myocytes (NRVMs) impaired protein folding in the ER and cardiomyocyte viability during simulated I/R. However, this was not due to MANF-mediated protection from reactive oxygen species generated during reperfusion. Because I/R impairs oxygen-dependent ER protein disulfide formation and such impairment can be caused by reductive stress in the ER, we examined the effects of the reductive ER stressor DTT. MANF knockdown in NRVMs increased cell death from DTT-mediated reductive ER stress, but not from nonreductive ER stresses caused by thapsigargin-mediated ER Ca2+ depletion or tunicamycin-mediated inhibition of ER protein glycosylation. In vitro, recombinant MANF exhibited chaperone activity that depended on its conserved cysteine residues. Moreover, in cells, MANF bound to a model ER protein exhibiting improper disulfide bond formation during reductive ER stress but did not bind to this protein during nonreductive ER stress. We conclude that MANF is an ER chaperone that enhances protein folding and myocyte viability during reductive ER stress.

CHAPTER 1: Introduction of the dissertation

The ER is a subcellular location where 35% of all protein synthesis occurs, and proteins synthesized here in cardiac myocytes include G-protein coupled receptors, receptor tyrosine kinases, ion channels, and calcium handling proteins required for cardiac myocyte contractility.[1] Proteins synthesized here also include those that serve extracellular functions including extracellular matrix proteins such as collagen and proteins known as chemokines that mediate intracellular communication between cardiac myocytes and non-myocytes that reside in the heart such as stem cells, immune cells, and fibroblasts[1, 2]. In order for these proteins to successfully traverse the ER and maintain the heart's function they must be folded into their functional three-dimensional conformations[3, 4]. The endoplasmic reticulum maintains a carefully balanced set of conditions that create a nurturing environment for proteins to fold, and these conditions include pH, redox potential, and the concentrations of calcium, O_2, and glucose[5-9] (**Figure 1.1A**); additionally, within the ER exists a class of proteins known as chaperones that catalyze the folding of proteins into their 3-dimensional conformations, and protein degradation machinery which catalyzes extraction and destruction of proteins that do not achieve a folded, functional conformation[10, 11].

A condition known as ER stress, defined as an imbalance between the amount of proteins that need to be folded and the protein folding and degradation machinery, can be brought about by changes in any of the conditions needed for protein folding, increased protein synthesis, or by accumulation of misfolded proteins (**Figure 1.1A**)[2, 12]. The Glembotski lab has demonstrated that accumulation of misfolded proteins in the ER of cardiac myocytes is toxic and leads to cardiac myocyte dysfunction and death ultimately resulting in heart failure (**Figure 1.1B**)[5, 9]. However, the Glembotski lab has also demonstrated that the heart has the capacity, albeit limited, to prevent accumulation of toxic misfolded proteins in the ER, and this capacity is mediated by what is known as the endoplasmic reticulum unfolded protein response[7, 11]. One of the key orchestrators of the ER unfolded protein response is a protein embedded in the ER membrane known as activating

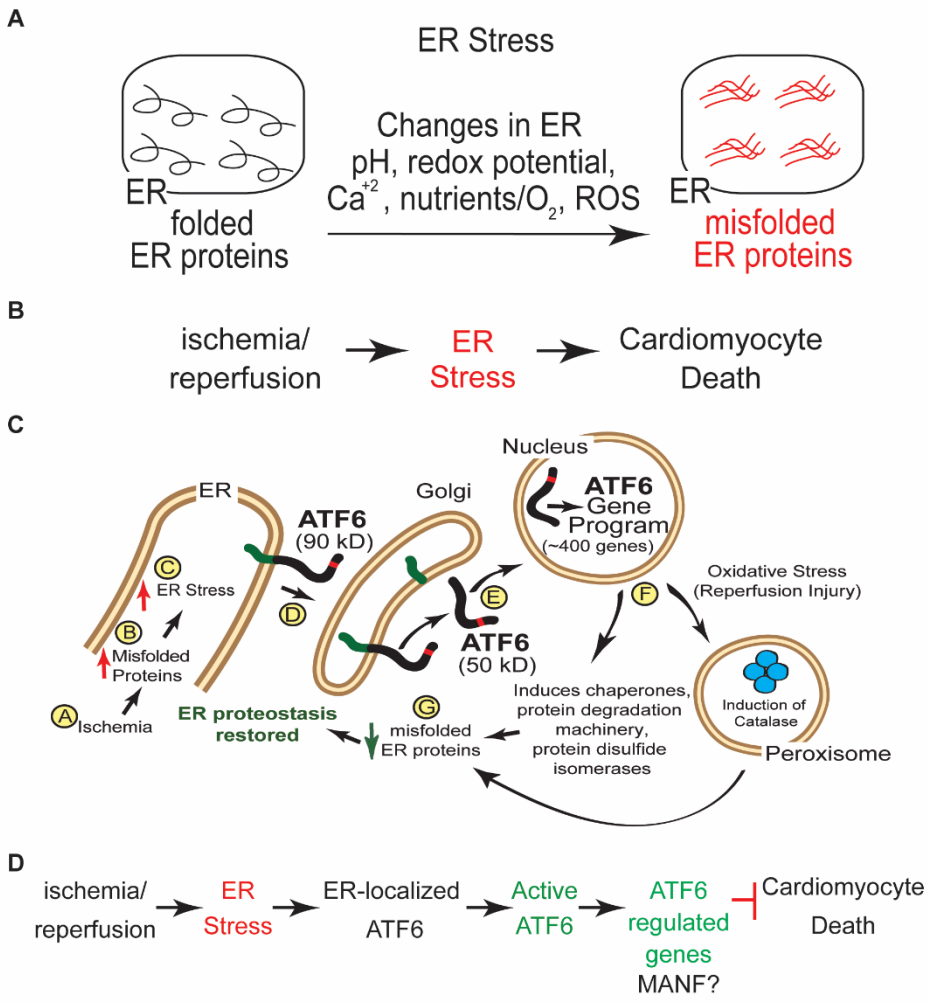

Figure 1.1: Overview of how ER stress is caused in cardiac myocytes, how ATF6 is activated upon ER stress to prevent myocyte death, and the hypothesis addressed in this study.

A. The protein folding environment is dependent several critically tuned factors including pH, redox potential, concentration of O_2 and other nutrients; changes in any of these factors can result in protein misfolding and ER stress. **B.** Ischemia/reperfusion injury in the heart, which alters several of the factors listed in **A**, results in ER stress which can lead to myocyte death. **C.** Upon sensing misfolded proteins ATF6 trafficks to the Golgi where it is cleaved, liberating a transcriptionally active fragment that induces ~400 genes which include ER-targeted chaperones and misfolded protein degradation machinery, as well as non-ER targeted proteins such as Catalase which is targeted to the peroxisome and neutralizes reactive oxygen species generated during reperfusion injury. **D**. Hypothesis: During ER stress caused by ischemia/reperfusion, ATF6 induces MANF, a protein with unknown function, which may exert a unique function to prevent cardiomyocyte death during ischemia/reperfusion injury.

transcription factor 6 (ATF6), which is able to sense the accumulation of misfolded proteins in the ER[2, 5]. Upon sensing misfolded proteins, ATF6 mobilizes to the nucleus where it increases expression of 400 genes that predominantly encode proteins such as ER chaperones that aid in restoring optimal protein folding conditions in the ER to prevent cardiac myocyte death (**Figure 1.1C**)[10, 12, 13]. Recently, the Glembotski lab has demonstrated that ATF6 also increases expression of proteins not targeted to the ER, such as the antioxidant protein catalase proteins which protects against oxidative stress associated with reperfusion injury[7, 14], indicating that ATF6 exerts its protective function across various forms of cardiac pathology. One of the genes induced by ATF6 encodes a protein known as mesencephalic astrocyte-derived neurotrophic factor (MANF)[6, 13, 15]. MANF is an ER-targeted, structurally unique protein, the function of which was unknown prior to the study presented in this dissertation[6, 15]. These observations lead to the hypothesis addressed in chapters two, three, and four that MANF exerts a unique mechanism of protection thereby elucidating a novel molecular mechanism of heart disease (**Figure 1.1D**).

Chapter 2: The Glembotski lab has previously demonstrated that ischemia/reperfusion (I/R) injury in the adult mammalian heart, during which occlusion of one or more of the major arteries of the heart results in cessation of blood flow to downstream cardiac tissue, results in ER protein misfolding and activation of ATF6[5, 7]. To combat ER protein misfolding that contributes to myocyte death, ATF6 upregulates ER-targeted chaperones and protein degradation machinery to restore ER protein folding as well as well as antioxidant proteins that protect against oxidative stress that occurs with reperfusion[7]. ATF6 also upregulates MANF in the adult mammalian heart[12, 13], however it has yet to be determined whether MANF exerts any protective effects during I/R injury. A series of experiments presented in the first chapter of this dissertation illustrate that MANF loss of function in adult cardiac myocytes and in the intact heart results in increased cardiac injury and decreased cardiac function following I/R, demonstrating a cardioprotective function for MANF in the adult mammalian heart.

Chapter 3: The Glembotski lab has recently reported that, while ATF6 induces gene targets that are protective against several forms of different cardiac pathologies, it also induces its gene targets depending on the type of stress cardiac myocytes are experiencing[2, 12, 14]. During ischemia, ATF6 induces targets that specifically protect against misfolded proteins such as the ER-resident chaperone GRP78, but during I/R injury, ATF6 will induce genes encoding antioxidant proteins such as Catalase which neutralizes damaging reactive oxygen species[2, 7, 12, 14]. Since in the first chapter of this study it was demonstrated that MANF loss of function results in increased cardiac injury during I/R, a series of experiments in this second chapter of this dissertation were performed to determine whether MANF is protective against ischemic injury or reperfusion injury. Experiments performed in this chapter of the dissertation demonstrate that MANF exerts its protective function during reperfusion injury by maintaining ER protein folding, and is specifically protective against protein misfolding caused by reductive ER stress[8, 16-18].

Chapter 4: The Glembotski lab has previous demonstrated that MANF possesses an ER retention signal, and previous studies from our labs and others have demonstrated that MANF is part of an interactome composed of several ER-resident chaperones[6, 19]. These previous studies, along with our observations in the second chapter of this dissertation that demonstrate MANF maintains ER protein folding during I/R injury, that MANF is protective against protein misfolding caused by reductive ER stress, and that MANF possesses evolutionarily conserved cysteine residues which are typically associated with redox functions[20], led to the hypothesize that MANF may act as a chaperone, and that this chaperone function is dependent on its cysteine residues. In the third chapter of this dissertation, this hypothesis was addressed by assessing whether MANF prevents aggregation of misfolded proteins and refolds misfolded proteins into a functional conformation, both of which are hallmark biochemical activities of a chaperone[3, 21]. Lastly, experiments were performed to determine whether the conserved cysteine residues of MANF are required for its structure and function.

References

1. Glembotski, C.C., Roles for the sarco-/endoplasmic reticulum in cardiac myocyte contraction, protein synthesis, and protein quality control. Physiology (Bethesda), 2012. **27**(6): p. 343-50.

2. Stauffer, W.T., A. Arrieta, E.A. Blackwood, and C.C. Glembotski, Sledgehammer to Scalpel: Broad Challenges to the Heart and Other Tissues Yield Specific Cellular Responses via Transcriptional Regulation of the ER-Stress Master Regulator ATF6alpha. Int J Mol Sci, 2020. **21**(3).

3. Balchin, D., M. Hayer-Hartl, and F.U. Hartl, In vivo aspects of protein folding and quality control. Science, 2016. **353**(6294): p. aac4354.

4. Vincenz, L. and F.U. Hartl, Sugarcoating ER Stress. Cell, 2014. **156**(6): p. 1125-1127.

5. Doroudgar, S., D.J. Thuerauf, M.C. Marcinko, P.J. Belmont, and C.C. Glembotski, Ischemia activates the ATF6 branch of the endoplasmic reticulum stress response. J Biol Chem, 2009. **284**(43): p. 29735-45.

6. Glembotski, C.C., D.J. Thuerauf, C. Huang, J.A. Vekich, R.A. Gottlieb, and S. Doroudgar, Mesencephalic astrocyte-derived neurotrophic factor protects the heart from ischemic damage and is selectively secreted upon sarco/endoplasmic reticulum calcium depletion. J Biol Chem, 2012. **287**(31): p. 25893-904.

7. Jin, J.K., E.A. Blackwood, K. Azizi, D.J. Thuerauf, A.G. Fahem, C. Hofmann, R.J. Kaufman, S. Doroudgar, and C.C. Glembotski, ATF6 Decreases Myocardial Ischemia/Reperfusion Damage and Links ER Stress and Oxidative Stress Signaling Pathways in the Heart. Circ Res, 2017. **120**(5): p. 862-875.

8. Chin, K.T., G. Kang, J. Qu, L.B. Gardner, W.A. Coetzee, E. Zito, G.I. Fishman, and D. Ron, The sarcoplasmic reticulum luminal thiol oxidase ERO1 regulates cardiomyocyte excitation-coupled calcium release and response to hemodynamic load. FASEB J, 2011. **25**(8): p. 2583-91.

9. Thuerauf, D.J., M. Marcinko, N. Gude, M. Rubio, M.A. Sussman, and C.C. Glembotski, Activation of the unfolded protein response in infarcted mouse heart and hypoxic cultured cardiac myocytes. Circ Res, 2006. **99**(3): p. 275-82.

10. Belmont, P.J., W.J. Chen, M.N. San Pedro, D.J. Thuerauf, N. Gellings Lowe, N. Gude, B. Hilton, R. Wolkowicz, M.A. Sussman, and C.C. Glembotski, Roles for endoplasmic reticulum-associated degradation and the novel endoplasmic reticulum stress response gene Derlin-3 in the ischemic heart. Circ Res, 2010. **106**(2): p. 307-16.

11. Doroudgar, S., M. Volkers, D.J. Thuerauf, M. Khan, S. Mohsin, J.L. Respress, W. Wang, N. Gude, O.J. Muller, X.H. Wehrens, M.A. Sussman, and C.C. Glembotski, Hrd1 and ER-Associated Protein Degradation, ERAD, are Critical Elements of the Adaptive ER Stress Response in Cardiac Myocytes. Circ Res, 2015. **117**(6): p. 536-46.

12. Blackwood, E.A., C. Hofmann, M. Santo Domingo, A.S. Bilal, A. Sarakki, W. Stauffer, A. Arrieta, D.J. Thuerauf, F.W. Kolkhorst, O.J. Muller, T. Jakobi, C. Dieterich, H.A. Katus, S. Doroudgar, and C.C. Glembotski, ATF6 Regulates Cardiac Hypertrophy by Transcriptional Induction of the mTORC1 Activator, Rheb. Circ Res, 2019. **124**(1): p. 79-93.

13. Martindale, J.J., R. Fernandez, D. Thuerauf, R. Whittaker, N. Gude, M.A. Sussman, and C.C. Glembotski, Endoplasmic reticulum stress gene induction and protection from ischemia/reperfusion injury in the hearts of transgenic mice with a tamoxifen-regulated form of ATF6. Circ Res, 2006. **98**(9): p. 1186-93.

14. Blackwood, E.A., K. Azizi, D.J. Thuerauf, R.J. Paxman, L. Plate, J.W. Kelly, R.L. Wiseman, and C.C. Glembotski, Pharmacologic ATF6 activation confers global protection in widespread disease models by reprograming cellular proteostasis. Nat Commun, 2019. **10**(1): p. 187.

15. Glembotski, C.C., Functions for the cardiomyokine, MANF, in cardioprotection, hypertrophy and heart failure. J Mol Cell Cardiol, 2011. **51**(4): p. 512-7.

16. Ellgaard, L., C.S. Sevier, and N.J. Bulleid, How Are Proteins Reduced in the Endoplasmic Reticulum? Trends Biochem Sci, 2018. **43**(1): p. 32-43.

17. Oka, O.B., M.A. Pringle, I.M. Schopp, I. Braakman, and N.J. Bulleid, ERdj5 is the ER reductase that catalyzes the removal of non-native disulfides and correct folding of the LDL receptor. Mol Cell, 2013. **50**(6): p. 793-804.

18. Poet, G.J., O.B. Oka, M. van Lith, Z. Cao, P.J. Robinson, M.A. Pringle, E.S. Arner, and N.J. Bulleid, Cytosolic thioredoxin reductase 1 is required for correct disulfide formation in the ER. EMBO J, 2017. **36**(5): p. 693-702.

19. Yan, Y., C. Rato, L. Rohland, S. Preissler, and D. Ron, MANF antagonizes nucleotide exchange by the endoplasmic reticulum chaperone BiP. Nat Commun, 2019. **10**(1): p. 541.

20. Ellgaard, L. and L.W. Ruddock, The human protein disulphide isomerase family: substrate interactions and functional properties. EMBO Rep, 2005. **6**(1): p. 28-32.

21. Buchner, J., H. Grallert, and U. Jakob, Analysis of chaperone function using citrate synthase as nonnative substrate protein. Methods Enzymol, 1998. **290**: p. 323-38.

Chapter 2: MANF loss of function in vivo decreases myocyte viability and cardiac function during ischemia/reperfusion injury.

Abstract

During I/R injury in the heart, cardiac myocytes downstream of the included artery suffer from decreased perfusion of blood carrying oxygen and nutrients required for cardiac myocyte contractility and viability. In the endoplasmic reticulum, oxygen and nutrients are also required for the synthesis and folding of proteins required for myocyte contractility and viability. Upon re-opening of the occluded artery, the sudden re-introduction of oxygen and nutrients results in malignant re-initiation of cardiac metabolism, resulting in generation of reactive oxygen species (ROS) which can further compromise the function of proteins residing in the ER. During ischemia, the ER transmembrane-bound protein ATF6 senses the accumulation of misfolded proteins, upon which it mobilizes to the Golgi Apparatus, where it is proteolytically cleaved, liberating a transcriptionally active fragment that localizes to the nucleus to upregulate genes encoding ER-targeted chaperones that restore ER protein folding and maintain ER function, as well as antioxidant proteins such as catalase which neutralize ROS generated during reperfusion injury. In addition to upregulation of these cardioprotective genes, ATF6 upregulates the gene encoding MANF, an ER-resident, protein of unknown function that possesses a unique amino acid sequence and three-dimensional structure, suggesting that MANF also exerts a novel function in the heart. To determine whether MANF is cardioprotective, here a cardiomyocyte-specific MANF-knockdown mouse model was generated. MANF knockdown increased cardiac damage after I/R, and AAV9-mediated re-expression of MANF in the heart was sufficient to restore the effects of MANF loss-of-function during following I/R injury, demonstrating that MANF exerts a cardioprotective function in the adult mammalian heart.

Introduction

The endoplasmic reticulum (ER) is a major site of the synthesis of proteins that are critical for proper function of the heart, including many calcium-handling proteins, receptors, and secreted proteins, such as hormones, stem cell homing factors, and growth factors[1, 2]. Therefore, proper

folding of proteins synthesized in the ER of cardiac myocytes is essential for maintaining optimal cardiac function. Furthermore, many post-translational modifications occur in the ER, including disulfide bond formation, which are critical for protein stability and function[3]. Disulfide bond formation in the ER, also known as oxidative protein folding, is an oxygen-dependent process[3-7]. Some time ago, this led to the hypothesis that ER protein folding would be impaired in cardiac myocytes in response to a lack of oxygen during pathophysiological conditions of ischemia and ischemia/reperfusion[3, 4]. Subsequently, it was demonstrated in cultured cardiac myocytes and in mouse hearts, in vivo, that I/R disrupts protein folding in the ER, leading to activation of the ER stress response, also called the unfolded protein response (UPR)[5, 8].

The UPR is controlled in all mammalian cells by several ER-transmembrane sensors of ER protein misfolding, including the adaptive transcription factor, ATF6[9, 10]. When protein synthesis surpasses the capacity of the protein folding machinery, increases in misfolded proteins cause the translocation of the ER-transmembrane, 90 kD form of ATF6, to the Golgi, where it is clipped, liberating an N-terminal fragment that, after nuclear translocation, serves as a transcription factor[9, 10]. This 50 kD active form of ATF6 regulates a gene program that is responsible for the expression of numerous proteins that enhance ER protein folding, which adaptively restores the balance between protein synthesis and folding[11, 12]. The Glembotski lab previously generated a transgenic (TG) mouse line in which ATF6 could be activated at will, selectively in cardiac myocytes; using this mouse line we showed that ATF6 protected hearts from I/R damage[13].

Transcript profiling of these ATF6 TG mouse hearts, as well as ATF6 knockout mouse hearts, defined the ATF6 gene program in the heart and it was posited that these genes might contribute to the protective effects of ATF6[11-13]. One of those genes encodes mesencephalic astrocyte-derived neurotrophic factor (MANF), which was originally isolated from astrocytes, but later found in all eukaryotic cells examined to date[13-15]. One of the striking features of MANF is

that it has a noncanonical but functional ER retention sequence at the C-terminus, but otherwise shares little structural homology with other proteins[15]. This finding spawned the hypothesis that MANF exerts a unique function within the ER to maintain ER function and myocyte contractility and prevent myocyte death during I/R injury; however, such a concept has not been studied. Accordingly, the current study was undertaken to examine the effects of MANF loss-of-function in the adult mouse heart on myocyte viability and cardiac function following I/R injury.

Hypothesis: MANF is required for myocyte viability and cardiac function during I/R injury.

Aims:

1. Assess whether MANF loss of function affects basal cardiac function and results in cardiac pathology.
2. Assess whether MANF loss of function affects myocyte viability and cardiac function following I/R injury.
3. Assess whether re-expression of MANF is sufficient to restore the effects of MANF loss of function on myocyte viability and cardiac function following I/R injury.

Methods

Generation of MANF Knockdown (MANF KD) Transgenic Mice:

An oligonucleotide coding for an RNA hairpin targeting the mouse MANF transcript was cloned into the α-MHC vector, a gift from J. Robbins (University of Cincinnati). The αMHC-MANF KD construct was linearized and injected into the pronuclei of fertilized B6D2F1 (Harlan Sprague–Dawley) embryos. The resulting TG mice were back-crossed into the FVB background strain for at least 10 generations.

MANF KD Hairpin sequence:

5’TGCTGT**TATCTTCCGGATATAGTCAG**GTTTTGGCCACTGACTGACCTGACTATCCGGAAG ATAA-3’

Animals were genotyped by isolating DNA from tail biopsies and performing PCR with the following primers:

Forward Primer targeting the αMHC promoter:

5'-CGGCACTCTTAGCAAACCTC-3'

Reverse Primer:

5'-CAGATCTGGGCCATTTGTTC-3'

Tissue protein extraction:

Mouse hearts were excised, washed briefly in ice-cold DPBS and snap frozen in liquid nitrogen. Approximately 20mg of frozen tissue was extracted in 250µL of ice-cold tissue homogenization buffer composed of 20mM Tris (pH 7.5), 150mM NaCl, 1% Triton X-100, 1% SDS, and 0.5% sodium deoxycholate with 1x protease/phosphatase mixture. Tissue homogenates were then clarified by centrifugation at 20,000xg for 10 minutes at 4°C.

Immunoblotting:

Following determination of protein concentration of clarified tissue extracts using the BCA protein assay kit (Bio-Rad, Cat. No. 5000111), between 5 and 40µg of protein extracts were subjected to reducing SDS-PAGE then electroeluted onto PVDF membranes. Membranes were blocked for 30 minutes at room temperature in 5% non-fat instant dry milk dissolved in Tris-buffered saline containing 150mM NaCl, 2.68mM KCl, 50 mM Tris-pH 7.5, 0.1% Tween (TBST) with gentle rocking. Membranes were probed with rabbit MANF antiserum, at 1:1000 (Anti-ARMET, Cat. No. ab67203, Abcam; Anti-MANF, Cat. No. SAB3500384, Sigma-Aldrich), a mouse KDEL antiserum at 1:8000 (ENZO Life Sciences; Cat. No. ADI-SPA-827), a mouse FLAG antibody at 1:8000 (Sigma-Aldrich; Cat. No. F1804), and a B-actin antibody (Santa Cruz, Cat. No. sc-47778). Antibodies were diluted in 5% milk dissolved in TBST. Membranes were incubated with antibody solutions for 12-16 hours at 4°C. Membranes were then washed 3 times for 15 minutes in TBST and then incubated for 1 hour at room temperature with the appropriate

horseradish peroxidase–conjugated anti-IgG (Jackson ImmunoResearch Laboratories, Inc.) diluted at 1:2000 in 5% milk dissolved in TBST. Membranes were then washed 3 times for 15 minutes with gentle rocking in TBST and subjected to enhanced chemiluminescence and exposed to autoradiography film or imaging using an ImageQuant 4000 from GE Healthcare Life Sciences. Immunoblots were quantified using ImageJ software densitometry.

Tissue mRNA extraction and Quantitative real-time PCR (qRT-PCR):

Total RNA was isolated from mouse hearts using the RNeasy Mini kit (Qiagen, Cat. No. 74104) as per manufacturer's instructions. cDNA synthesis was performed using SuperScript III First-Strand Synthesis System (Thermo Fisher). qRT-PCR was performed using Maxima SYBR Green/ROX qPCR Master Mix in a StepOnePlus RT-PCR System (Thermo Fisher). The following primers were used:

Manf:

Forward: 5'-TGGGTGCGTTCTTCGACAT-3'

Reverse: 5'-GACGGTTGCTGGATCATTGAT-3'

β-Actin:

Forward: 5'-GACGGCCAGGTCATCACTAT-3'

Reverse: 5'-GTACTTGCGCTCAGGAGGAG-3'

Gapdh:

5'-ATGTTCCAGTATGACTCCACTCACG-3'

5'-GAAGACACCAGTAGACTCCACGACA-3'

Nppa:

5-'TTGTGGTGTGTCACGCAGCT-3'

5'-TGTTCACCACGCCACAGTG-3'

Nppb:

5'-AAGTCGGAGGAAATGGCCC-3'

5'-TTGTGAGGCCTTGGTCCTTC-3'

Col1a1:

5'-AAGACGGGAGGGCGAGTGCT-3'

5'-TCTCACCGGGCAGACCTCGG-3'

Echocardiography:

Echocardiography was carried out on anesthetized mice using a Visualsonics Vevo 770, or a Visualsonics Vevo 2100 high-resolution echocardiograph, as previously described[16].

Plasmid generation:

Construct 1: pcDNA3.1(-) Mouse MANF

The open reading frame of mouse Manf (NM_029103) was amplified by PCR and then ligated into the XhoI and HindIII sites of multiple cloning site of pcDNA3.1(-).

Construct 2: pcDNA3.1(-) Mouse MANF signal sequence

Using construct 1 as a template, PCR was carried out to introduce a NheI restriction site and Kozak sequence, and an ApaI restriction site, into the 5' and 3' ends respectively of the PCR amplified product coding for the MANF signal sequence MWATRGLAVALALSVLPDSRA. This PCR product and pcDNA3.1(-) were digested with NheI and ApaI and ligated together. The ApaI site is immediately followed by sequential XbaI and XhoI restriction sites.

Construct 3: pcDNA3.1(-) 3x-FLAG:

A version of pcDNA3.1(-) containing an N-terminal 3x-FLAG sequence was constructed by annealing the following oligonucleotides:

5'ctagcGCC**ATGGACTACAAAGACCACGACGGTGATTATAAAGATCACGATATCGATTACA AAGGATGACGATGACAAGt**-3'

5'-ctaga**CTTGTCATCGTCATCCTTGTAATCGATATCGTGATCTTTATAATCACCGTCGTGG-TCTTTGTAGTCCAT**GGCg-3'

The NheI and XbaI overhangs of the annealed oligonucleotides were used to ligate the product into the XbaI site of pcDNA3.1(-), resulting in the creation of 3x FLAG-pcDNA3.1, as previously described[17].

Construct 4: pcDNA3.1(-) Mouse MANF signal sequence + 3x-FLAG.

Using **construct 3** as a template, PCR was performed to introduce XbaI and XhoI sites to the 5' and 3' ends, respectively, of the region coding for the 3x-FLAG tag, DYKDHDGDYKDHDIDYKDDDDK. This PCR product and **construct 2** were digested with XbaI and XhoI and ligated together to create a construct encoding the MANF signal sequence followed by 3x-FLAG.

Construct 5: pcDNA3.1(-) Mouse MANF signal sequence + 3x-FLAG + $MANF_{WT}$ (referred to hereafter as FLAG-$MANF_{WT}$)

Using construct 1 as a template, PCR was performed with the following primers:
5'GGAACG**CTCGAG**CTGCGGCCAGGAGAC-3'
5'-GGAGCTGACACGGAAGAT-3' (pcDNA 3.1(-) reverse primer)
The resulting PCR product and **construct 4** were digested with XhoI and HindIII and ligated together to generate a construct encoding the MANF signal sequence followed by 3x-FLAG and MANF, with the following amino acid sequence:
MWATRGLAVALALSVLPDSRAGPSRDYKDHDGDYKDHDIDYKDDDDKLELRPGDCEVCISYLG
RFYQDLKDRDVTSSPATIEEELIKFCREARGKENRLCYYIGATDDAATKIINEVSKPLAHHIPVEKI
CEKLKKKDSQICELKYDKQIDLSTVDLKKLRVKELKKILDDWGEMCKGCAEKSDYIRKINELMPK
YAPKAASARTDL

Adeno-associated virus serotype 9 (AAV9) Preparation and Tail Vein Injection:

To generate recombinant AAV9-control and AAV9-FLAG-$MANF_{WT}$, shuttle vectors for these recombinants were constructed and co-transfected with AAV9 helper, pDG-9 (a gift from

Dr. Roger Hajjar) into HEK293T cells to produce virus, as described previously[18]. The shuttle vector pTRUF12-CMV was constructed by modifying pTRUF12 (a gift from Dr. Roger Hajjar) by first removing the region encoding GFP that was down-stream of the IRES. New restriction sites were inserted into the multiple cloning site to include Nhe1, Pme1, Xho1, and Mlu1. The coding region of FLAG-$MANF_{WT}$ (**construct 5,** above) was excised and ligated into the NheI and HindIII restriction sites of the shuttle vector pTRUF12-CMV. To reduce recognition of the AAV9mediated FLAG-MANF transcripts by the MANF KD hairpin, silent mutations were introduced into the pTRUF12-CMV plasmid by site directed mutagenesis with the following primers:
5'-GCAGAAAAGTCTGATTACATTAGGAAAATCAATGAACTGATGC-3'
5'-GCATCAGTTCATTGATTTTCCTAATGTAATCAGACTTTTCTGC-3'

To prepare the recombinant AAV9, HEK293T cells were plated a density of $8x10^6$ per T-175 flask and maintained in DMEM/F12 containing 10% FBS, penicillin/streptomycin at 37°C and 5% CO2. For each virus preparation, 48 flasks were used. Twenty-four hours after plating, cultures were transfected using Polyethylenimine "Max" (MW 40,000, Polysciences, cat# 24765) as follows: For each T-175 flask, 15µg of helper plasmid and 5µg of pTRUF12 plasmid were mixed with 1mL of DMEM:F12 (no antibiotics) and 160µL of polyethylenimine (0.517 mg/mL), vortexed for 30 seconds, and incubated for 15 minutes at room temperature. This was then mixed with 18mL DMEM/F12 containing 2% FBS, penicillin/ streptomycin then used to replace the media on the cultures. The cultures were then rocked intermittently for 15 minutes before being placed in a CO2 incubator. Three days later, the cells collected from six T-175 flasks were centrifuged at 500xg for 10 minutes, then resuspended in 10mL of lysis buffer (150mM NaCl, 50mM TrisHCL). The resuspended cells were then subjected to three rounds of freeze-thaw, followed by treatment with benzonase (1500U of benzonase; Novagen) and 1mM $MgCl_2$ at 37°C for 30 minutes. The cell debris was collected by centrifugation at 3,400xg for 20 minutes. The supernatant obtained from six T-175 flasks containing the AAV9 was then purified on an iodixanol gradient comprised

of the following four phases: 7.3mL of 15%, 4.9mL of 25%, 4mL of 40%, and 4mL of 60% iodixanol (Optiprep; Sigma-Aldrich) overlayed with 10mL of cell supernatant. The gradients were centrifuged in a 70Ti rotor (Beckman Coulter) at 69,000rpm for 1 hour using OptiSeal Polyallomer Tubes (Beckman Coulter). Virus was collected by inserting a needle 2mm below the 40%-60% interface and collecting 4 or 5 fractions (~4mL) of this interface and most of the 40% layer. The fractions were analyzed for viral content and purity by examining 10µL of each fraction on a 12% SDS-PAGE gel (BioRad), followed by staining with InstantBlue (Expedeon) to visualize the viral capsid proteins, VP1, VP2 and VP3. The virus was then collected from the fractions of several gradients and the buffer was exchanged with lactated Ringer's using an ultrafiltration device, Vivaspin 20, 100kDa MWCO (GE Healthcare). The final viral preparation was then fractionated on a 12% SDS-PAGE gel, stained with Coomassie blue (Expedeon, Cat. No. ISB1L), and then compared with a similarly stained gel of a virus of a known titer (an analogous control AAV9 with a CMV_{enh}MLC800 composite promoter with no downstream open reading frame). To administer recombinant AAV, mice were injected with 100µL of 37ºC heated Lactated Ringer's solution containing 10^{11} genome-containing units per mouse were injected via tail vein.

Isolation and sI/R treatment of adult mouse ventricular myocytes (AMVM)[5]:

Briefly, hearts were rapidly cannulated via the ascending aorta, mounted on a perfusion apparatus and retrograde perfused at 3 mL/min for 4 minutes at 37°C with heart medium (Joklik Modified Minimum Essential Medium; Cat. No. M-0518, Sigma-Aldrich, supplemented with 10mM HEPES, 30mM taurine, 2mM D-L-carnitine, 20mM creatine, 5mM inosine, 5mM adenosine, and 10mM butanedione monoxime (BDM), pH 7.36). Collagenase digestion of hearts was performed by perfusing for 13 minutes with heart medium supplemented with type 2 collagenase (50-60mg; ~320U/mL, Cat. No. LS004176, Worthington) and 12.5µM $CaCl_2$. Hearts were removed from the cannula and submerged in 2.5mL of effluent collected off the heart during the collagenase digestion and dissociated using forceps. Collagenase was neutralized by adding 2.5mL of heart

medium supplemented with 10% FBS, and the final concentration of $CaCl_2$ was adjusted to 12.5μM. Cells were dissociated further by gently triturating for 4 minutes. The cell suspension was then filtered through a 100μm mesh filter and myocytes were allowed to sediment by gravity for 6 minutes at room temperature. The supernatant containing nonviable cells and non-myocytes was discarded and the remaining myocytes were resuspended in 5mL of heart medium containing 5% FBS and 37.5μM $CaCl_2$. The concentration of $CaCl_2$ in this suspension was slowly increased in a careful stepwise manner as follows: Step 1- add 50μL of 10mM $CaCl_2$, mix gently, allow to sit for 4 minutes; Step 2- repeat Step 1; Step 3- add 100μL of 10mM $CaCl_2$ and wait 4 minutes; Step 4- add 80μL of 100mM $CaCl_2$ and wait 4 min. Cells were resuspended in plating medium (MEM medium; Cat. No. 12350-039, Thermo Fisher Scientific, Waltham, MA, 1x insulin-transferrin-selenium; Cat. No. 41400-045, Thermo Fisher, 10mM HEPES, 100 units/mL penicillin and 100 μg/mL streptomycin, 10 mM BDM and 4% FBS). Cells were plated at 5 x 10^4 cells per well in 12-well culture plates coated with laminin (10μg/mL). After at least 2 hours, the medium was changed to maintaining medium (MEM medium, 1x insulin-transferrin-selenium, 10mM HEPES, 1.2mM $CaCl_2$ and 0.01% bovine serum albumin, 25μM blebbistatin). Cells were used for experiments 12-18 hours later. To induce ER stress, the medium was switched to maintaining media without blebbistatin and 7μM thapsigargin for 16 hours. To subject myocytes to simulated ischemia/reperfusion, the medium was changed to glucose-free DMEM (Cat. No. A14430-01) with dialyzed FBS and antibiotics and incubated at 0.1% O_2 for 3 hours in a hypoxia chamber with an oxygen controller. Following 3 hours of simulated ischemia, the medium was switched to reperfusion media for 24 hours (1x MEM containing 1x insulin, transferrin and selenium in 10mM HEPES, 1.2mM $CaCl_2$, and 0.1mg/mL bovine serum albumin with no blebbistatin.

AMVM Cell Viability Assay (Calcein AM staining)[5]:

Following sI/R treatment, Calcein AM (Thermo Fisher Cat. No. C1430) dissolved at 1mg/mL in DMSO was diluted 1:1000 directly into culture wells. Cultures were then incubated for

10 minutes at 37°C. Viable NRVM or AMVM were identified as calcein AM-positive and images were obtained using an IX70 fluorescence microscope (Olympus, Melville, NY). Numbers of viable, calcein AM-positive cells were counted using ImageJ. Parallel control cultures were maintained at ~20–21% O_2 in simulated ischemia medium supplemented with 17.5mM glucose.

Ex vivo Global Ischemia/Reperfusion[5, 13]:

Briefly, age-matched (10 to 11 weeks of age) WT and MANF KD TG mice were injected intraperitoneally with heparin (500U/kg) and after 10 minutes mice were anesthetized with sodium pentobarbital (150mg/kg). Hearts were isolated and rinsed with ice-cold modified Krebs-Henseleit buffer, the aortas were cannulated, and the hearts were mounted onto a Langendorff perfused heart apparatus. Hearts were perfused by gravity at a constant pressure of 80 mmHg, and a pressure sensor balloon was inserted into the left ventricle through the left atrium. Left ventricular developed pressure (LVDP, mmHg) was assessed using Powerlab software. Hearts were equilibrated for thirty minutes while submersed in buffer at 37°C and paced at 400Hz and 0.5mA. Hearts were subjected to global no-flow ischemia without pacing for twenty minutes and then reperfused for sixty minutes.

LDH Assay[13]:

LDH release from isolated perfused hearts was assayed using a CytoTox 96® NonRadioactive Cytotoxicity Assay from Promega. From the kit, 12mL of room temperature assay buffer were used to dissolve one bottle of substrate mix. 100µL of perfusate from cultures were transferred to a clear round-bottom 96-well plate. 50µL of assay buffer mixed with assay substrate was added to each perfusate sample. The absorbance of the resulting solution was [7]measured at 490nm, using a VersaMax microplate reader set at 29°C.

Triphenyl Tetrazolium Chloride Staining[13]:

Hearts exposed to global ischemia/reperfusion were briefly frozen (5 minutes) at -80°C. Hearts were partially thawed and sliced into 1-mm sections. Sections were incubated in 1% triphenyl tetrazolium chloride (TTC) in phosphate buffer (88mM Na_2HPO4, NaH_2PO4 1.8mM) at 37°C for 10 minutes. Sections were then incubated in 10% formalin diluted in phosphate buffer overnight at 4°C. Sections were placed on glass slides and scanned on a Canon scanner. Images were quantified using ImageJ to outline the infarct and area at risk.

Results

MANF loss of function in the heart increases cardiac damage during ischemia/reperfusion injury

To determine the effects of MANF loss-of-function in the heart, a mouse model was generated in which the α-MHC promoter drives expression of a Manf-specific microRNA in a cardiac myocyte-restricted manner. The choice was made to knockdown endogenous MANF, instead of completely deleting it because the deletion of many ER stress response genes has been shown to lead to embryonic lethality[18]. Immunoblots of mouse hearts showed that, compared to wild-type (WT) mice, MANF knockdown (KD) mice exhibited a four-fold reduction in MANF (**Figure 2.1A-B**). As the effects of MANF knockdown on mouse heart function have not been previously examined, basal cardiac function was assessed by echocardiography. Compared to WT mouse hearts, MANF KD mice exhibited increased ejection fraction; MANK KD female mice had slightly decreased left ventricular systolic volume, while male MANF KD mice had slightly increased left ventricular diastolic volume (**Table 2.1**). To assess whether the increase in cardiac contractility elicited cardiac pathology, mRNA levels of cardiac pathology markers Nppa, Nppb, and Col1a1 and protein levels of ER stress markers, i.e. GRP94 and GRP78, as well as hearts and lung weights from WT and MANF KD mice were measured. Expression of ER stress and cardiac pathology markers (**Figure 2.1C-G**) and heart and lung weights (**Figure 2.1H-J**) were

unaffected by MANF knockdown. Overall, these results show that knocking down MANF in cardiac myocytes of mouse hearts by approximately 80% increases contractility but does not induce any overt cardiac pathology. Since no overt cardiac pathology was observed, further experiments were performed to assess the effects of MANF knockdown in pathophysiological models of ER stress.

To determine the consequences of MANF knockdown on myocyte viability during conditions known to induce ER stress, adult mouse ventricular myocytes (AMVM) were isolated from WT and MANF KD mice and subjected to simulated ischemia/reperfusion (sI/R), a model of pathophysiological ER stress. Compared to WT myocytes, MANF KD myocytes exhibited more death in response to sI/R (**Figure 2.1K**). To examine functional roles for MANF in the heart, WT and MANF KD mouse hearts were subjected to *ex vivo* I/R[5, 13]. Compared to WT mouse hearts, MANF KD mouse hearts exhibited significantly lower functional recovery, significantly increased tissue damage, and greater LDH release, the last of which is an indicator of necrotic tissue damage (**Figure 2.2A-E**)[13], though in this experiment this measure did not reach statistical significance. These results indicate that MANF knockdown in the heart decreases myocyte viability during I/R resulting in increased tissue damage and decreased cardiac function.

Re-expression of MANF reverses the effects of MANF knockdown on cardiac damage following ischemia/reperfusion

To determine whether ectopic expression of FLAG-MANF$_{WT}$ could restore the functional and structural defects observed in the MANF KD mice, a recombinant AAV9[5, 12, 18] was engineered encoding FLAG-MANF using nucleotide sequences that are not targeted by the MANF-specific microRNA that is expressed in MANF KD mouse hearts. The hearts of MANF KD mice that were

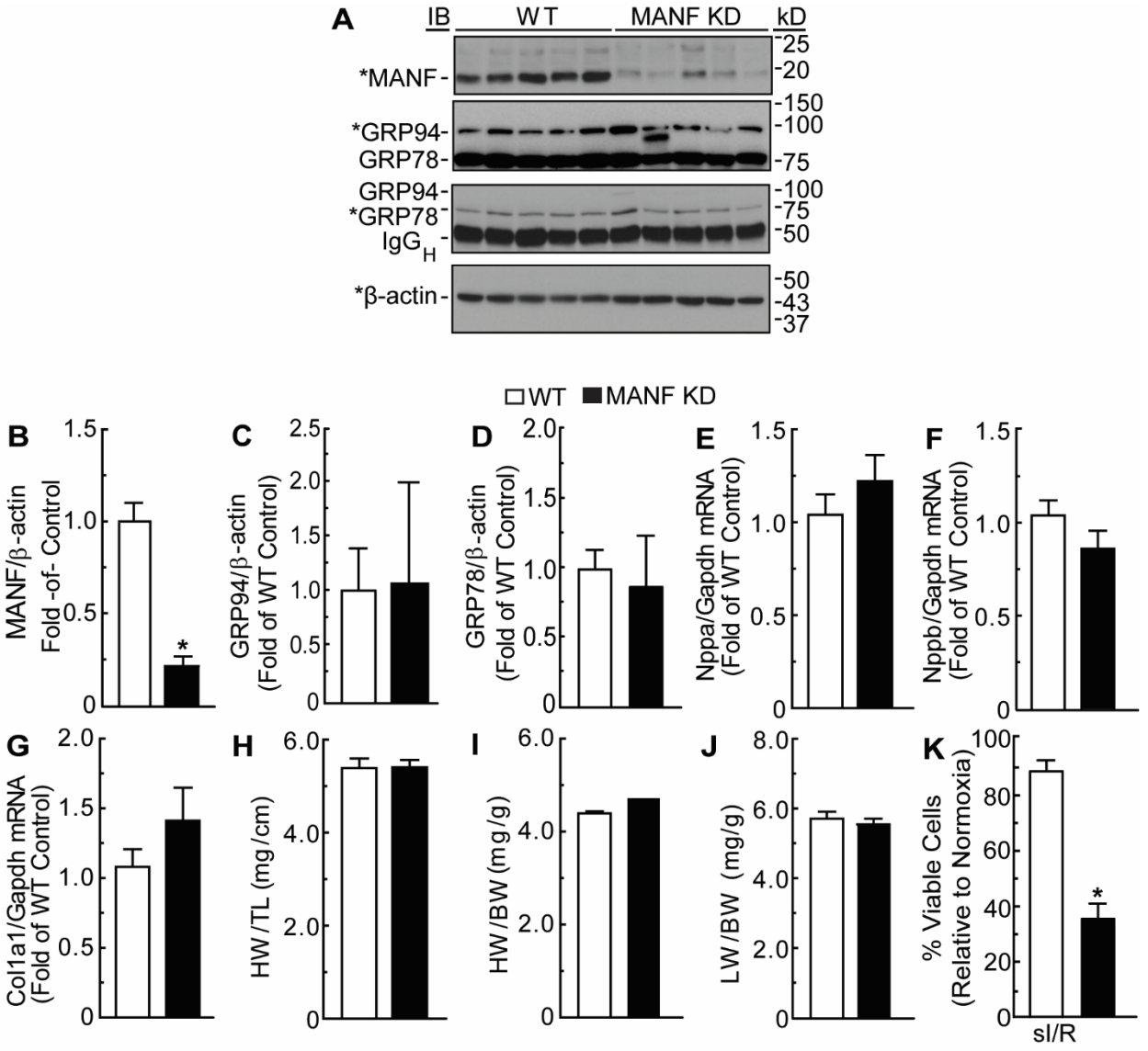

Figure 2.1: Effect of MANF knockdown in the heart on expression of GRP94 andGRP78, expression of fetal genes, heart and lung weights, and viability of isolated adult mouse ventricular myocytes during sI/R. **A**, MANF, GRP94, GRP78, and β-actin immunoblots of mouse heart extracts from 10-week-old female WT (n=5) or MANF KD mice (n=5). *, band of interest that was quantified in **B**–**D**. IgG_H indicates position of immunoglobulin heavy chain. **B**–**D**, densitometry of immunoblots shown in **A**. Band intensities were normalized to those for β-actin and displayed as fold of WT control level. **E**–**G**, fetal gene mRNA levels were determined by RT-qPCR. **H** and **I**, heart weights were normalized to tibia length (**H**) or body weight (**I**). **J**, lung weights were normalized to body weight. Echocardiography data and statistical analysis can be found in Table 1. **K**, myocytes were isolated from 10-week-old adult WT and MANF KD mice and then subjected to sI/R followed by determination of cell viability. To determine percentage cell viability, the number of calcein AM–positive cells per field was divided by the total number of cells in the same field. *, statistically significant difference by Student's unpaired t-test, $p \leq 0.05$. Note that GRP78 and GRP94 immunoblotting was performed using an anti-KDEL antibody. Error bars, S.E.M.

Table 2.1: Echocardiographic parameters of wild type (WT) and transgenic (MANF KD) mice.

Parameter	Female WT (n = 6)	Female MANF KD (n = 7)	Male WT (n = 6)	Male MANF KD (n = 7)
FS (%)	39.80±3.11	50.47±0.75*	36.89±1.87	45.96±1.72*
EF (%)	70.61±2.72	82.62±0.74*	67.91±2.35	77.82±1.83*
LVEDV (µl)	53.17±2.37	49.82±3.25	41.83±3.02	56.93±3.86*
LVESV (µl)	15.97±2.18	8.74±0.87*	13.18±0.72	12.99±1.94
LVIDD (mm)	3.58±0.09	3.40±0.06	3.22±0.10	3.66±0.10
LVIDS (mm)	2.10±0.14	1.65±0.11*	2.02±0.04	1.98±0.11
PWTD (mm)	0.89±0.05	0.77±0.06	0.92±0.07	1.05±0.14
PWTS (mm)	1.15±0.06	1.32±0.08	1.25±0.12	1.45±0.07
AWTD (mm)	0.85±0.06	0.95±0.11	1.03±0.07	0.94±0.04
AWTS (mm)	1.45±0.07	1.58±0.06	1.43±0.07	1.56±0.08
LV mass (mg)	99.16±8.22	92.65±7.72	106.75±6.94	124.01±14.04
HR (bpm)	472.96±2.98	458.69±5.51	473.88±11.14	453.20±4.58

FS = fractional shortening
EF = ejection fraction
LVEDV = left ventricular end diastolic volume
LVESV = left ventricular end systolic volume
LVIDD = left ventricular inner diameter in diastole
LVIDS = left ventricular inner diameter in systole
PWTD = left ventricular posterior wall thickness in diastole
PWTS = left ventricular posterior wall thickness in systole
AWTD = left ventricular anterior wall thickness in diastole
AWTS = left ventricular anterior wall thickness in systole
LV mass = left ventricular mass
HR = heart rate in beats per minute
Statistical analyses used student's unpaired t-test.

* = $p \leq 0.05$ different between WT and transgenic MANF KD mice of the same sex.

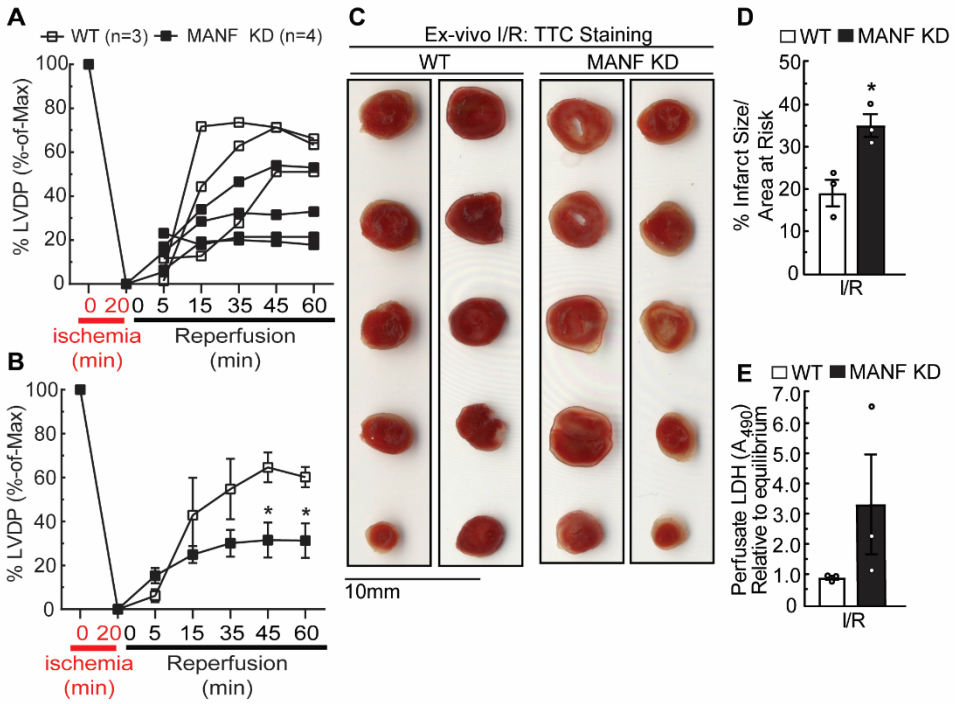

Figure 2.2: Effect of MANF knockdown in the heart on cardiac contractility and cardiac damage following I/R. A–E, ex vivo I/R of WT and MANF KD mouse hearts. Hearts from female WT (n=3) or MANF KD (n=4) were subjected to ex vivo ischemia for 20 min, followed by 60 min of reperfusion (I/R). **A** and **B**, LVDP upon reperfusion was normalized to the LVDP obtained during equilibration, the latter of which was set to 100%. **A**, plot of individual LVDP time courses from different mouse hearts. **B**, average of the plots shown in **A**. **C** and **D**, heart sections were stained with TTC to assess the extent of myocardial damage (**C**); shown is the average infarct size divided by area at risk (**D**). **E**, samples of ex vivo heart perfusates were obtained after 45 min of reperfusion and then assayed for LDH activity relative to LDH activity in the equilibrium perfusate. *, statistically significant difference by Student's unpaired t-test, $p \leq 0.05$. Error bars, S.E.M.

treated with AAV9-FLAG-MANF$_{WT}$ had about the same level of MANF as WT hearts **(Figure 2.3A)**. When hearts were subjected to *ex vivo* I/R, compared to AAV9-Con treated mice, AAV9-FLAG-MANF treated mice exhibited smaller infarcts, greater contractile function, and less necrosis **(Figure 2.3B-F)**. In fact, the AAV9-FLAG-MANF completely restored these cardiac parameters to those seen in WT mice. Thus, it is the depletion of endogenous MANF in the MANF KD mouse hearts that results in their greater I/R injury and decreased cardiac function.

Discussion

The Glembotski lab has previously demonstrated that during ischemia, ATF6 up-regulates genes that encode ER-resident chaperones, such as GRP78 and GRP94, which are protective by contributing to ER protein folding, and we have shown that during I/R, ATF6 up-regulates genes encoding antioxidant proteins, such as catalase which neutralize ROS generated during reperfusion injury[4, 5]. Here, *in vivo* it was observed that MANF loss of function decreases myocyte viability and cardiac function following I/R injury, and that ectopic re-expression of MANF was sufficient to reverse the effect of MANF loss of function in the heart. Additionally, the acute nature of the ex vivo experiments performed in this study reveals important aspects of MANF function in the adult mammalian heart. Specifically, ex vivo experiments allow interrogation of the function of MANF without the long term effects of I/R injury such as genetic reprogramming that occurs at the site of injury; furthermore, the observation that MANF loss of function increases cardiac damage in this model of I/R injury indicates that MANF expressed at baseline is protective against necrotic cell death (**Figure 2.2, 2.3**)[5].

During necrotic cell death, ROS generated at the mitochondria are what orchestrates cellular necrosis. While ROS generated at the mitochondria can damage electron transport machinery, impairing OxPhos-mediated ATP generation, they can also damage ER/SR-resident Ca^{2+} handling proteins including SERCA, IP3R, and RyR. Impairment function of Ca^{2+} handling results in mitochondrial accumulation of calcium, further contributing to ROS generation at the

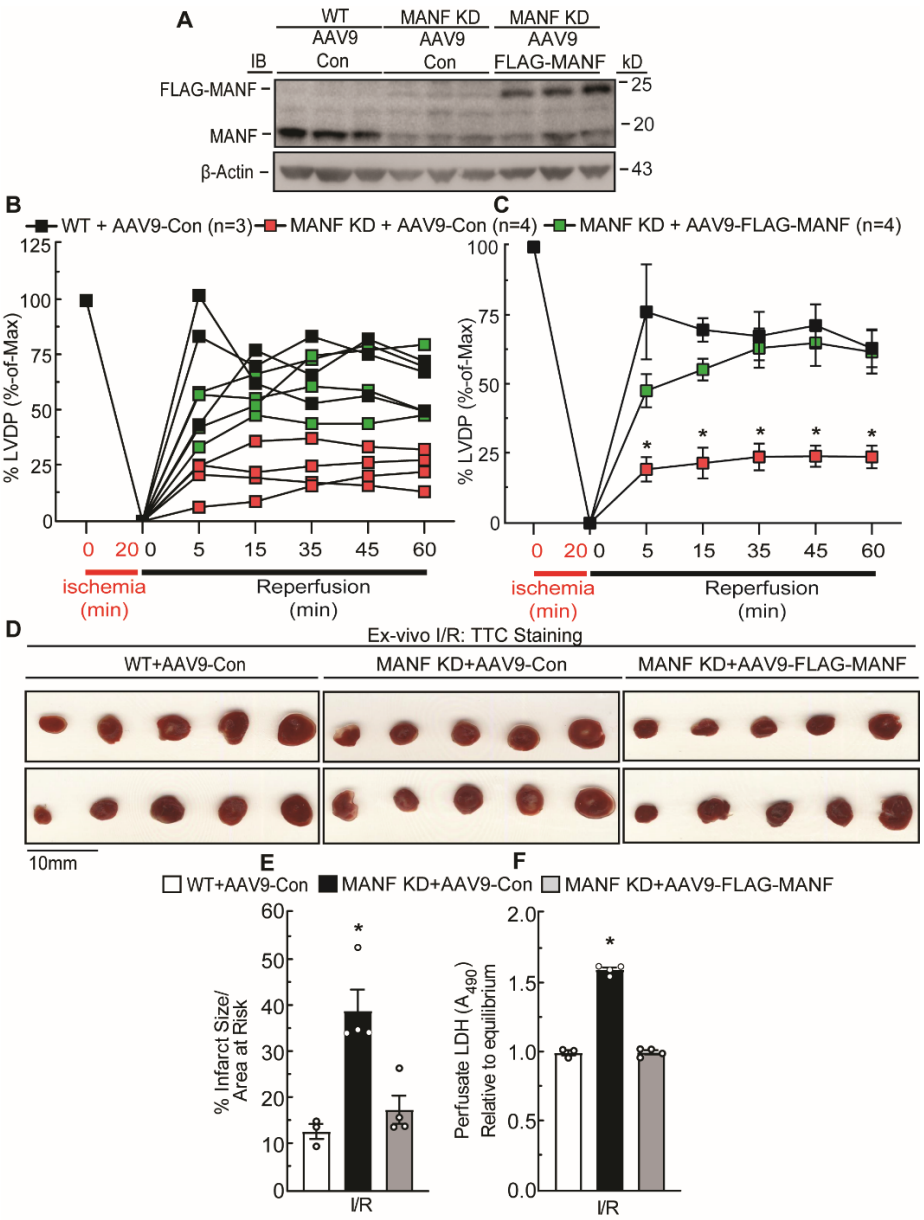

Figure 2.3: Effect of MANF re-expression in MANF KD mouse hearts on cardiac damage and contractility following I/R. AAV9-Con or AAV9-FLAG-MANF was administered to WT and MANF KD mice by tail vein injection. Seven days later, male hearts were extracted and subjected to MANF and β-actin immunoblotting (**A**), and female hearts were subjected to ex vivo I/R (**B**–**F**). For ex vivo I/R, hearts from WT mice injected with AAV-Con (n=3) or MANF KD mice injected with AAV-Con (n = 4) or AAV-FLAG-MANF (n = 4) were subjected to 20 min of ex vivo global ischemia and then 60 min of reperfusion. **B** and **C**, LVDP upon reperfusion was normalized to the LVDP obtained during equilibration, the latter of which was set to 100%. **B**, plot of individual LVDP time courses from different mouse hearts. **C**, average of the plots shown in **B**. **D** and **E**, heart sections were stained with TTC to assess myocardial damage (**D**); shown is the average infarct size divided by area at risk (**E**). **F**, samples of perfusate were obtained after 45 min of reperfusion to assess LDH activity relative to LDH activity in the equilibrium perfusate. *, statistically significant difference from all other groups by two-way ANOVA followed by Tukey's post hoc analysis, $p \leq 0.05$. These experiments were performed twice using separate cohorts of mice. Error bars, S.E.M.

mitochondria. Accumulation of ROS at the mitochondria ultimately leads to mitochondrial permeability transitions pore opening and complete collapse of mitochondrial membrane potential and initiation of cellular necrosis, characterized in part by uncontrolled release of intracellular proteins such as LDH (**Figure 2.2E, 2.3F**) into the extracellular space. As MANF resides in the ER as indicated by the presence of an ER retention signal[19], MANF likely exerts its cardioprotective function in the ER. One potential way MANF could be protective against necrotic cell death is by maintaining optimal function of Ca^{2+} handling proteins during I/R injury i.e. the lack of MANF may impair the activity of ER/SR localized calcium handling proteins. Future experiments will be needed to interrogate the MANF interactome for calcium handling proteins and assess the functional consequences of these interactions.

Most if not all co-translationally translocated ER/SR proteins interact with GRP78 as part of their folding and maturation[20], which likely includes calcium handling proteins like SERCA, IP3R, and RyR. Furthermore, it has been established that MANF directly interacts with GRP78[19, 21], thus it's possible that MANF may modulate the folding activity of GRP78 when GRP78 is bound to Ca^{2+} handling proteins, and loss of MANF may result in suboptimal folding of calcium handling proteins by GRP78. Additionally, MANF forms a calcium dependent complex with GRP78[19] and in future studies it might be illuminating to discern whether MANF loss of function alters the basal ER/SR and cytosolic calcium concentration, which is to say, MANF loss of function may affect calcium handling in cardiac myocytes both by affecting the function of calcium handling proteins and/or altering the calcium storage capacity of the ER/SR, in turn priming cardiac myocytes for necrosis and ultimately decreased cardiac function.

References

1. Glembotski, C.C., Roles for the sarco-/endoplasmic reticulum in cardiac myocyte contraction, protein synthesis, and protein quality control. Physiology (Bethesda), 2012. **27**(6): p. 343-50.

2. Gidalevitz, T., F. Stevens, and Y. Argon, Orchestration of secretory protein folding by ER chaperones. Biochim Biophys Acta, 2013. **1833**(11): p. 2410-24.

3. Thuerauf, D.J., M. Marcinko, N. Gude, M. Rubio, M.A. Sussman, and C.C. Glembotski, Activation of the unfolded protein response in infarcted mouse heart and hypoxic cultured cardiac myocytes. Circ Res, 2006. **99**(3): p. 275-82.

4. Doroudgar, S., D.J. Thuerauf, M.C. Marcinko, P.J. Belmont, and C.C. Glembotski, Ischemia activates the ATF6 branch of the endoplasmic reticulum stress response. J Biol Chem, 2009. **284**(43): p. 29735-45.

5. Jin, J.K., E.A. Blackwood, K. Azizi, D.J. Thuerauf, A.G. Fahem, C. Hofmann, R.J. Kaufman, S. Doroudgar, and C.C. Glembotski, ATF6 Decreases Myocardial Ischemia/Reperfusion Damage and Links ER Stress and Oxidative Stress Signaling Pathways in the Heart. Circ Res, 2017. **120**(5): p. 862-875.

6. Koritzinsky, M., F. Levitin, T. van den Beucken, R.A. Rumantir, N.J. Harding, K.C. Chu, P.C. Boutros, I. Braakman, and B.G. Wouters, Two phases of disulfide bond formation have differing requirements for oxygen. J Cell Biol, 2013. **203**(4): p. 615-27.

7. Lodish, H.F. and N. Kong, The secretory pathway is normal in dithiothreitol-treated cells, but disulfide-bonded proteins are reduced and reversibly retained in the endoplasmic reticulum. J Biol Chem, 1993. **268**(27): p. 20598-605.

8. Blackwood, E.A., K. Azizi, D.J. Thuerauf, R.J. Paxman, L. Plate, J.W. Kelly, R.L. Wiseman, and C.C. Glembotski, Pharmacologic ATF6 activation confers global protection in widespread disease models by reprograming cellular proteostasis. Nat Commun, 2019. **10**(1): p. 187.

9. Stauffer, W.T., A. Arrieta, E.A. Blackwood, and C.C. Glembotski, Sledgehammer to Scalpel: Broad Challenges to the Heart and Other Tissues Yield Specific Cellular Responses via Transcriptional Regulation of the ER-Stress Master Regulator ATF6alpha. Int J Mol Sci, 2020. **21**(3).

10. Haze, K., H. Yoshida, H. Yanagi, T. Yura, and K. Mori, Mammalian transcription factor ATF6 is synthesized as a transmembrane protein and activated by proteolysis in response to endoplasmic reticulum stress. Mol Biol Cell, 1999. **10**(11): p. 3787-99.

11. Belmont, P.J., W.J. Chen, M.N. San Pedro, D.J. Thuerauf, N. Gellings Lowe, N. Gude, B. Hilton, R. Wolkowicz, M.A. Sussman, and C.C. Glembotski, Roles for endoplasmic reticulum-associated degradation and the novel endoplasmic reticulum stress response gene Derlin-3 in the ischemic heart. Circ Res, 2010. **106**(2): p. 307-16.

12. Blackwood, E.A., C. Hofmann, M. Santo Domingo, A.S. Bilal, A. Sarakki, W. Stauffer, A. Arrieta, D.J. Thuerauf, F.W. Kolkhorst, O.J. Muller, T. Jakobi, C. Dieterich, H.A. Katus, S. Doroudgar, and C.C. Glembotski, ATF6 Regulates Cardiac Hypertrophy by Transcriptional Induction of the mTORC1 Activator, Rheb. Circ Res, 2019. **124**(1): p. 79-93.

13. Martindale, J.J., R. Fernandez, D. Thuerauf, R. Whittaker, N. Gude, M.A. Sussman, and C.C. Glembotski, Endoplasmic reticulum stress gene induction and protection from

ischemia/reperfusion injury in the hearts of transgenic mice with a tamoxifen-regulated form of ATF6. Circ Res, 2006. **98**(9): p. 1186-93.

14. Petrova, P., A. Raibekas, J. Pevsner, N. Vigo, M. Anafi, M.K. Moore, A.E. Peaire, V. Shridhar, D.I. Smith, J. Kelly, Y. Durocher, and J.W. Commissiong, MANF: a new mesencephalic, astrocyte-derived neurotrophic factor with selectivity for dopaminergic neurons. J Mol Neurosci, 2003. **20**(2): p. 173-88.

15. Glembotski, C.C., Functions for the cardiomyokine, MANF, in cardioprotection, hypertrophy and heart failure. J Mol Cell Cardiol, 2011. **51**(4): p. 512-7.

16. Tsujita, Y., T. Kato, and M.A. Sussman, Evaluation of left ventricular function in cardiomyopathic mice by tissue Doppler and color M-mode Doppler echocardiography. Echocardiography, 2005. **22**(3): p. 245-53.

17. Thuerauf, D.J., H. Hoover, J. Meller, J. Hernandez, L. Su, C. Andrews, W.H. Dillmann, P.M. McDonough, and C.C. Glembotski, Sarco/endoplasmic reticulum calcium ATPase-2 expression is regulated by ATF6 during the endoplasmic reticulum stress response: intracellular signaling of calcium stress in a cardiac myocyte model system. J Biol Chem, 2001. **276**(51): p. 48309-17.

18. Doroudgar, S., M. Volkers, D.J. Thuerauf, M. Khan, S. Mohsin, J.L. Respress, W. Wang, N. Gude, O.J. Muller, X.H. Wehrens, M.A. Sussman, and C.C. Glembotski, Hrd1 and ER-Associated Protein Degradation, ERAD, are Critical Elements of the Adaptive ER Stress Response in Cardiac Myocytes. Circ Res, 2015. **117**(6): p. 536-46.

19. Glembotski, C.C., D.J. Thuerauf, C. Huang, J.A. Vekich, R.A. Gottlieb, and S. Doroudgar, Mesencephalic astrocyte-derived neurotrophic factor protects the heart from ischemic damage and is selectively secreted upon sarco/endoplasmic reticulum calcium depletion. J Biol Chem, 2012. **287**(31): p. 25893-904.

20. Alder, N.N., Y. Shen, J.L. Brodsky, L.M. Hendershot, and A.E. Johnson, The molecular mechanisms underlying BiP-mediated gating of the Sec61 translocon of the endoplasmic reticulum. J Cell Biol, 2005. **168**(3): p. 389-99.

21. Yan, Y., C. Rato, L. Rohland, S. Preissler, and D. Ron, MANF antagonizes nucleotide exchange by the endoplasmic reticulum chaperone BiP. Nat Commun, 2019. **10**(1): p. 541.

Chapter 3: MANF contributes to ER protein folding during reperfusion injury and reductive stress

Abstract

In the second chapter of this dissertation, it was demonstrated that MANF serves a cardioprotective role in the heart during maneuvers that induce I/R injury. Since ATF6 induces genes that are protective, specifically during ischemia or during reperfusion, and since ATF6 induced MANF, here we examined whether MANF is protective by examining the effects of MANF loss of function on viability of cultured cardiac myocytes during simulated ischemia and simulated ischemia/reperfusion (sI and sI/R). Here, it was observed that MANF is protective during simulated reperfusion; however, its protective function is not through protecting against oxidative stress. Rather, it was observed that MANF maintains ER protein folding during reperfusion injury and is specifically protective against protein misfolding caused by reductive ER stress.

Introduction

During cardiac pathology, proteins that compose cardiac myocytes are subjected to a broad array of conditions that result in ER protein misfolding, leading to compromised myocyte function and contributing to cardiac myocyte death[1-6]. During ischemia/reperfusion, ischemia results in decreased levels of oxygen and nutrients that are required to power the protein folding machinery[3]. Upon reperfusion, the sudden reintroduction of oxygen and nutrients results in oxidative and reductive stresses that directly damage protein structure[5, 7, 8]. During cardiac hypertrophy that occurs in response to increased mechanical loading of the heart e.g. chronic hypertension, protein synthesis increases in cardiac myocytes, resulting in increased cellular levels of nascent unfolded proteins and increased levels of misfolded proteins that must be degraded by cellular protein degradation machinery[2, 4]. Each protein folding challenge myocytes face requires specific protein folding resources to maintain cellular protein folding homeostasis[1]. If these protein folding challenges are not met with the induction of the appropriate protein folding

response, this leads to activation of cell death pathways results in apoptotic and necrotic forms of cell death[5].

The Glembotski laboratory has previously demonstrated that various types of cardiac pathologies activate ATF6, which, in turn, induces genes that protect against specific types of protein folding stressors. This concept is exemplified by the observation that ATF6 induces ER-resident chaperones, such as GRP78, in cardiac myocytes in response to impaired protein glycosylation by the prototypical ER stressor, tunicamycin, or in response to the depletion of ATP and O_2 required for ER protein folding that occurs during ischemia[2, 3]. Interestingly, ATF6 induces the antioxidant, catalase, in myocytes in response to ischemia/reperfusion injury, during which reintroduction of O_2 and nutrients results in oxidative stress, which can result in oxidative damage and misfolding of proteins in the ER, as well as other subcellular compartments[2, 5, 9]. The Glembotski lab also showed that genes induced by ATF6 are stimulus-specific, exemplified by the observation that in cardiac myocytes subjected response to growth stimulus, ATF6 is activated and upregulates Rheb, the key regulator of the growth-promoting mTOR pathway; however, under growth-promoting conditions, activated ATF6 does not upregulate catalase[10]. Additionally, it has been previously reported that ATF6 is activated in response lipotoxic stress, which then induces genes encoding fatty acid oxidation enzymes[11], in further support of the concept that the ATF6 gene program can be fine-tuned in a stress-specific manner.

In the second chapter of this dissertation MANF was shown to be cardioprotective against I/R injury in the heart, but it remains unknown whether MANF exerts its protective function during ischemia or reperfusion. Additionally, it is also unknown how MANF exerts its cardioprotective function. However, the Glembotski lab has previously demonstrated that MANF possesses a canonical ER-retention signal, and that MANF directly interacts with the ATF6-inducible, ER-resident, cardioprotective chaperone GRP78, indicating that MANF may exert its protective function by enhancing ER protein folding[12, 13]. Therefore, here, it was determined whether MANF

is protective during ischemia or reperfusion, and whether MANF loss of function impairs ER proteostasis under specific ER protein folding stress conditions.

Hypothesis: MANF contributes to ER proteostasis during sI/R in a stimulus specific manner.

Aim 1: Assess whether MANF is protective during ischemia or ischemia/reperfusion.

Aim 2: Assess whether MANF contributes to ER proteostasis during sI/R.

Aim 3: Assess whether MANF contributes to ER proteostasis and myocyte viability in a stimulus-specific manner.

Methods

Culturing of neonatal rat ventricular myocytes[4, 5]:

Neonatal rat ventricular myocytes (NRVM) were prepared from 1 to 3-day-old Sprague-Dawley rat hearts using a neonatal cardiomyocyte isolation system (Cat. No. LK003300 Worthington Biochemical Corp.). Myocytes were then purified on a discontinuous Percoll density gradient. Briefly, isolated cells were counted and then collected by centrifugation at 250×g for 5 min in an Eppendorf 5810R using the swinging bucket rotor. 40 to 60 million cells were then resuspended in 2mL 1×ADS buffer (116mM NaCl, 18mM HEPES, 845µM NaHPO4, 5.55mM Glucose, 5.37mM KCl, 831µM MgSO4, 0.002% Phenol Red, pH 7.35±0.5). Stock Percoll was prepared by combining 9 parts of Percoll (cat# 170891-02, GE healthcare, Piscataway, NJ) with 1 part of clear (without phenol red) 10×ADS. The stock Percoll was used to make the Percoll for the top (density= 1.059g/mL; 1 part Percoll stock added to 1.2 parts clear 1×ADS) and bottom (density= 1.082g/mL; 1 part Percoll stock added to 0.54 parts red 1×ADS) layers. The gradient, consisting of 4mL top Percoll and 3mL bottom Percoll, was set in a 15mL conical tube by pipetting the top Percoll first, and layering the bottom Percoll gently underneath, and the cells (in 2mL red 1×ADS buffer) were layered on the top. Subsequently, the Percoll gradient was centrifuged at 1500×g for 30 minutes with no deceleration brake at 4°C. The isolated myocytes, which concentrated in the layer located between the lower red ADS layer and the middle clear ADS

layer, were carefully collected and washed twice with 50mL of 1×ADS and were then resuspended in plating medium and counted. This procedure is also effective for purifying myocytes that have been isolated by trypsin digestion, as previously described[14]. Following Percoll purification, myocytes were plated at the desired density on plastic culture plates that had been pre-treated with 5µg/mL fibronectin in Dulbecco's modified Eagle's medium (DMEM)/F:12 (cat# 11330-32, Invitrogen, Carlsbad, CA) at 37°C for one hour in a 5% CO_2 incubator. Cultures were then maintained in (DMEM)/F:12, supplemented with 10% FBS and antibiotics (100units/mL penicillin and 100µg/mL streptomycin).

NRVM plating density:

In experiments where cell viability was assessed by MTT assay, NRVM were plated at $7.5x10^4$ cells/well on 48-well dishes with 250µL culture medium/well (Corning, Cat. No. 3548; 0.95cm² growth area per well). For all other experiments NRVM were plated at $6x10^5$ cells/well on 12-well dishes with 1mL culture medium/well (Corning, Cat. No. 3513; 3.8cm² growth area per well).

siRNA Transfection of Neonatal Rat Ventricular Myocytes

Twenty-four hours after plating, NRVM were transfected with control siRNA (Integrated DNA Technologies (IDT), Negative Control siRNA Cat. No. 51-01-14-04) or siRNA targeting the *Manf* mRNA (Integrated DNA Technologies (IDT) siRNA, 3'UTR custom synthesis). In brief, siRNAs were diluted to a concentration of 120nM in (DMEM)/F:12 supplemented with v/v 0.5% FBS and 0.675% HiPerfect reagent (Qiagen, Cat No./ID: 301704) without antibiotics. The resulting solutions were incubated for 15 minutes at room temperature (21ºC). NRVM were incubated with the relevant siRNA solutions for 16 hours (125µL/well on 48-well plates, 500 µL/well on 12-well plates) after which the medium was changed to (DMEM)/F:12 supplemented with 2% FBS and antibiotics (250µL/well on 48-well plates, 1mL/well on 12-well plates) for 72 hours, after which cultures were subjected to ER stress treatments, simulated ischemia, or

simulated ischemia/reperfusion.

Manf siRNA sequence: 5'-UGGGCUCCUGACAAUGAGAUGUGAA-3'

siRNAs were dissolved in molecular grade H_2O to a 20μM stock concentration.

Simulated Ischemia/reperfusion[3]:

To simulate ischemia, NRVM cultures ($6x10^5$ cells/well on 12-well culture dishes) were washed twice with pre-warmed (37°C) 0.5mL of serum-free and glucose-free DMEM (ThermoFisher Scientific Cat. No. A1443001) supplemented with antibiotics; after washing, cultures were incubated in 1mL of serum-free and glucose-free DMEM with antibiotics at 0.1% O_2 for 6-12 hours in a hypoxia chamber with an oxygen controller. Parallel control cultures were maintained at ~20–21% O_2 in serum-free and glucose-free DMEM supplemented with antibiotics and 17.5mM glucose. To simulate reperfusion, serum-free and glucose-free medium was replaced with DMEM/F:12, supplemented with 1mg/mL bovine serum albumin (Sigma-Aldrich, Cat. No. A6003) and antibiotics for 1-24 hours and incubated at ~20–21% O_2.

Intracellular reactive oxygen species measurement[5]:

The levels of intracellular ROS were determined with the CellROX Orange fluorescent dye (Thermo Fisher Cat. No. C10443). After 8hr of sI and 1Hr R, NRVM were incubated with 5 μM CellROX Orange for 20 min at 37°C in DMEM/F:12, supplemented with 1mg/mL bovine serum albumin (Sigma-Aldrich, Cat. No. A6003) and antibiotics, and then washed 3 times with PBS (1mL/well). PBS was replaced with DMEM/F:12 supplemented with 1mg/mL bovine serum albumin (Sigma-Aldrich, Cat. No. A6003) and antibiotics. Cultures were then imaged using an IX70 fluorescence microscope (Olympus, Melville, NY). Fluorescence intensity in a field was measured with ImageJ software, which was normalized to the number of cells in that field to yield the mean cell fluorescence.

NRVM Cell Death Assay[3]:

Following sI (12 h) and sI/R (6h sI, 24 h R) treatment, 2µL of a 10mg/mL propidium iodide (PI) stock solution and 1uL of a 1mg/mL stock solution of Hoescht 33342 were added to 22µL of DPBS. The total 25µL were then added direction to a well of a 12-well culture dish which were then incubated for no more than 5 minutes at 37ºC. Cultures were then imaged using an IX70 fluorescence microscope (Olympus, Melville, NY). Numbers of PI and Hoescht positive cells were counted using ImageJ. For cultures subjected to simulated ischemia alone, we observed that it was important to keep the imaging time under 30 minutes so as to prevent increased cell death from the rapid onset of reperfusion injury[15].

NRVM Cell Viability Assay Following ER stress or H_2O_2 treatments[4]**:**

Following siRNA transfection, medium from NRVM plated on 48-wells was replaced with DMEM/F:12 supplemented with antibiotics and 10-20µg/mL tunicamycin (TM), 4µM thapsigargin (TG), 2mM dithiothreitol (DTT) (250µL/well) for 12-24 hours, or 180µM H_2O_2 for 5 hours. Following treatment, culture medium was replaced with fresh 250µL/well DMEM/F:12 supplemented with antibiotics and 180µg/mL 3-(4,5-Dimethylthiazol-2-yl)-2,5-diphenyltetrazolium bromide (MTT) labeling reagent (Millipore-Sigma/Roche Cat. No. 11465007001**)** from a 5 mg/ml stock solution using phosphate buffered saline (PBS). Cultures were incubated for a further four hours at 37°C. The MTT-containing medium was manually pipetted away from the wells and 50 µL of DMSO was added to each culture well. The absorbance at 560nm of the resulting solution was measured on a clear round bottom 96-well plates using a VersaMax microplate reader.

Plasmid Generation:

Construct 1: pcDNA3.1(-) Mouse MANF

The open reading frame of mouse Manf (NM_029103) was amplified by PCR and then ligated into the XhoI and HindIII sites of multiple cloning site of pcDNA3.1(-).

Construct 2: pcDNA3.1(-) Mouse MANF signal sequence

Using construct 1 as a template, PCR was carried out to introduce a NheI restriction site and Kozak sequence, and an ApaI restriction site, into the 5' and 3' ends respectively of the PCR amplified product coding for the signal sequence MWATRGLAVALALSVLPDSRA. This PCR product and pcDNA3.1(-) were digested with NheI and ApaI and ligated together. The ApaI site is immediately followed by sequential XbaI and XhoI restriction sites.

Construct 3: pcDNA3.1(-) 3x-FLAG:

A version of pcDNA3.1(-) containing an N-terminal 3x-FLAG sequence was constructed by annealing the following oligonucleotides:

5'ctagcGCC**ATGGACTACAAAGACCACGACGGTGATTATAAAGATCACGATATCGATTACA**
AGGATGACGATGACAAGt-3'

5'-ctaga**CTTGTCATCGTCATCCTTGTAATCGATATCGTGATCTTTA-**
TAATCACCGTCGTGGTCTTTGTAGTCCATGGCg-3'

The NheI and XbaI overhangs of the annealed oligonucleotides were used to ligate the product into the XbaI site of pcDNA3.1(-), resulting in the creation of 3x FLAG-pcDNA3.1, as previously described[16].

Construct 4: pcDNA3.1(-) Mouse MANF signal sequence + 3x-FLAG.

Using **construct 3** as a template, PCR was performed to introduce XbaI and XhoI sites to the 5' and 3' ends, respectively, of the region coding for the 3x-FLAG tag, DYKDHDGDYKDHDIDYKDDDDK. This PCR product and **construct 2** were digested with XbaI and XhoI and ligated together to create a construct encoding the MANF signal sequence followed by 3x-FLAG.

Construct 5: pcDNA3.1(-) Mouse MANF signal sequence + 3x-FLAG + $MANF_{WT}$ (referred to hereafter as FLAG-$MANF_{WT}$)

Using construct 1 as a template, PCR was performed with the following primers:

5’GGAACG**CTCGAG**CTGCGGCCAGGAGAC-3’

5’-GGAGCTGACACGGAAGAT-3’ (pcDNA 3.1(-) reverse primer)

The resulting PCR product and **construct 4** were digested with XhoI and HindIII and ligated together to generate a construct encoding the MANF signal sequence followed by 3x-FLAG and MANF, with the following amino acid sequence:

MWATRGLAVALALSVLPDSRAGPSRDYKDHDGDYKDHDIDYKDDDDKLELRPGDCEVCISYL
GRFYQDLKDRDVTSSPATIEEELIKFCREARGKENRLCYYIGATDDAATKIINEVSKPLAHHIPVE
KICEKLKKKDSQICELKYDKQIDLSTVDLKKLRVKELKKILDDWGEMCKGCAEKSDYIRKINELM
PKYAPKAASARTDL

Construct 6: pcDNA3.1(-) 3x-HA

A version of pcDNA3.1(-) encoding a C-terminal 3x-HA sequence was constructed by sequential annealing and ligating the following oligonucleotides into pcDNA3.1(-).The first set of oligonucleotides were annealed and digested with EcoR1 and BamH1 before ligation into pcDNA3.1(-) to generate a form of pcDNA3.1(-) encoding a C-terminal 1x-HA:

5'-GAATTCTACCCATACGATGTTCCAGATTACGCTTAATGAGGATCC-3'

5'-GGATCCTCATTAAGCGTAATCTGGAACATCGTATGGGTAGAATTC-3'

The second set of oligonucleotides were annealed and directly ligated into the EcoR1 site into the above vector pcDNA3.1(-) encoding a C-terminal 1x-HA:

5'-AATTCTATCCGTATGACGTACCTGACTATGCGGGCTATCCCTATGACGTGCCG-
GACTATGCAC-3'

5'-AATTGTGCATAGTCCGGCACGTCATAGGGATAGCCCGCATAGTCAGGTACGTCA-
TACGGATAG-3'

Construct 7 and 8: α1 Antitrypsin (α1AT).

A construct encoding human α-1 antitrypsin (A1AT, NCBI RefSeq NM_000295) was generated by PCR using the appropriate primers to create an amplicon with Xho1 on the 5' end of the start site, and a termination codon and EcoRI on the 3' end. This PCR product was cloned into the pCDNA3.1 vector (**Construct 7**) or pcDNA3.1 vector modified to encode a C-terminal 3x-HA epitope (**Construct 8**).

Construct 9 and **10**:

To generate constructs encoding Mutant α-1Antitrypsin[17], α1AT ΔCT (**Construct 9**) and α1AT-HA ΔCT (**Construct 10**), site directed mutagenesis was performed with the following primers:

5'-CAATGGGGCTGACCTCCGGGGTCACAG-3'

5'-CTGTGACCCCGGAGGTCAGCCCCATTG-3'

Adenovirus (AdV) generation and NRVM infection:

The AdEasy system was used for preparing recombinant adenoviral strains using previously described methods[2, 3]. Recombinant Adv encoding FLAG-MANF$_{WT}$ was produced by excising the coding region of FLAG-MANF$_{WT}$ (**constructs 5**, above) then ligating it into a version of the adenovirus shuttle vector, pAdTrack-CMV, that does not contain the GFP coding region. Recombinant Adv encoding α1AT ΔCT was produced by excising the coding region of α1AT ΔCT (**constructs 9**, above) then ligating them into a version of the adenovirus shuttle vector, pAdTrack-CMV containing the GFP coding region. pAdTrack-CMV-FLAG-MANF$_{WT}$ and pAdTrack-CMV-α1AT ΔCT[17] were linearized and then co-transformed with the adenoviral vector, pAdEasy-1, into E. coli strain BJ5183. This strain of E. coli allows for homologous recombination of pAdEasy-1 and the pAdTrack-CMV shuttle vector containing the gene of interest. Recombinants were selected on kanamycin and screened by restriction digestion with PacI.

Recombinant plasmids were then retransformed into E. coli DH5α for propagation purposes. To generate recombinant adenoviruses, these recombinant adenoviral plasmids were linearized with PacI and then transfected into 293 human embryonic kidney cells using LipofectAMINE® (Life Technologies, Inc.). The recombinant viruses were then harvested 7–10 days post-infection. Viral titers were determined by qPCR as compared to a virus of a known titer. NRVM cultures were infected with the relevant Adv by diluting it into DMEM/F12 containing 2% FBS, penicillin/streptomycin. NRVM cultures were incubated with the relevant virus solutions solutions for 24 hours (500 µL/well on 12-well plates) after which the medium was changed to (DMEM)/F:12 supplemented with 2% FBS and antibiotics (250µL/well on 48-well plates, 1mL/well on 12-well plates) for 24 hours, after which cultures were subjected to ER stress treatments.

Immunoblotting:

Medium was removed from 12-well culture dishes and adherent cells were washed with ice-cold DPBS and then lysed with 60-100µL of cell lysis buffer composed of 20mM Tris (pH 7.5), 150mM NaCl, 1% Triton X-100, 0.1% SDS, 1x protease/phosphatase inhibitor mixture (Roche Applied Science; Catalog No. 05892791001 and 4906837001). Lysates were scraped and transferred to microcentrifuge tubes and stored at -80°C. Following determination of protein concentration of clarified cell or tissue extracts using the BCA protein assay kit (Bio-Rad, Cat. No. 5000111), between 5 and 40µg of protein extracts or 25µL of cell culture medium were subjected to reducing SDS-PAGE then electroeluted onto PVDF membranes. Membranes were blocked for 30 minutes at room temperature in 5% non-fat instant dry milk dissolved in Tris-buffered saline containing 150mM NaCl, 2.68mM KCl, 50 mM Tris-pH 7.5, 0.1% Tween (TBST) with gentle rocking. Membranes were probed with rabbit MANF antiserum, at 1:1000 (Anti-ARMET, Cat. No. ab67203, Abcam; Anti-MANF, Cat. No. SAB3500384, Sigma-Aldrich), a mouse KDEL antiserum at 1:8000 (ENZO Life Sciences; Cat. No. ADI-SPA-827), a mouse FLAG antibody at 1:8000 (Sigma-Aldrich; Cat. No. F1804), an HMGB1 antiserum at 1:1000 (Abcam Cat. No. 18256), an

HA antibody at 1:1000 (Santa Cruz Cat. No. sc-7392), an α1AT antiserum at 1:2000 (Dako Cat No. A0012), a PARP antiserum at 1:1000 (Cell Signaling, Cat. No. 9542) and a mouse GAPDH antiserum at 1:6,000,000 (Fitzgerald, Cat. No. 10R-G109a). Antibodies were diluted in 5% milk dissolved in TBST. Membranes were incubated with antibody solutions for 12-16 hours at 4°C. Membranes were then washed 3 times for 15 minutes in TBST and then incubated for 1 hour at room temperature with the appropriate horseradish peroxidase–conjugated anti-IgG (Jackson ImmunoResearch Laboratories, Inc.) diluted at 1:2000 in 5% milk dissolved in TBST. Membranes were then washed 3 times for 15 minutes with gentle rocking in TBST and subjected to enhanced chemiluminescence and exposed to autoradiography film or imaging using an ImageQuant 4000 from GE Healthcare Life Sciences. Immunoblots were quantified using ImageJ software densitometry.

FLAG immunoprecipitation Following ER Stress Treatments:

HeLa Cells were maintained in DMEM supplemented with 10% FBS and antibiotics not allowing confluency to surpass 80%. HeLa cells were resuspended at $6x10^6$ cells/400 µl of ice-cold Dulbecco's PBS and electroporated with 1-20µg of the relevant plasmids in a 0.4-cm gap electroporation cuvette at 250 V and 950 microfarads using a GenePulser II Electroporator (Bio-Rad). The cells were then plated at a density of $3x10^6$ cells on a 10cm dishes and incubated for 24 h in DMEM supplemented with 10% FBS and antibiotics. Transfected HeLa cell cultures were then treated for 1 h with vehicle or 2.5 mM DTT in serum-free DMEM/F-12 supplemented with antibiotics. NRVMs plated at $1x10^6$ cells per well on 6-well culture dishes were incubated with the relevant adenoviruses suspended in DMEM/F:12 supplemented with 2% FBS and antibiotics for 24 h. NRVMs were then treated for 1 h with vehicle, 2µM TG, or 2.5 mM DTT in serum-free DMEM/F-12 supplemented with antibiotics. The culture media containing TG or DTT was then removed and cultures were briefly washed with ice-cold DPBS containing 20mM N-ethyl maleimide (NEM; Sigma-Aldrich, Cat. No. E376). Cultures were then lysed with cell lysis buffer

composed of 20mM Tris (pH 7.5), 150mM NaCl, 1% Triton X100, 20mM NEM, and 1x protease/phosphatase inhibitors. The resulting cell lysates were then clarified by centrifugation at 20,000xg. Between 80 and 200µg of clarified protein cell extracts were diluted to 0.5-1µg protein/µL using cell lysis buffer composed of 20mM Tris (pH 7.5), 150mM NaCl, 1% Triton X100, 20mM NEM, and 1x protease/phosphatase inhibitors (maximum volume of 200µL in 1.5mL microcentrifuge tubes). 1µg of FLAG antibody (Sigma-Aldrich; Cat. No. F1804) was added to the resulting solutions which were then gently rocked overnight (~16 hours) at 4°C. To this mixture, 20µL of protein A agarose beads (ThermoFisher, Cat. No. 20333, 50% slurry) that had been prewashed with ice-cold lysis buffer (20mM Tris (pH 7.5), 150mM NaCl, 1% Triton X100) were added to each microcentrifuge tube. The resulting mixture was gently rocked for 2 hours at 4°C. The beads were sedimented to the bottom of the microcentrifuge tubes by centrifugation at 4000xg for 1-2 minutes at 4°C. The supernatant removed with a 1mL pipetteman without disrupting the sedimented beads. The beads were then washed with 1mL of ice-cold lysis buffer and sedimented by centrifugation at 4000xg for 1-2 minutes 4°C. This process was repeated 2 more times. To elute the FLAG-immunoprecipitated complexes, the isolated beads were incubated with 30µL cell lysis buffer composed of 20mM Tris (pH 7.5), 150mM NaCl, 1% Triton X100, 1x protease/phosphatase inhibitors, and 300µg/mL FLAG peptide. The resulting mixture was gently rocked for 3 hours at 4°C, and the eluate was separated from the beads by centrifugation at 4000xg for 1-2 minutes at room temperature (21°C). The eluates were then subjected to reducing or non-reducing SDS-PAGE on a 4-12% gradient polyacrylamide gel and then electroeluted onto PVDF membranes. Membranes were blocked for 30 minutes at room temperature in 5% non-fat instant dry milk dissolved in TBST with gentle rocking. Membranes were probed with a mouse FLAG antibody at 1:8000 (Sigma-Aldrich; Cat. No. F1804), an HA antibody at 1:1000 (Santa Cruz Cat. No. sc-7392), or an α1AT antiserum at 1:2000 (Dako Cat No. A0012).

Results

MANF improves ER proteostasis during reperfusion injury

In the second chapter of this dissertation, it was demonstrated that MANF loss of function decreases myocyte viability and cardiac function following I/R. However, myocyte death can occur during ischemia, and/or reperfusion. Thus, to determine whether MANF could provide protection under one, or both of these conditions, MANF levels were determined in cultured neonatal rat ventricular myocytes (NRVM) subjected to simulated ischemia (sI), or simulated ischemia followed by simulated reperfusion (sI/R). MANF levels increased upon sI and further upon sI/R, suggesting that MANF could contribute to preserving myocyte viability under either, or both conditions (**Figure 3.1A**). To further examine functional roles for MANF, it was knocked down using siRNA **(Figure 3.1B)**. MANF knockdown had no effect on cell death during sI (**Figure 3.1C**); however, MANF knockdown increased necrotic cell death during reperfusion, as indicated by the increased number of propidium iodide (PI)-positive cells (**Figure 3.1D**), the release of HMGB1 into the culture medium during reperfusion (**Figure 3.2A** (**top**))**, Figure 3.2B),** and lack of significant change in PARP cleavage **(Figure 3.2A, 3.2C**). Since cell death in cardiac myocytes can be caused by reactive oxygen species (ROS) generated during reperfusion injury [5, 18], the effects of MANF knockdown on ROS generation during sI/R was examined. Under these conditions, MANF knockdown significantly increased ROS (**Figure 3.2D**).

Since ROS increased when MANF was knocked down in sI/R-treated NRVM, and since the accumulation of cellular ROS can precipitate ER stress[19], the effect MANF knockdown on molecular markers of ER protein misfolding during sI/R was determined. One way to measure ER protein-folding is to examine the levels of ER chaperones, which are known to increase when ER protein-folding is impaired. Indeed, MANF knockdown impaired ER protein-folding during sI/R, as evidenced by increased expression of the ER chaperones GRP94, GRP78, and PDIA6 (**Figure 3.2A (lower) and 3.2E**). Thus, endogenous MANF enhances myocyte viability, at least partly by

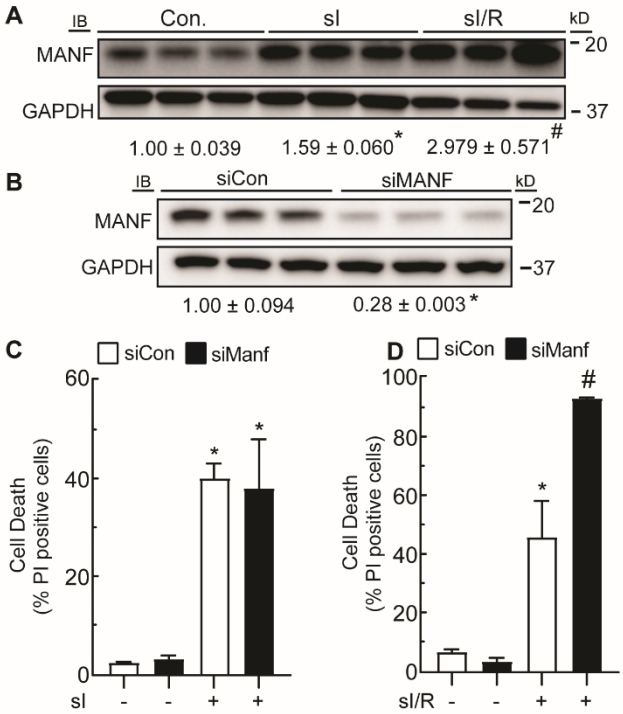

Figure 3.1: Effect of sI and sI/R on MANF expression and the effect of MANF knockdown on myocyte death during sI and sI/R. A, immunoblots of MANF and GAPDH from NRVMs subjected to 8 h of sI or 8 h of sI followed by 24 h of simulated reperfusion (sI/R). Band intensities were normalized to those for GAPDH and displayed as fold of control level ± SEM *, statistically significant difference from control by Student's unpaired t test, $p \leq 0.05$. #, statistically significant difference from all other groups by one-way ANOVA followed by Newman–Keuls post hoc analysis. **B**, immunoblots of MANF and GAPDH from NRVMs transfected with siCon or siManf demonstrating MANF knockdown. Band intensities were normalized to those for GAPDH and displayed as fold of control. *, statistically significant difference by Student's unpaired t test, $p \leq 0.05$. **C** and **D**, siCon- or siManf-transfected NRVMs were subjected to 12 h of sI (**C**) or 6 h of sI followed by 24 h of reperfusion (sI/R) (**D**), and percentage cell death was assessed by staining cell cultures with Hoechst 33342 and PI and dividing the number of PI-positive cells by the number of Hoechst-positive cells in a given field. * and #, statistically significant difference from all other groups by two-way ANOVA followed by Tukey's post hoc analysis, $p \leq 0.05$. Error bars, S.E.M.

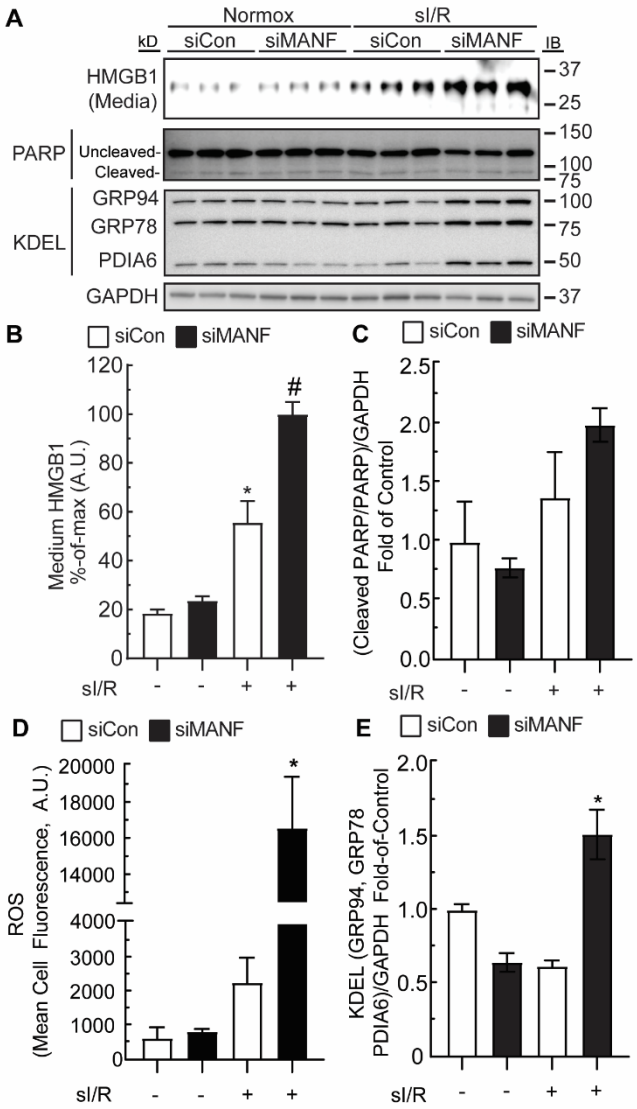

Figure 3.2: Effect MANF knockdown on HMGB1 release into culture medium, PARP cleavage, ROS generation, and expression of ER stress markers during sI/R. A, HMGB1 immunoblots of the culture medium indicating cell death and immunoblots of PARP, GRP94, GRP78, PDIA6, and GAPDH from NRVMs transfected with siCon or siManf and subjected to 6 h of sI followed by 24 h of reperfusion (sI/R). **B**, densitometry of HMGB1 immunoblot shown in **A**.**C**, Densitometry of uncleaved and cleaved PARP immunoblot shown in **A**. The ratio of cleaved to uncleaved PARP signals was normalized to GAPDH and displayed as fold of control. **D**, siCon- or siManf-transfected NRVMs were subjected to sI/R followed by ROS measurement with CellROX. **E**, densitometry of GRP94, GRP78, PDIA6, and GAPDH immunoblots shown in E. Band intensities of GRP94, GRP78, and PDIA6 were normalized to those for GAPDH and displayed as fold of control. * and #, statistically significant difference from all other groups by two-way ANOVA followed by Tukey's post hoc analysis, $p \leq 0.05$. Note that GRP78, GRP94, and PDIA6 immunoblots were performed using an anti-KDEL antibody. Error bars, S.E.M.

contributing to maintaining ER protein-folding during sI/R. Since the increase in ROS upon MANF knockdown might be responsible for increases in protein misfolding and decreases in myocyte viability during sI/R, the effects of MANF knockdown on cell viability in NRVM treated with the ROS-generator, H_2O_2 were examined[5, 18, 20]. While MANF knockdown and H_2O_2 each decreased myocyte viability, when examined together, their effects were approximately additive (**Figure 3.3A**), suggesting that MANF does not directly protect against protein misfolding caused by ROS. The probable independence of the effects of MANF knockdown and H_2O_2 on NRVM viability was further supported by a two-way ANOVA, which statistically demonstrated that MANF knockdown and H_2O_2 independently affected viability. Since MANF-mediated protection of myocytes did not appear to involve mitigating the effects of ROS generated during reperfusion, it was determined whether MANF could protect myocytes against other types of ER protein misfolding that occur during I/R injury.

MANF is protective against reductive stress

While ROS generated during I/R can result in protein misfolding, protein misfolding can also be caused by impaired disulfide bond formation in the ER. Disulfide bonds, formed in nascent ER proteins, are dependent on the presence of oxygen and the optimal redox environment of the ER, which is likely to shift toward a reductive environment during reperfusion, as the ER redox machinery needs time to recover during oxygen reintroduction, much like how mitochondria need time to recover[7, 8, 21-28]. Accordingly, it was determined whether MANF is protective during reductive stress by treating NRVM with the reducing agent, DTT. Additionally, for the sake of comparison to non-reductive forms of ER stress that also occur during I/R[13, 29, 30], NRVM were treated with thapsigargin, which inhibits SERCA, reducing ER Ca^{+2} and causing ER protein-misfolding, or tunicamycin, which impairs ER protein glycosylation required for folding and trafficking of secreted and membrane-bound proteins through the classical secretory pathway[31-33]. MANF knockdown and DTT treatment separately decreased myocyte viability, and together

appeared to synergistically decrease myocyte viability **(Figure 3.3B)**, suggesting that MANF is required for optimal myocyte viability during protein misfolding caused by reductive ER stress. In contrast to DTT, MANF knockdown and TG treatment separately decreased myocyte viability, and when combined, their effects on viability were approximately additive (**Figure 3.3C**), and MANF knockdown had no effect on NRVM viability when under TM treatment (**Figure 3.3D)**.These results suggest that MANF is not required for optimal myocyte viability during protein misfolding caused by non-reductive ER stress. Furthermore, the synergistic effects of MANF knockdown and DTT treatment, and lack thereof with TG or TM treatment, were also supported by a two-way ANOVA.

Next, it was considered whether MANF might bind to misfolded ER proteins and, in so doing, act as a chaperone during reductive stress. Accordingly, to examine whether MANF binds to misfolded ER proteins during reductive stress, NRVM were infected with adenoviruses encoding FLAG-MANF and a known misfolded ER protein, α1-antitrypsin (α1AT ΔCT) [17, 34-36], then treated with TG or DTT. The decreased expression of FLAG-MANF and α1AT ΔCT during treatment with TG and DTT (**Figure 3.3E, FLAG IB, α1AT ΔCT IB)** is probably due to the global repression of translation of mRNAs encoding non-ER stress response genes that takes place during ER stress[3, 37, 38]. When cell lysates were subjected to FLAG immunoprecipitation (IP) followed by FLAG or α1AT ΔCT immunoblotting (IB) it was apparent that MANF co-immunoprecipitated with misfolded α1AT ΔCT, but only upon treatment with DTT and not TG (**Figure 3.3E**). Thus, MANF appears to improve ER protein-folding during DTT-mediated (reductive) ER stress, but not during ER Ca^{+2} depletion-mediated (non-reductive) ER stress. Additionally, these results were also observed in HeLa cells, indicating that MANF also exerts this function in non-cardiac cells (**Figure 3.3F**).

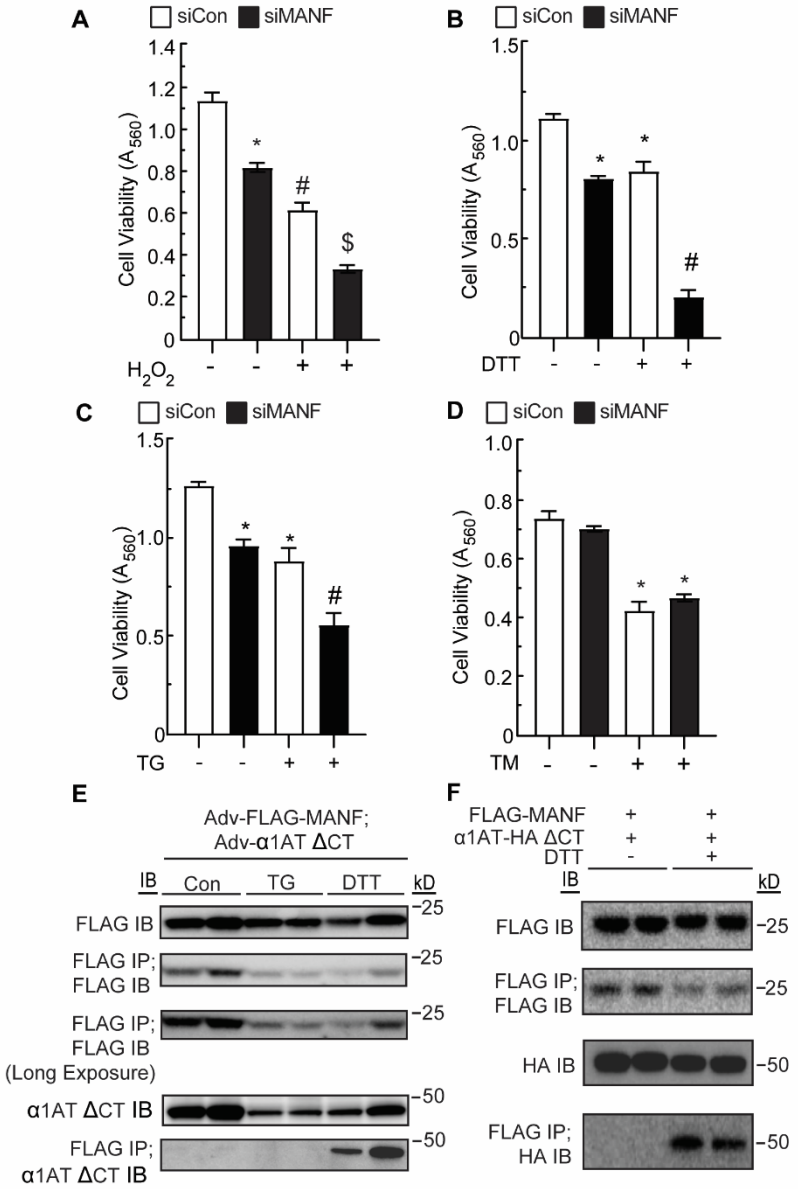

Figure 3.3: Effect of MANF loss of function and pharmacological ER stressors on myocyte viability, effect of TG or DTT on FLAG-MANF and α1AT ΔCT co-immunoprecipitation. **A**–**D**, NRVMs were transfected with siCon or siManf, and after 72 h, cells were treated with H_2O_2 (**A**), DTT(**B**), TG(**C**), TM(**D**), or vehicle. Viability was then assessed by an MTT assay. * and #, statistically significant difference from all other groups by two-way ANOVA followed by Tukey's post hoc analysis, $p \leq 0.05$. **E**, NRVM cultures were co-infected with adenoviruses encoding FLAG-MANF and α1AT ΔCT, as shown, and treated with TG or DTT for 1 h. Cell extracts were subjected to SDS-PAGE followed by immunoblotting for FLAG or α1AT ΔCT. The cell extracts were also subjected to FLAG IP followed by SDS-PAGE and then IB for FLAG or α1AT ΔCT, as shown. **F**, HeLa cell cultures were co-transfected with plasmid constructs encoding FLAG-MANF and/or α1AT-HA ΔCT, as shown. The cell extracts were subjected to SDS-PAGE followed by immunoblotting for HA or FLAG. The cell extracts were also subjected to FLAG IP followed by SDS-PAGE and then IB for FLAG or HA, as shown.

Discussion

In the second chapter of this dissertation, it was observed that MANF loss of function in the adult mammalian heart increases cardiac injury in a model of *ex vivo* I/R injury via increased necrotic cell death. Since the function of MANF to this point was unknown, and ATF6 up-regulates genes that are protective during both phases of I/R injury[3, 5, 9], it was important to dissect during which phase of I/R MANF is protective to further elucidate its function. Here, it was found that MANF was dispensable for cardiac myocyte viability during simulated ischemia, but was critical for myocyte viability following I/R. Additionally, it was observed that MANF knockdown did not sensitize NRVMs to oxidative stress mediated by H_2O_2, suggesting that the protective function of MANF was separate from oxidative stress and ROS generation associated with reperfusion injury. Furthermore, it was found that in combination with MANF knockdown, I/R increased expression of GRP78, GRP94, and another ATF6-inducible chaperone and protein disulfide isomerase, PDIA6[39], demonstrating, for the first time, that MANF exerts its protective function by maintaining ER protein folding specifically during reperfusion.

The Glembotski lab has recently demonstrated that the genes in cardiac myocytes that are induced by ATF6 are stimulus-specific i.e. the ER stress response is tuned depending on what type of ER protein folding challenge the cell is facing[1, 10]. Additionally, it has been demonstrated previously that various components of the ER protein-folding machinery have dedicated roles in maintaining ER protein folding and/or dedicated client proteins in the ER[40]. To determine how MANF could maintain ER protein folding during reperfusion injury, we pharmacologically mimicked nonreductive and reductive ER stress using TG or TM and DTT, respectively[7, 13, 22, 24, 29, 30, 41]. We observed that MANF was required for myocyte viability during reductive ER stress mediated by DTT, but it was dispensable during nonreductive ER stress mediated by TG or TM. Furthermore, we found that MANF forms a complex with the misfolded protein α1AT ΔCT during reductive, but not during nonreductive, ER stress. These results are

consistent with findings from the Glembotski laboratory and others that the ER stress response can be protective in a stimulus-specific manner[1, 10], and demonstrate for the first time that MANF exerts its protective function under the specific proteotoxic stimulus reductive ER stress.

While there is mounting evidence that reductive stress contributes to various types of cardiac pathology[7, 21, 22, 24], it has yet to be elucidated how ER reductive stress contributes to reperfusion injury. However, it has been established in non-cardiac cells that during ischemia, newly synthesized co-translationally translocated proteins that normally undergo oxidative protein folding to achieve their final function conformation are unable to do so as a result of decreased cellular oxygen levels[23, 27]. This results in an accumulation of “reduced” unfolded proteins i.e. that contain free cysteine residues, and upon reperfusion oxidative protein folding can resume. However, the protein folding challenge remains as the ER oxidative protein folding machinery must contend with both accumulated free cysteine-containing proteins, as well as improper/non-native disulfides that form as part of the oxidative protein folding process[26, 28, 31, 34, 42]. These effects are recapitulated with DTT treatment, and future experiments may include assessing what ER-targeted proteins are misfolded during both DTT-mediated reductive stress and sI/R mediated reductive stress and which of them form complexes with MANF.

References

1. Stauffer, W.T., A. Arrieta, E.A. Blackwood, and C.C. Glembotski, Sledgehammer to Scalpel: Broad Challenges to the Heart and Other Tissues Yield Specific Cellular Responses via Transcriptional Regulation of the ER-Stress Master Regulator ATF6alpha. Int J Mol Sci, 2020. **21**(3).

2. Blackwood, E.A., C. Hofmann, M. Santo Domingo, A.S. Bilal, A. Sarakki, W. Stauffer, A. Arrieta, D.J. Thuerauf, F.W. Kolkhorst, O.J. Muller, T. Jakobi, C. Dieterich, H.A. Katus, S. Doroudgar, and C.C. Glembotski, ATF6 Regulates Cardiac Hypertrophy by Transcriptional Induction of the mTORC1 Activator, Rheb. Circ Res, 2019. **124**(1): p. 79-93.

3. Doroudgar, S., D.J. Thuerauf, M.C. Marcinko, P.J. Belmont, and C.C. Glembotski, Ischemia activates the ATF6 branch of the endoplasmic reticulum stress response. J Biol Chem, 2009. **284**(43): p. 29735-45.

4. Doroudgar, S., M. Volkers, D.J. Thuerauf, M. Khan, S. Mohsin, J.L. Respress, W. Wang, N. Gude, O.J. Muller, X.H. Wehrens, M.A. Sussman, and C.C. Glembotski, Hrd1 and ER-Associated Protein Degradation, ERAD, are Critical Elements of the Adaptive ER Stress Response in Cardiac Myocytes. Circ Res, 2015. **117**(6): p. 536-46.

5. Jin, J.K., E.A. Blackwood, K. Azizi, D.J. Thuerauf, A.G. Fahem, C. Hofmann, R.J. Kaufman, S. Doroudgar, and C.C. Glembotski, ATF6 Decreases Myocardial Ischemia/Reperfusion Damage and Links ER Stress and Oxidative Stress Signaling Pathways in the Heart. Circ Res, 2017. **120**(5): p. 862-875.

6. Thuerauf, D.J., M. Marcinko, N. Gude, M. Rubio, M.A. Sussman, and C.C. Glembotski, Activation of the unfolded protein response in infarcted mouse heart and hypoxic cultured cardiac myocytes. Circ Res, 2006. **99**(3): p. 275-82.

7. Yu, Q., C.F. Lee, W. Wang, G. Karamanlidis, J. Kuroda, S. Matsushima, J. Sadoshima, and R. Tian, Elimination of NADPH oxidase activity promotes reductive stress and sensitizes the heart to ischemic injury. J Am Heart Assoc, 2014. **3**(1): p. e000555.

8. Eaton, P., H.L. Byers, N. Leeds, M.A. Ward, and M.J. Shattock, Detection, quantitation, purification, and identification of cardiac proteins S-thiolated during ischemia and reperfusion. J Biol Chem, 2002. **277**(12): p. 9806-11.

9. Blackwood, E.A., K. Azizi, D.J. Thuerauf, R.J. Paxman, L. Plate, J.W. Kelly, R.L. Wiseman, and C.C. Glembotski, Pharmacologic ATF6 activation confers global protection in widespread disease models by reprograming cellular proteostasis. Nat Commun, 2019. **10**(1): p. 187.

10. Glembotski, C.C., A. Arrieta, E.A. Blackwood, and W.T. Stauffer, ATF6 as a Nodal Regulator of Proteostasis in the Heart. Front Physiol, 2020. **11**: p. 267.

11. Tam, A.B., L.S. Roberts, V. Chandra, I.G. Rivera, D.K. Nomura, D.J. Forbes, and M. Niwa, The UPR Activator ATF6 Responds to Proteotoxic and Lipotoxic Stress by Distinct Mechanisms. Dev Cell, 2018. **46**(3): p. 327-343 e7.

12. Glembotski, C.C., Functions for the cardiomyokine, MANF, in cardioprotection, hypertrophy and heart failure. J Mol Cell Cardiol, 2011. **51**(4): p. 512-7.

13. Glembotski, C.C., D.J. Thuerauf, C. Huang, J.A. Vekich, R.A. Gottlieb, and S. Doroudgar, Mesencephalic astrocyte-derived neurotrophic factor protects the heart from ischemic damage and is selectively secreted upon sarco/endoplasmic reticulum calcium depletion. J Biol Chem, 2012. **287**(31): p. 25893-904.

14. Hoover, H.E., D.J. Thuerauf, J.J. Martindale, and C.C. Glembotski, alpha B-crystallin gene induction and phosphorylation by MKK6-activated p38. A potential role for alpha B-crystallin as a target of the p38 branch of the cardiac stress response. J Biol Chem, 2000. **275**(31): p. 23825-33.

15. Vanden Hoek, T.L., Z. Shao, C. Li, R. Zak, P.T. Schumacker, and L.B. Becker, Reperfusion injury on cardiac myocytes after simulated ischemia. Am J Physiol, 1996. **270**(4 Pt 2): p. H1334-41.

16. Thuerauf, D.J., H. Hoover, J. Meller, J. Hernandez, L. Su, C. Andrews, W.H. Dillmann, P.M. McDonough, and C.C. Glembotski, Sarco/endoplasmic reticulum calcium ATPase-2 expression is regulated by ATF6 during the endoplasmic reticulum stress response: intracellular signaling of calcium stress in a cardiac myocyte model system. J Biol Chem, 2001. **276**(51): p. 48309-17.

17. Belmont, P.J., W.J. Chen, M.N. San Pedro, D.J. Thuerauf, N. Gellings Lowe, N. Gude, B. Hilton, R. Wolkowicz, M.A. Sussman, and C.C. Glembotski, Roles for endoplasmic reticulum-associated degradation and the novel endoplasmic reticulum stress response gene Derlin-3 in the ischemic heart. Circ Res, 2010. **106**(2): p. 307-16.

18. Marshall, K.D., M.A. Edwards, M. Krenz, J.W. Davis, and C.P. Baines, Proteomic mapping of proteins released during necrosis and apoptosis from cultured neonatal cardiac myocytes. Am J Physiol Cell Physiol, 2014. **306**(7): p. C639-47.

19. Malhotra, J.D. and R.J. Kaufman, Endoplasmic reticulum stress and oxidative stress: a vicious cycle or a double-edged sword? Antioxid Redox Signal, 2007. **9**(12): p. 2277-93.

20. Siman, R., T.K. McIntosh, K.M. Soltesz, Z. Chen, R.W. Neumar, and V.L. Roberts, Proteins released from degenerating neurons are surrogate markers for acute brain damage. Neurobiol Dis, 2004. **16**(2): p. 311-20.

21. Dimmeler, S. and A.M. Zeiher, A "reductionist" view of cardiomyopathy. Cell, 2007. **130**(3): p. 401-2.

22. Rajasekaran, N.S., P. Connell, E.S. Christians, L.J. Yan, R.P. Taylor, A. Orosz, X.Q. Zhang, T.J. Stevenson, R.M. Peshock, J.A. Leopold, W.H. Barry, J. Loscalzo, S.J. Odelberg, and I.J. Benjamin, Human alpha B-crystallin mutation causes oxido-reductive stress and protein aggregation cardiomyopathy in mice. Cell, 2007. **130**(3): p. 427-39.

23. Chin, K.T., G. Kang, J. Qu, L.B. Gardner, W.A. Coetzee, E. Zito, G.I. Fishman, and D. Ron, The sarcoplasmic reticulum luminal thiol oxidase ERO1 regulates cardiomyocyte excitation-coupled calcium release and response to hemodynamic load. FASEB J, 2011. **25**(8): p. 2583-91.

24. Handy, D.E. and J. Loscalzo, Responses to reductive stress in the cardiovascular system. Free Radic Biol Med, 2017. **109**: p. 114-124.

25. Cuozzo, J.W. and C.A. Kaiser, Competition between glutathione and protein thiols for disulphide-bond formation. Nat Cell Biol, 1999. **1**(3): p. 130-5.

26. Ellgaard, L., C.S. Sevier, and N.J. Bulleid, How Are Proteins Reduced in the Endoplasmic Reticulum? Trends Biochem Sci, 2018. **43**(1): p. 32-43.

27. Koritzinsky, M., F. Levitin, T. van den Beucken, R.A. Rumantir, N.J. Harding, K.C. Chu, P.C. Boutros, I. Braakman, and B.G. Wouters, Two phases of disulfide bond formation have differing requirements for oxygen. J Cell Biol, 2013. **203**(4): p. 615-27.

28. Sevier, C.S. and C.A. Kaiser, Formation and transfer of disulphide bonds in living cells. Nat Rev Mol Cell Biol, 2002. **3**(11): p. 836-47.

29. Garcia-Dorado, D., M. Ruiz-Meana, J. Inserte, A. Rodriguez-Sinovas, and H.M. Piper, Calcium-mediated cell death during myocardial reperfusion. Cardiovasc Res, 2012. **94**(2): p. 168-80.

30. Wang, Z.V., Y. Deng, N. Gao, Z. Pedrozo, D.L. Li, C.R. Morales, A. Criollo, X. Luo, W. Tan, N. Jiang, M.A. Lehrman, B.A. Rothermel, A.H. Lee, S. Lavandero, P.P.A. Mammen, A. Ferdous, T.G. Gillette, P.E. Scherer, and J.A. Hill, Spliced X-box binding protein 1 couples the unfolded protein response to hexosamine biosynthetic pathway. Cell, 2014. **156**(6): p. 1179-1192.

31. Poet, G.J., O.B. Oka, M. van Lith, Z. Cao, P.J. Robinson, M.A. Pringle, E.S. Arner, and N.J. Bulleid, Cytosolic thioredoxin reductase 1 is required for correct disulfide formation in the ER. EMBO J, 2017. **36**(5): p. 693-702.

32. Vincenz, L. and F.U. Hartl, Sugarcoating ER Stress. Cell, 2014. **156**(6): p. 1125-1127.

33. Glembotski, C.C., Finding the missing link between the unfolded protein response and O-GlcNAcylation in the heart. Circ Res, 2014. **115**(6): p. 546-8.

34. Ushioda, R., J. Hoseki, K. Araki, G. Jansen, D.Y. Thomas, and K. Nagata, ERdj5 is required as a disulfide reductase for degradation of misfolded proteins in the ER. Science, 2008. **321**(5888): p. 569-72.

35. Preissler, S., J.E. Chambers, A. Crespillo-Casado, E. Avezov, E. Miranda, J. Perez, L.M. Hendershot, H.P. Harding, and D. Ron, Physiological modulation of BiP activity by trans-protomer engagement of the interdomain linker. Elife, 2015. **4**: p. e08961.

36. Sifers, R.N., S. Brashears-Macatee, V.J. Kidd, H. Muensch, and S.L. Woo, A frameshift mutation results in a truncated alpha 1-antitrypsin that is retained within the rough endoplasmic reticulum. J Biol Chem, 1988. **263**(15): p. 7330-5.

37. Yang, Q. and P. Sarnow, Location of the internal ribosome entry site in the 5' non-coding region of the immunoglobulin heavy-chain binding protein (BiP) mRNA: evidence for specific RNA-protein interactions. Nucleic Acids Res, 1997. **25**(14): p. 2800-7.

38. Rainbolt, T.K., J.M. Saunders, and R.L. Wiseman, Stress-responsive regulation of mitochondria through the ER unfolded protein response. Trends Endocrinol Metab, 2014. **25**(10): p. 528-37.

39. Vekich, J.A., P.J. Belmont, D.J. Thuerauf, and C.C. Glembotski, Protein disulfide isomerase-associated 6 is an ATF6-inducible ER stress response protein that protects cardiac myocytes from ischemia/reperfusion-mediated cell death. J Mol Cell Cardiol, 2012. **53**(2): p. 259-67.

40. Behnke, J., M.J. Mann, F.L. Scruggs, M.J. Feige, and L.M. Hendershot, Members of the Hsp70 Family Recognize Distinct Types of Sequences to Execute ER Quality Control. Mol Cell, 2016. **63**(5): p. 739-52.

41. Kranias, E.G. and R.J. Hajjar, Modulation of cardiac contractility by the phospholamban/SERCA2a regulatome. Circ Res, 2012. **110**(12): p. 1646-60.

42. Oka, O.B., M.A. Pringle, I.M. Schopp, I. Braakman, and N.J. Bulleid, ERdj5 is the ER reductase that catalyzes the removal of non-native disulfides and correct folding of the LDL receptor. Mol Cell, 2013. **50**(6): p. 793-804.

Chapter 4: MANF contributes to ER protein folding by acting as a chaperone

Abstract

In the third chapter of this dissertation, it was demonstrated that MANF is protective against reperfusion injury by maintaining ER proteostasis, and that it is specifically protective against protein misfolding caused by reductive stress. However, it still remains to be determined how MANF contributes to ER protein folding. Since MANF is protective by maintaining ER protein folding during I/R, and is induced by ATF6, which canonically upregulates genes encoding ER protein folding chaperones, here it was determined whether MANF acts as a chaperone. It was demonstrated that MANF is able to both prevent the aggregation of misfolded proteins and to refold misfolded proteins into a functional conformation, even though bioinformatic analysis suggests that MANF does not possess structural features found in other well-known chaperones. Since MANF was protective against reductive ER stress, here it was determined whether the chaperone activity of MANF was dependent on its evolutionarily conserved cysteine residues. It was found that these cysteine residues are required for the chaperone activity of MANF, and that they are also required for MANF to form complexes with misfolded proteins during reductive ER stress.

Introduction

A significant number of genes induced by ATF6 during ER stress encode ER-resident chaperones, which, along with chaperones in other cellular compartments, maintains protein folding homeostasis which is required for all known cellular functions[1]. During ER stress, which occurs during cardiac I/R, toxic misfolded proteins accumulate in the ER of cardiac myocytes and impair its functions, which include the folding and trafficking of ER/SR transmembrane bound Ca^{+2} handling proteins and GPCRs required for cardiac myocyte contractility, and the secretion of proteins that make up the extracellular matrix or act as chemokines[2]. Chaperones, such as the heat shock protein 70kDa and 90kDa family of proteins, recognize and bind to misfolded proteins or nascent polypeptides that have yet to be folded into a functional conformation. Chaperone

binding to misfolded proteins sequesters them until they undergo post-translation modifications required for proper folding, or actively fold into their mature functional conformations[1, 3]. In the ER, the HSP90 and HSP70 homologs, GRP78 and GRP94, form a protein folding complex with the lectin-binding chaperones, calreticulin and calnexin, which recognize and fold glycosylated nascent proteins[4, 5]. Additionally, GRP94 and GRP78 form protein folding complexes with ER-resident PDIs, which possess a thioredoxin domain that catalyzes disulfide bond formation in nascent proteins which stabilize the final structure of client proteins[6]. While ER-resident protein folding machinery is calibrated to ensure optimal ER protein folding and, thus, optimal ER function, there are also mechanisms that prevent accumulation of client proteins that do not reach their functional conformation, as well as to manage increases in protein folding demand which occurs during cardiac pathology.

A significant portion of newly synthesized nascent proteins targeted to the ER do not achieve a functional conformation and must be managed both by ER-resident chaperones and ER-associated degradation machinery[7, 8]. When client proteins do not reach a functional conformation, they remain bound by GRP78 and GRP94 and are trafficked to the ER retrotranslocon, which serves to extract terminally misfolded proteins from the ER, after which they are ubiquitylated by the E3 ubiquitin ligase Hrd1[9, 10]. The actions of GRP78 and GRP94 as pro-folding or pro-degradation chaperones are dictated by their interactions with co-chaperones, which also possess chaperone activity[9, 11]. The co-chaperones that typically regulate the pro-folding or pro-degradation functions of GRP94 and GRP78 contain a Dna-J domain, which can alter the ATPase activity of GRP78 and GRP94, in turn altering the strength or time of interaction between the chaperone activity domain of GRP78 or GRP94 and a misfolded client protein[9, 11]. Thus, the ER-resident chaperone network composed of the various proteins described above works in concert to determine the fate of unfolded proteins in the ER, to ultimately maintain ER protein folding homeostasis, ER function, and myocyte viability.

While the various ER-resident chaperones play myriad roles in protein folding, post-translational modification, and degradation, all chaperones studied to date share two common properties the define the chaperone function of a protein: the ability to slow the aggregation of misfolded proteins and fold misfolded proteins into a functional confirmation[1, 12]. Both of these chaperone properties can be assessed using *in vitro* chaperone assays, in which the denatured client protein is incubated with a putative or known chaperone, after which the client/substrate mixture is assessed for aggregation via spectrophotometric turbidity measurement, or biochemical function of the client protein e.g. enzymatic activity. In the third chapter of this dissertation, it was demonstrated that MANF loss of function decreased myocyte viability during I/R and during reductive ER stress. Additionally, it was demonstrated that MANF contributes to ER protein folding homeostasis during I/R injury, and forms a complex with misfolded proteins during reductive ER stress. However, it is not known whether MANF contributes to ER protein folding by acting as a chaperone. Accordingly, here, it was determined whether MANF possesses chaperone activity, and whether highly conserved cysteine residues, of MANF contribute to the structure and function of MANF.

Hypothesis: The conserved cysteine residues of MANF are required for its chaperone function.

Aim 1: Assess whether MANF possesses chaperone activity in vitro

Aim 2: Assess whether the conserved cysteine residues of MANF modulate its structure.

Aim 3: Assess whether the conserved cysteine residues are required for its chaperone function

Methods

Plasmid Generation:

Construct 1: pcDNA3.1(-) Mouse MANF

The open reading frame of mouse Manf (NM_029103) was amplified by PCR and then ligated into the XhoI and HindIII sites of multiple cloning site of pcDNA3.1(-).

Construct 2: pcDNA3.1(-) Mouse MANF signal sequence

Using construct 1 as a template, PCR was carried out to introduce a NheI restriction site and Kozak sequence, and an ApaI restriction site, into the 5' and 3' ends respectively of the PCR amplified product coding for the signal sequence MWATRGLAVALALSVLPDSRA. This PCR product and pcDNA3.1(-) were digested with NheI and ApaI and ligated together. The ApaI site is immediately followed by sequential XbaI and XhoI restriction sites.

Construct 3: pcDNA3.1(-) 3x-FLAG:

A version of pcDNA3.1(-) containing an N-terminal 3x-FLAG sequence was constructed by annealing the following oligonucleotides:

5'ctagcGCC**ATGGACTACAAAGACCACGACGGTGATTATAAAGATCACGATATCGATTACA**

AGGATGACGATGACAAGt-3'

5'-ctaga**CTTGTCATCGTCATCCTTGTAATCGATATCGTGATCTTTA-**

TAATCACCGTCGTGGTCTTTGTAGTCCATGGCg-3'

The NheI and XbaI overhangs of the annealed oligonucleotides were used to ligate the product into the XbaI site of pcDNA3.1(-), resulting in the creation of 3x FLAG-pcDNA3.1, as previously described[13].

Construct 4: pcDNA3.1(-) Mouse MANF signal sequence + 3x-FLAG.

Using **construct 3** as a template, PCR was performed to introduce XbaI and XhoI sites to the 5' and 3' ends, respectively, of the region coding for the 3x-FLAG tag, DYKDHDGDYKDHDIDYKDDDDK. This PCR product and **construct 2** were digested with XbaI and XhoI and ligated together to create a construct encoding the MANF signal sequence followed by 3x-FLAG.

Construct 5: pcDNA3.1(-) Mouse MANF signal sequence + 3x-FLAG + $MANF_{WT}$ (referred to hereafter as FLAG-$MANF_{WT}$)

Using construct 1 as a template, PCR was performed with the following primers:

5'GGAACG**CTCGAG**CTGCGGCCAGGAGAC-3'

5'-GGAGCTGACACGGAAGAT-3' (pcDNA 3.1(-) reverse primer)

The resulting PCR product and **construct 4** were digested with XhoI and HindIII and ligated together to generate a construct encoding the MANF signal sequence followed by 3x-FLAG and MANF, with the following amino acid sequence:

MWATRGLAVALALSVLPDSRAGPSRDYKDHDGDYKDHDIDYKDDDDKLELRPGDCEVCISYL
GRFYQDLKDRDVTSSPATIEEELIKFCREARGKENRLCYYIGATDDAATKIINEVSKPLAHHIPVE
KICEKLKKKDSQICELKYDKQIDLSTVDLKKLRVKELKKILDDWGEMCKGCAEKSDYIRKINELM
PKYAPKAASARTDL

Construct 6: pcDNA3.1(-) Mouse MANF signal sequence + 3x-FLAG + $MANF_{Mut.}$ (referred to hereafter as FLAG-$MANF_{Mut.}$)

To mutate all eight cysteines in mouse MANF to alanine, serial site directed mutagenesis was performed with the following primers:

Cysteines at positions 27 and 30:

5'-CGGCCAGGAGACGCTGAAGTTGCTATTTCTTATCTGG-3'

5'-CCAGATAAGAAATAGCAACTTCAGCGTCTCCTGGCCG-3'

Cysteines at positions 61 and 72

5'-CTTATAAAGTTTGCCCGTGAAGCAAGAGGCAAAGAGAATCGGTTGGCCTACTACA-
TTGGAG-3'

5'-CTCCAATGTAGTAGGCCAACCGATTCTCTTTGCCTCTTGCTTCACGGGCAAACTT-

TATAAG-3’

Cysteines at positions 103 and 114

5’-GTGGAAAAGATCGCTGAGAAGCTGAAGAAGAAAGACAGCCAGATCGCTGAACT-

AAAATC-3’

5’-GTATTTTAGTTCAGCGATCTGGCTGTCTTTCTTCTTCAGCTTCTCAGCGATCTT-

TTCCAC-3’

Cysteines at positions 148 and 151

5’-GACTGGGGGGAGATGGCCAAAGGCGCTGCAGAAAAGTCTG-3’

5’-CAGACTTTTCTGCAGCGCCTTTGGCCATCTCCCCCCAGTC-3’

Construct 7: pcDNA3.1(-) 3x-HA

A version of pcDNA3.1(-) encoding a C-terminal 3x-HA sequence was constructed by sequential annealing and ligating the following oligonucleotides into pcDNA3.1(-).The first set of oligonucleotides were annealed and digested with EcoR1 and BamH1 before ligation into pcDNA3.1(-) to generate a form of pcDNA3.1(-) encoding a C-terminal 1x-HA

5'-GAATTCTACCCATACGATGTTCCAGATTACGCTTAATGAGGATCC-3'

5'-GGATCCTCATTAAGCGTAATCTGGAACATCGTATGGGTAGAATTC-3'

The second set of oligonucleotides were annealed and directly ligated into the EcoR1 site into the above vector pcDNA3.1(-) encoding a C-terminal 1x-HA

5'-AATTCTATCCGTATGACGTACCTGACTATGCGGGCTATCCCTATGACGTGCCG-

GACTATGCAC-3'

5'-AATTGTGCATAGTCCGGCACGTCATAGGGATAGCCCGCATAGTCAGGTACGTCA-

TACGGATAG-3'

Construct 8 and 9:

α1 Antitrypsin (α1AT). A construct encoding human α-1 antitrypsin (A1AT, NCBI RefSeq NM_000295) was generated by PCR using the appropriate primers to create an amplicon with Xho1 on the 5' end of the start site, and a termination codon and EcoRI on the 3' end. This PCR product was cloned into the pCDNA3.1 vector (**Construct 8**) or pcDNA3.1 vector modified to encode a C-terminal 3x-HA epitope (**Construct 9**).

Construct 10 and **11**:

To generate constructs encoding Mutant α-1Antitrypsin[14], α1AT ΔCT (**Construct 10**) and α1AT-HA ΔCT (**Construct 11**), site directed mutagenesis was performed with the following primers:

5'-CAATGGGGCTGACCTCCGGGGTCACAG-3'

5'-CTGTGACCCCGGAGGTCAGCCCCATTG-3'

Purification of recombinant WT and mutant forms of 6x-His–tagged MANF:

BL21 *E. coli* were transformed with constructs (prSET-B, Invitrogen catalog no. V351-20) encoding 6x-His–tagged $MANF_{WT}$ or $MANF_{Mut}$. and then maintained in 1 liter of Luria broth with 50 mg/liter ampicillin at 37 °C and 300 rpm until reaching an *A*600 of 0.6–0.7. Isopropyl-D-1-thiogalactopyranoside was added to the culture flask to a final concentration of 1mM, and cultures were incubated at 37 °C and 300 rpm for an additional 4 h. Cells were then collected by centrifugation at 4 °C and 4000 rpm for 30 min in an Eppendorf 5810R using the swinging bucket rotor. The cells were then frozen at -20°C until the next step in the process. Cell pellets were thawed and then resuspended in 100 ml of Buffer Z (8 M urea, 100mM NaCl, 20 mM HEPES, pH 8.0, and 20 mM imidazole), after which they were subjected to 10 rounds of sonication. Each round consisted of 20 s of sonication, followed by placement of the cells in an ice-water bath for at least 1 min. Lysates were clarified by centrifugation at 3220 relative centrifugal force for 15 min

at 10 °C. The lysate was then applied to a pre-equilibrated 2.5-ml nickel-nitrilotriacetic acid nickel affinity column at room temperature (Qiagen, Valencia, CA). The column was then washed with 200 ml of Buffer Z and then eluted with 10 ml of Buffer Z to which 250mM imidazole had been added. The eluate was then applied to PD-10 desalting columns (GE Healthcare Life Sciences, catalog no. 17085101) (2.5 ml/column) that had been equilibrated with PBS. The PD-10 eluates were then concentrated using Centricon Plus-70 centrifugal filter units (Millipore–Sigma, catalog no. UFC701008). The protein concentration was calculated using the BCA protein assay kit as described above and verified by SDS-PAGE and Coomassie Blue staining (Expedeon, catalog no. ISB1L).

Insulin aggregation assay[15]:

Insulin (Sigma–Aldrich, Cat. No. I0516) was diluted to a final concentration of 113µM (0.652 mg/ml) in phosphate buffer composed of 100mM potassium phosphate (KH2PO4), 2.5mM EDTA, pH 7.0, with or without 330µM DTT, with or without 7.8–23.4 µM rMANF. Samples were transferred to a 96-well clear round-bottom plate (100µl/well), and absorbance at 360 nm was observed as a function of time using a VersaMax microplate reader set to 21 °C.

Lactalbumin aggregation assay[16]:

Reduced α-lactalbumin (rLA) was prepared by dissolving α-lactalbumin (Sigma–Aldrich, Cat. No. L6010) to a concentration of 18.28µM (2.55mg/ml) in phosphate buffer (14mM KH2PO4, 86mM Na_2HPO_4, and 150mM KCl, pH 7.5) containing 2.5mM EDTA and 5mM DTT for 30 min at 21 °C. Denatured BSA was prepared by dissolving BSA (Sigma–Aldrich, Cat. No. A6003) to a concentration of 210µM (13.97 mg/ml) in 7.2M guanidine hydrochloride dissolved in phosphate buffer and incubation at 21°C overnight. To initiate rLA aggregation, rLA was mixed with the denatured BSA at a final concentration of 14µM rLA and 2.6µM BSA in phosphate buffer. rMANF forms were added to the rLA and BSA mixture at final concentrations of 14–28µM, after which

samples were added to a clear 96-well round-bottom plate (100 µL/well), and absorbance at 360 nm was observed as a function of time using a VersaMax microplate reader set to 37 °C.

Citrate synthase activity assay[12]:

Citrate synthase (Cat. No. C3260, Sigma–Aldrich) was suspended at 1µM in TSC buffer composed of 10mM Tris-HCl (pH 7.2), 150 mM NaCl, and 5 mM CaCl2 and kept on ice. An aliquot of the TSC/citrate synthase solution was incubated at 50°C for 1 h to cause denaturation. Recombinant GRP78 (ProSpec, catalog no. HSP-037, HSPA5) or MANF was added at 1 µM to the TSC/citrate synthase solution after denaturation and incubated at 25°C for 0.5–1 h. To measure the enzyme activity of citrate synthase, the TSC/citrate synthase solution was rapidly diluted 80-fold into a solution of TE (50 mM Tris, 2mM EDTA, pH 8.0) containing 0.204mM 5,5'-dithiobis-(2-nitrobenzoic acid) (Sigma-Aldrich, Cat. No. D8130), 0.204mM oxaloacetic acid (Sigma–Aldrich, Cat. No. O9504), and 0.306mM acetyl-CoA (Sigma–Aldrich, Cat. No. A2056). Citrate synthase activity was assessed by measuring the absorbance of the solution at 412 nm over time, using a VersaMax microplate reader set to 29°C.

Clustal Analysis:

Clustal analysis of MANF and chaperone/co-chaperone families: For a given family of chaperones, co-chaperones, or annotated chaperone functional domains, amino acid sequences (**Table 4.1**) were analyzed using the Clustal Omega Multiple Sequence Alignment tool with default settings (https://www.ebi.ac.uk/Tools/msa/clustalo/), and compared to the sequence of mature mouse MANF without the signal sequence (Uniprot reference Q9CXI5, aa 22-179). The resulting percent identity matrices were used to generate the average sequence identities. The average sequence identities of the chaperone/co-chaperone/chaperone domain family members subjected to Clustal Omega analysis with MANF were plotted on a 95% confidence interval.

Adeno-associated virus serotype 9 (AAV9) Preparation and Tail Vein Injection:

To generate recombinant AAV9-control and AAV9-FLAG-MANF$_{WT}$, shuttle vectors for these recombinants were constructed and co-transfected with AAV9 helper, pDG-9 (a gift from Dr. Roger Hajjar) into HEK293T cells to produce virus, as described previously[10]. The shuttle vector pTRUF12-CMV was constructed by modifying pTRUF12 (a gift from Dr. Roger Hajjar) by first removing the region encoding GFP that was down-stream of the IRES. New restriction sites were inserted into the multiple cloning site to include Nhe1, Pme1, Xho1, and Mlu1. The coding region of FLAG-MANF$_{WT}$ (**construct 5**, **6** above) was excised and ligated into the NheI and HindIII restriction sites of the shuttle vector pTRUF12-CMV. To reduce recognition of the AAV9-mediated FLAG-MANF transcripts by the MANF KD hairpin, silent mutations were introduced into the pTRUF12-CMV plasmid by site directed mutagenesis with the following primers:
5'-GCAGAAAAGTCTGATTACATTAGGAAAATCAATGAACTGATGC-3'
5'-GCATCAGTTCATTGATTTTCCTAATGTAATCAGACTTTTCTGC-3'

To prepare the recombinant AAV9, HEK293T cells were plated a density of 8x10^6 per T-175 flask and maintained in DMEM/F12 containing 10%FBS, penicillin/streptomycin at 37°C and 5% CO2. For each virus preparation, 48 flasks were used. Twenty-four hours after plating, cultures were transfected using Polyethylenimine "Max" (MW 40,000, Polysciences, cat# 24765) as follows: For each T-175 flask, 15µg of helper plasmid and 5µg of pTRUF12 plasmid were mixed with 1mL of DMEM:F12 (no antibiotics) and 160µL of polyethylenimine (0.517 mg/mL), vortexed for 30 seconds, and incubated for 15 minutes at room temperature. This was then mixed with 18mL DMEM/F12 containing 2% FBS, penicillin/streptomycin then used to replace the media on the cultures. The cultures were then rocked intermittently for 15 minutes before being placed in a CO2 incubator. Three days later, the cells collected from six T-175 flasks were centrifuged at 500xg for 10 minutes, then resuspended in 10mL of lysis buffer (150mM NaCl, 50mM TrisHCL). The resuspended cells were then subjected to three rounds of freeze-thaw, followed by treatment

with benzonase (1500U of benzonase; Novagen) and 1mM $MgCl_2$ at 37°C for 30 minutes. The cell debris was collected by centrifugation at 3,400xg for 20 minutes. The supernatant obtained from six T-175 flasks containing the AAV9 was then purified on an iodixanol gradient comprised of the following four phases: 7.3mL of 15%, 4.9mL of 25%, 4mL of 40%, and 4mL of 60% iodixanol (Optiprep; Sigma-Aldrich) overlayed with 10mL of cell supernatant. The gradients were centrifuged in a 70Ti rotor (Beckman Coulter) at 69,000rpm for 1 hour using OptiSeal Polyallomer Tubes (Beckman Coulter). Virus was collected by inserting a needle 2mm below the 40%-60% interface and collecting 4 or 5 fractions (~4mL) of this interface and most of the 40% layer. The fractions were analyzed for viral content and purity by examining 10µL of each fraction on a 12% SDS-PAGE gel (BioRad), followed by staining with InstantBlue (Expedeon) to visualize the viral capsid proteins, VP1, VP2 and VP3. The virus was then collected from the fractions of several gradients and the buffer was exchanged with lactated Ringer's using an ultrafiltration device, Vivaspin 20, 100kDa MWCO (GE Healthcare). The final viral preparation was then fractionated on a 12% SDS-PAGE gel, stained with Coomassie blue (Expedeon, Cat. No. ISB1L), and then compared with a similarly stained gel of a virus of a known titer (an analogous control AAV9 with a CMV_{enh}MLC800 composite promoter with no downstream open reading frame). To administer recombinant AAV, mice were injected with 100µL of 37ºC heated Lactated Ringer's solution containing 10^{11} genome-containing units per mouse were injected via tail vein.

Heart Tissue RT-qPCR:

Total RNA was isolated from mouse hearts using the RNeasy Mini kit (Qiagen). cDNA synthesis was performed using the SuperScript III First-Strand Synthesis System (Thermo Fisher Scientific). RT-qPCR was performed using Maxima SYBR Green/ROX qPCR Master Mix in a StepOnePlus RT-PCR system (Thermo Fisher Scientific). The following primers were used:
β-actin

5'-GACGGCCAGGTCATCACTAT-3'

5’-GTACTTGCGCTCAGGAGGAG-3’

FLAG-Manf

5’-ATCACGATATCGATTACAAGGATG-3’

5’-GGCTTCGACACCTCATTGAT-3’

Culturing of NRVM and infection of NRVM with AAV9[10, 17-19]*:*

Neonatal rat ventricular myocytes (NRVM) were prepared from 1 to 3-day-old Sprague-Dawley rat hearts using a neonatal cardiomyocyte isolation system (Cat. No. LK003300 Worthington Biochemical Corp.). Myocytes were then purified on a discontinuous Percoll density gradient. Briefly, isolated cells were counted and then collected by centrifugation at 250×g for 5 min in an Eppendorf 5810R using the swinging bucket rotor. 40 to 60 million cells were then resuspended in 2mL 1×ADS buffer (116mM NaCl, 18mM HEPES, 845µM NaHPO4, 5.55mM Glucose, 5.37mM KCl, 831µM MgSO4, 0.002% Phenol Red, pH 7.35±0.5). Stock Percoll was prepared by combining 9 parts of Percoll (cat# 170891-02, GE healthcare, Piscataway, NJ) with 1 part of clear (without phenol red) 10×ADS. The stock Percoll was used to make the Percoll for the top (density= 1.059g/mL; 1 part Percoll stock added to 1.2 parts clear 1×ADS) and bottom (density= 1.082g/mL; 1 part Percoll stock added to 0.54 parts red 1×ADS) layers. The gradient, consisting of 4mL top Percoll and 3mL bottom Percoll, was set in a 15mL conical tube by pipetting the top Percoll first, and layering the bottom Percoll gently underneath, and the cells (in 2mL red 1×ADS buffer) were layered on the top. Subsequently, the Percoll gradient was centrifuged at 1500×g for 30 minutes with no deceleration brake at 4°C. The isolated myocytes, which concentrated in the layer located between the lower red ADS layer and the middle clear ADS layer, were carefully collected and washed twice with 50mL of 1×ADS and were then resuspended in plating medium and counted. This procedure is also effective for purifying myocytes that have been isolated by trypsin digestion, as previously described[1]. Following Percoll purification, myocytes were plated at the desired density on plastic culture plates that had been pre-treated

with 5µg/mL fibronectin in Dulbecco's modified Eagle's medium (DMEM)/F:12 (cat# 11330-32, Invitrogen, Carlsbad, CA) at 37°C for one hour in a 5% CO_2 incubator. Cultures were then maintained in (DMEM)/F:12, supplemented with 10% FBS and antibiotics (100units/mL penicillin and 100µg/mL streptomycin). 24 hours after plating, NRVMs plated at $1x10^6$ cells per well on 6-well dished were treated for 30 minutes with (DMEM)/F:12, supplemented with 10% FBS, antibiotics (100units/mL penicillin and 100µg/mL streptomycin), and 1µM bortezomib. After 30 minutes the bortezomib-containing media was then replaced with (DMEM)/F:12, supplemented with 10% FBS and antibiotics (100units/mL penicillin and 100µg/mL streptomycin) containing the appropriate AAV9 at an MOI of 10,000. After 24 hours, AAV9-containing medium was removed and adherent cells were washed with ice-cold DPBS and then lysed with 60-100µL of cell lysis buffer composed of 20mM Tris (pH 7.5), 150mM NaCl, 1% Triton X-100, 0.1% SDS, 1x protease/phosphatase inhibitor mixture (Roche Applied Science; Catalog No. 05892791001 and 4906837001). Lysates were scraped and transferred to microcentrifuge tubes and stored at -80°C.

Heart tissue protein extraction:

Mouse hearts were excised, washed briefly in ice-cold DPBS and snap frozen in liquid nitrogen. Approximately 20mg of frozen tissue was extracted in 250µL of ice-cold tissue homogenization buffer composed of 20mM Tris (pH 7.5), 150mM NaCl, 1% Triton X-100, 1% SDS, and 0.5% sodium deoxycholate with 1x protease/phosphatase mixture. Tissue homogenates were then clarified by centrifugation at 20,000xg for 10 minutes at 4°C.

Immunoblotting:

Following determination of protein concentration of clarified tissue extracts using the BCA protein assay kit (Bio-Rad, Cat. No. 5000111), between 5 and 40µg of protein extracts were subjected to reducing SDS-PAGE then electroeluted onto PVDF membranes. Membranes were blocked for 30 minutes at room temperature in 5% non-fat instant dry milk dissolved in Tris-

buffered saline containing 150mM NaCl, 2.68mM KCl, 50 mM Tris-pH 7.5, 0.1% Tween (TBST) with gentle rocking. Membranes were probed with a FLAG antibody (1:8,000; Sigma-Aldrich; Cat. No. F1804 (rabbit MANF antiserum, at 1:1000 (Anti-ARMET, Cat. No. ab67203, Abcam; Anti-MANF, Cat. No. SAB3500384, Sigma-Aldrich), and a B-actin antibody (1:80,000; Santa Cruz, Cat. No. sc-47778). Antibodies were diluted in 5% milk dissolved in TBST. Membranes were incubated with antibody solutions for 12-16 hours at 4°C. Membranes were then washed 3 times for 15 minutes in TBST and then incubated for 1 hour at room temperature with the appropriate horseradish peroxidase–conjugated anti-IgG (Jackson ImmunoResearch Laboratories, Inc.) diluted at 1:2000 in 5% milk dissolved in TBST. Membranes were then washed 3 times for 15 minutes with gentle rocking in TBST and subjected to enhanced chemiluminescence and exposed to autoradiography film or imaging using an ImageQuant 4000 from GE Healthcare Life Sciences. Immunoblots were quantified using ImageJ software densitometry.

FLAG immunoprecipitation and Immunoblotting Following ER Stress Treatments:

HeLa Cells were maintained in DMEM supplemented with 10% FBS and antibiotics not allowing confluency to surpass 80%. HeLa cells were resuspended at $6x10^6$ cells/400 µl of ice-cold Dulbecco's PBS and electroporated with 1-20µg of the relevant plasmids in a 0.4-cm gap electroporation cuvette at 250 V and 950 microfarads using a GenePulser II Electroporator (Bio-Rad). The cells were then plated at a density of $3x10^6$ cells on a 10cm dishes and incubated for 24 h in DMEM supplemented with 10% FBS and antibiotics. Transfected HeLa cell cultures were then treated for 1 h with vehicle or 2.5 mM DTT in serum-free DMEM/F-12 supplemented with antibiotics. The culture media containing DTT was then removed and cultures were briefly washed with ice-cold DPBS containing 20mM N-ethyl maleimide (NEM; Sigma-Aldrich, Cat. No. E376). Cultures were then lysed with cell lysis buffer composed of 20mM Tris (pH 7.5), 150mM NaCl, 1% Triton X100, 20mM NEM, and 1x protease/phosphatase inhibitors. The resulting cell lysates were then clarified by centrifugation at 20,000xg. Between 80 and 200µg of clarified protein cell

extracts were diluted to 0.5-1µg protein/µL using cell lysis buffer composed of 20mM Tris (pH 7.5), 150mM NaCl, 1% Triton X100, 20mM NEM, and 1x protease/phosphatase inhibitors (maximum volume of 200µL in 1.5mL microcentrifuge tubes). 1µg of FLAG antibody (Sigma-Aldrich; Cat. No. F1804) was added to the resulting solutions which were then gently rocked overnight (~16 hours) at 4°C. To this mixture, 20µL of protein A agarose beads (ThermoFisher, Cat. No. 20333, 50% slurry) that had been prewashed with ice-cold lysis buffer (20mM Tris (pH 7.5), 150mM NaCl, 1% Triton X-100) were added to each microcentrifuge tube. The resulting mixture was gently rocked for 2 hours at 4°C. The beads were sedimented to the bottom of the microcentrifuge tubes by centrifugation at 4000xg for 1-2 minutes at 4°C. The supernatant removed with a 1mL pipetteman without disrupting the sedimented beads. The beads were then washed with 1mL of ice-cold lysis buffer and sedimented by centrifugation at 4000xg for 1-2 minutes 4°C. This process was repeated 2 more times. To elute the FLAG-immunoprecipitated complexes, the isolated beads were incubated with 30µL cell lysis buffer composed of 20mM Tris (pH 7.5), 150mM NaCl, 1% Triton X100, 1x protease/phosphatase inhibitors, and 300µg/mL FLAG peptide. The resulting mixture was gently rocked for 3 hours at 4°C, and the eluate was separated from the beads by centrifugation at 4000xg for 1-2 minutes at room temperature (21°C). The eluates were then subjected to reducing or non-reducing SDS-PAGE on a 4-12% gradient polyacrylamide gel and then electroeluted onto PVDF membranes. Membranes were blocked for 30 minutes at room temperature in 5% non-fat instant dry milk dissolved in 150mM NaCl, 2.68mM KCl, 50 mM Tris-pH 7.5, 0.1% Tween (TBST) with gentle rocking. Membranes were probed with a mouse FLAG antibody at 1:8000 (Sigma-Aldrich; Cat. No. F1804) and an HA antibody at 1:1000 (Santa Cruz Cat. No. sc-7392).

NRVM immunocytofluorescence:

NRVM were plated at approximately $1.25x10^5$ cells on fibronectin coated 4-chamber glass slides (Falcon). After siRNA transfection and adenovirus treatment as described above, slides

were washed 2 times with 0.5mL per well ice-cold DPBS. Slides were then fixed with 4% paraformaldehyde in DPBS on ice for 15 minutes. Slides were then washed 3 times with ice-cold DPBS, 5 minutes per wash, followed by permeabilization with 0.5% Triton X-100, 3mM EDTA for 10 minutes on ice, washed 3 times with DPBS, 5 minutes per wash, and then blocked for 1 hour with super block. Slides were then incubated with primary antibodies diluted in Superblock (ThermoFisher, Cat. No. 37515) for 16 hours at 4°C. Primary antibodies used for staining NRVM anti-FLAG (1:200 Sigma Cat. No. F1804) anti-GRP78 (C-20, 1:30, Cat. No. SC-1051, Santa Cruz). Slides were subsequently washed 6 times with ice-cold DPBS, 5 minutes per wash and then incubated at room temperature, in the dark for 90 minutes, with the appropriate fluorophore-conjugated secondary antibodies (Jackson ImmunoResearch Laboratories, West Grove, PA) diluted in Superblock including Cy3-conjugated anti-mouse IgG (1:250) or FITC-conjugated anti-goat IgG (1:250). Slides were subsequently washed 6 times with ice-cold DPBS, 5 minutes per wash. Nuclei were counterstained for 1 min with Topro-3 (1:1000, Thermo Fisher). Slides were subsequently washed 6 times with ice-cold DPBS. Images were obtained using laser scanning confocal microscopy on an LSM 710 confocal laser scanning microscope (Carl Zeiss, Oberkochen, Germany).

Results:

MANF acts as a chaperone to reduce ER protein misfolding caused by reductive ER stress.

In the previous chapter of this dissertation, it was demonstrated that MANF is protects during reperfusion by contributing to ER protein folding, and that MANF is specifically protective against reductive stress in the ER, during which MANF forms a complex with misfolded proteins. Thus, here it was determined whether MANF contributes to ER protein folding by acting as a chaperone. Chaperones are defined as any protein that interacts with, stabilizes, or helps another protein to acquire its functionally active conformation, without being present in its final structure[1]. In this regard, the two well established properties of chaperones are their abilities to 1) inhibit

aggregation of unfolded proteins and 2) fold proteins into their final functional conformations[1, 12]. Accordingly, it was determined whether recombinant MANF (rMANF) can inhibit the aggregation of insulin and α-lactalbumin and refold citrate synthase into its active conformation, as these are commonly employed *in vitro* chaperone assays (**Figure 4.1A**) [12, 15, 16]. rMANF decreased the aggregation of both insulin and α-lactalbumin in a concentration-dependent manner (**Figure 4.1B-E**) and was able to restore activity to unfolded, inactive citrate synthase, as did the positive control, recombinant GRP78 (**Figure 4.1E**). Taken together, the results in **Figure 4.1** indicate that during reductive ER stress MANF binds to misfolded ER proteins and acts as a chaperone.

The conserved cysteine residues of MANF are required for its chaperone function

To more deeply dissect the chaperone function of MANF, mutations were introduced into regions of MANF predicted to contribute to its chaperone function. To determine where to make such mutations, it was determined whether MANF bears any structural similarity to regions of other, well-studied chaperones, with an aim of mutating such regions in MANF. However, after extensive informatics assessments (**Table 4.1**) it was found that, compared to the known chaperones[3, 5, 6, 11, 12, 20-28], which align well and cluster together (**Figure 4.2A-B, black**), MANF exhibited poor alignment with most of the chaperone families tested, falling outside the 95% confidence interval of sequence similarity to the chaperones tested (**Figure 4.2A-B, red**). Since this comparative informatic analysis did not reveal any obvious domains that are shared between MANF and other chaperones, MANF alignment was examined across several different species in search of conserved potentially functional regions. In doing so, it was observed that there are several conserved domains, including the positions of the cysteine residues (**Figure 4.2C**). Since MANF protects against DTT-induced reductive ER stress, and since cysteine residues are susceptible to reduction during DTT treatment, the functional roles of the cysteine residues in MANF were examined. Accordingly, a construct encoding FLAG-MANF in which the 8 cysteine residues are mutated to alanine (**Figure 4.3A**, **FLAG-MANF$_{Mut.}$**) was made.

Immunocytofluorescence demonstrated that both FLAG-tagged forms of $MANF_{WT}$ and $MANF_{Mut}$ co-localized with the ER resident chaperone, Grp78 (**Figure 4.3B**-**C**), confirming that ectopically expressed MANF is properly located. Moreover, non-reducing gel studies demonstrated that redox status of the cysteine residues of MANF contribute to its structure. **(Figure 4.3D-F)**. Furthermore, while FLAG-$MANF_{WT}$ was able to form a intermolecular disulfide-dependent complex with misfolded α1AT ΔCT, in the ER, FLAG-$MANF_{Mut.}$ was unable to form this complex (**Figure 4.4A**). Moreover, and in contrast to $rMANF_{WT}$, $rMANF_{Mut.}$ did not exhibit chaperone activity (**Figure 4.4B-E**). These results are consistent with the hypothesis that the cysteine residues of MANF contribute to its chaperone function, at least in part by forming complexes with misfolded proteins in the ER.

While mutant $MANF_{Mut.}$ could be expressed in *E. coli*, which enabled the preparation of enough of the recombinant protein to test in this study, and while it properly localization in NRVM, FLAG-$MANF_{Mut.}$ detection in the hearts of AAV9-FLAG-$MANF_{Mut.}$-treated mice was very low (**Figure 4.5A-C**), as it was in NRVM infected with AAV9-FLAG-$MANF_{Mut.}$ (**Figure 4.5D-E**). Accordingly, because of the very low expression levels of FLAG-$MANF_{Mut.}$ in cultured cardiac myocytes and in the mouse heart, *in vivo,* it was not feasible to conduct experiments assessing whether the cysteine residues of MANF are required for its function, *in vivo,* or in NRVM.

Discussion

In the third chapter of this dissertation, it was found that MANF maintains ER protein folding during reperfusion injury and forms a complex with the model misfolded protein α1AT ΔCT during reductive ER stress. Consistent with those findings, here it was demonstrated that MANF is able to prevent the aggregation of and refold misfolded proteins, confirming the chaperone function of MANF[1, 12]. Since MANF exerts its protective functions during proteotoxic stimuli that impair oxidative protein folding[15, 29-33], it seems likely that MANF plays a role in the folding of client proteins that form disulfide bonds as part of their final functional conformations.

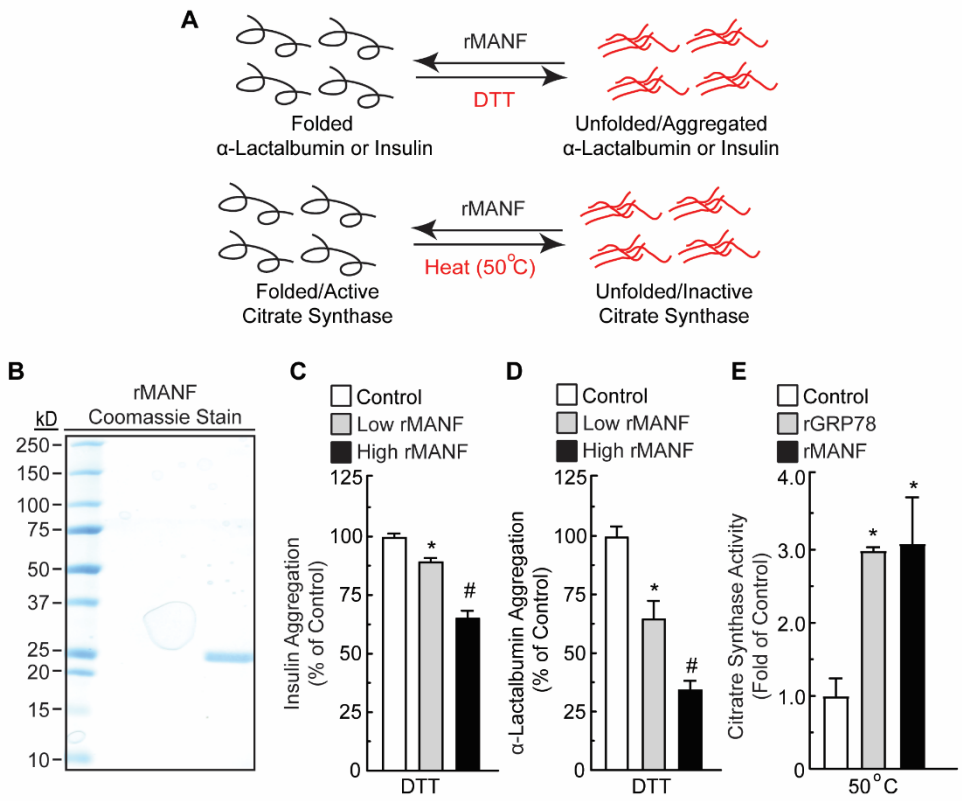

Figure 4.1: Effect of rMANF on protein aggregation and folding. A, diagram of chaperone assays performed in **C**-**E**. **B**, Coomassie Blue-stained gel of purified recombinant MANF (rMANF). **C**, effect of rMANF at low (7.8μM) or high (23.4μM) concentrations on the aggregation of insulin (113μM). **D**, effect of rMANF at low (14μM) or high (28μM) concentrations on the aggregation of α-lactalbumin (14μM). **E**, effect of recombinant GRP78 (1μM) or MANF (1μM) on activity of heat-denatured citrate synthase (1μM). Citrate synthase activity is displayed as fold heat-denatured control level. * and #, statistically significant difference from all other groups by one-way ANOVA, $p \leq 0.05$, followed by Newman–Keuls post hoc analysis. Error bars, S.E.M.

Table 4.1: Chaperone and co-chaperone amino acid sequences used in clustal omega analysis (Figure 4.2A, B)

Protein Name	Species	Uniprot Entry	Amino acids compared to MANF
Thioredoxin Domains			
PDIA1	*H. sapiens*	P07237	18-134
PDIA1	*H. sapiens*	P07237	349-475
PDIA2	*H. sapiens*	Q13087	27-152
PDIA2	*H. sapiens*	Q13087	367-496
PDIA3	*H. sapiens*	P30101	343-485
PDIA4	*H. sapiens*	P13667	158-301
PDIA4	*H. sapiens*	P13667	505-636
PDIA5	*H. sapiens*	Q14554	134-261
PDIA5	*H. sapiens*	Q14554	270-384
PDIA5	*H. sapiens*	Q14554	378-506
PDIA6	*H. sapiens*	Q15084	20-133
PDIA6	*H. sapiens*	Q15084	154-287
Erdj5	*H. sapiens*	Q8IXB1	130-232
Erdj5	*H. sapiens*	Q8IXB1	454-553
Erdj5	*H. sapiens*	Q8IXB1	557-662
Erdj5	*H. sapiens*	Q8IXB1	671-778
Tmx1	*H. sapiens*	Q9H3N1	27-132
Tmx2	*H. sapiens*	Q9Y320	114-269
Tmx3	*H. sapiens*	Q96JJ7	25-128
Tmx4	*H. sapiens*	Q9H1E5	30-137
Hsp70 ATPase Domains			
DnaK	*E. Coli*	P0A6Y8	1-388
Hsp71	*S. cerevisiae*	P10591	1-383
Hsp70	*H. sapiens*	P0DMV8	2-386
Grp78	*H. sapiens*	P11021	125-280
Hsc70	*H. sapiens*	P11142	2-386
Kar2	*S. cerevisiae*	P16474	146-300
Hsp70 Substrate Binding Domains			
DnaK	*E. Coli*	P0A6Y8	389-638
Hsp71	*S. cerevisiae*	P10591	384-642
Hsc70	*H. sapiens*	P11142	394-509
Grp78	*H. sapiens*	P11021	420-500
Hsp70	*H. sapiens*	P0DMV8	394-509
Kar2	*S. cerevisiae*	P16474	420-520
Hsp90 ATPase Domains			
Hsp90β	*H. sapiens*	P08238	1-236

Table 4.1: Chaperone and co-chaperone amino acid sequences used in clustal omega analysis (Figure 4.2A, B). (Continued)

Protein Name	Species	Uniprot Entry	Amino acids compared to MANF
Hsp82	*S. cerevisiae*	P02829	1-181
Grp94	*H. sapiens*	P14625	69-337
HtpG	*E. Coli*	A0A140ND61	27-184
Hsp90 Dimerization Domains			
HSP90β	*H. sapiens*	P08238	556-686
Hsp82	*S. cerevisiae*	P02829	543-709
Grp94	*H. sapiens*	P14625	611-746
HtpG	*E. Coli*	A0A140ND61	504-624
Full-length Hsp60			
T-complex protein 1 subunit α	*H. sapiens*	P17987	1-555
T-complex protein 1 subunit β	*H. sapiens*	P78371	1-535
T-complex protein 1 subunit γ	*H. sapiens*	P49368	1-545
T-complex protein 1 subunit Δ	*H. sapiens*	P50991	1-539
T-complex protein 1 subunit ε	*H. sapiens*	P48643	1-541
T-complex protein 1 subunit ζ	*H. sapiens*	P40227	1-531
Hsp100 AAA ATPases			
VCP	*H. sapiens*	P55072	1-806
ClpA	*E. Coli*	P0ABH9	1-758
Hsp104	*S. cerevisiae*	P31539	1-908
ClpB	*E. Coli*	P63284	1-857
Lectin Binding Chaperones			
Calreticulin	*M. musculus*	P35564	17-367
Calreticulin	*H. sapiens*	P27797	1-417
Calnexin	*H. sapiens*	P27824	1-592
Calreticulin	*D. magnia*	A0A0P6EVW0	1-409
Calnexin	*D. magnia*	A0A164QKC8	1-588
Calnexin	*S. cerevisiae*	P27825	1-502
Small Heat Shock Proteins			
HspB1	*H. sapiens*	P04792	1-205
HspB2	*H. sapiens*	Q16082	1-182

Table 4.1: Chaperone and co-chaperone amino acid sequences used in clustal omega analysis (Figure 4.2A, B). (Continued)

Protein Name	Species	Uniprot Entry	Amino acids compared to MANF
HspB3	*H. sapiens*	Q12988	1-150
HspB6	*H. sapiens*	O14558	1-160
HspB7	*H. sapiens*	Q9UBY9	1-170
HspB8	*H. sapiens*	Q9UJY1	1-196
α B-crystallin	*H. sapiens*	P02511	1-175
α A-crystallin	*H. sapiens*	P02489	1-173
Clusterin			
Clusterin	*H. sapiens*	P10909	23-449
Clusterin	*R. norvegicus*	P05371	22-447
Clusterin	*M. musculus*	Q06890	22-448
Clusterin	*D. rerio*	A0A0B5JQ03	21-449
Prefoldin Subunit 1			
Prefoldin Subunit 1	*H. sapiens*	O60925	1-122
Prefoldin Subunit 1	*R. norvegicus*	D3ZX38	1-122
Prefoldin Subunit 1	*M. musculus*	Q9CWM4	1-122
Prefoldin Subunit 1	*D. rerio*	Q5D016	1-122
Prefoldin Subunit 1	*S. cerevisiae*	P46988	1-109
(Probable) Prefoldin Subunit 1	*D. melanogaster*	Q9VMH8	1-126
(Probable) Prefoldin Subunit 1	*C. elegans*	Q17827	1-117
Prefoldin Subunit 2			
Prefoldin Subunit 2	*H. sapiens*	Q9UHV9	1-154
Prefoldin Subunit 2	*R. norvegicus*	B0BN18	1-154
Prefoldin Subunit 2	*M. musculus*	O70591	1-154
Prefoldin Subunit 2	*D. rerio*	Q1JPY6	1-156
Prefoldin Subunit 2	*S. cerevisiae*	P40005	1-111
(Probable) Prefoldin Subunit 2	*D. melanogaster*	Q9VTE5	1-143
Prefoldin Subunit 2	*C. elegans*	Q9N5M2	1-141
Prefoldin Subunit 3			
Prefoldin Subunit 3	*H. sapiens*	P61758	1-197
Prefoldin Subunit 3	*R. norvegicus*	M0R919	1-186
Prefoldin Subunit 3	*M. musculus*	P61759	1-196
Prefoldin Subunit 3	*D. rerio*	Q503D5	1-195
Prefoldin Subunit 3	*S. cerevisiae*	P48363	1-199
Prefoldin Subunit 3	*D. melanogaster*	Q9VGP6	1-194
Prefoldin Subunit 3	*S. cerevisiae*	P53900	1-199
(Probable) Prefoldin Subunit 3	*C. elegans*	O18054	1-185

Table 4.1: Chaperone and co-chaperone amino acid sequences used in clustal omega analysis (Figure 4.2A, B). (Continued)

Protein Name	Species	Uniprot Entry	Amino acids compared to MANF
Prefoldin Subunit 4			
Prefoldin Subunit 4	*H. sapiens*	Q9NQP4	1-134
Prefoldin Subunit 4	*R. norvegicus*	M0R5N4	1-139
Prefoldin Subunit 4	*M. musculus*	Q3UWL8	1-134
Prefoldin Subunit 4	*D. rerio*	F1R0Z8	1-135
Prefoldin Subunit 4	*S. cerevisiae*	P53900	1-129
(Probable) Prefoldin Subunit 4	*D. melanogaster*	Q9VRL3	1-138
(Probable) Prefoldin Subunit 4	*C. elegans*	Q17435	1-126
Full-length Prefoldin Subunit 5			
Prefoldin Subunit 5	*H. sapiens*	Q99471	1-154
(Predicted) Prefoldin Subunit 5	*R. norvegicus*	B5DFN4	1-154
Prefoldin Subunit 5	*M. musculus*	Q9WU28	1-154
Prefoldin Subunit 5	*D. rerio*	A9JT16	1-153
Prefoldin Subunit 5	*S. cerevisiae*	Q04493	1-163
(Probable) Prefoldin Subunit 5	*D. melanogaster*	Q9VCZ8	1-168
(Probable) Prefoldin Subunit 5	*C. elegans*	Q21993	1-152
Prefoldin Subunit 6			
Prefoldin Subunit 6	*H. sapiens*	O15212	1-129
Prefoldin Subunit 6	*R. norvegicus*	Q6MGC4	1-127
Prefoldin Subunit 6	*M. musculus*	Q03958	1-127
Prefoldin Subunit 6	*D. rerio*	Q7SX94	1-126
Prefoldin Subunit 6	*S. cerevisiae*	P52553	1-114
(Probable) Prefoldin Subunit 6	*D. melanogaster*	Q9VW56	1-125
(Probable) Prefoldin Subunit 6	*C. elegans*	P52554	1-126
Hsp40 DnaJ Domains			
DJB14	*H. sapiens*	Q8TBM8	108-172
DNJB2	*H. sapiens*	P25686	2-71
DNAJC5	*H. sapiens*	Q9H3Z4	13-82
DNAJC10	*H. sapiens*	Q8IXB1	35-100
DNAJC3	*H. sapiens*	Q13217	394-462
DNAJC7	*H. sapiens*	Q99615	381-451
DNAJC24	*H. sapiens*	Q6P3W2	10-81
DNAJA1	*H. sapiens*	P31689	6-68

Table 4.1: Chaperone and co-chaperone amino acid sequences used in clustal omega analysis (Figure 4.2A, B). (Continued)

Protein Name	Species	Uniprot Entry	Amino acids compared to MANF
DNAJB1	*H. sapiens*	P25685	2-70
DNAJB11	*H. sapiens*	Q9UBS4	25-90
DNAJC2	*H. sapiens*	Q99543	88-161
DNAJC21	*H. sapiens*	Q5F1R6	3-69
DNAJC9	*H. sapiens*	Q8WXX5	15-82
Unc45			
Unc45a	*H. sapiens*	Q9H3U1	1-944
Unc45b	*H. sapiens*	Q8IWX7	1-931
Unc45a	*M. musculus*	Q99KD5	1-944
Unc45b	*M. musculus*	8CGY6	1-931
Unc45	*C. elegans*	G5EG62	1-961
Unc45	*R. norvegicus*	Q32PZ3	1-944
Unc45	*D. melanogaster*	Q9VHW4	1-947

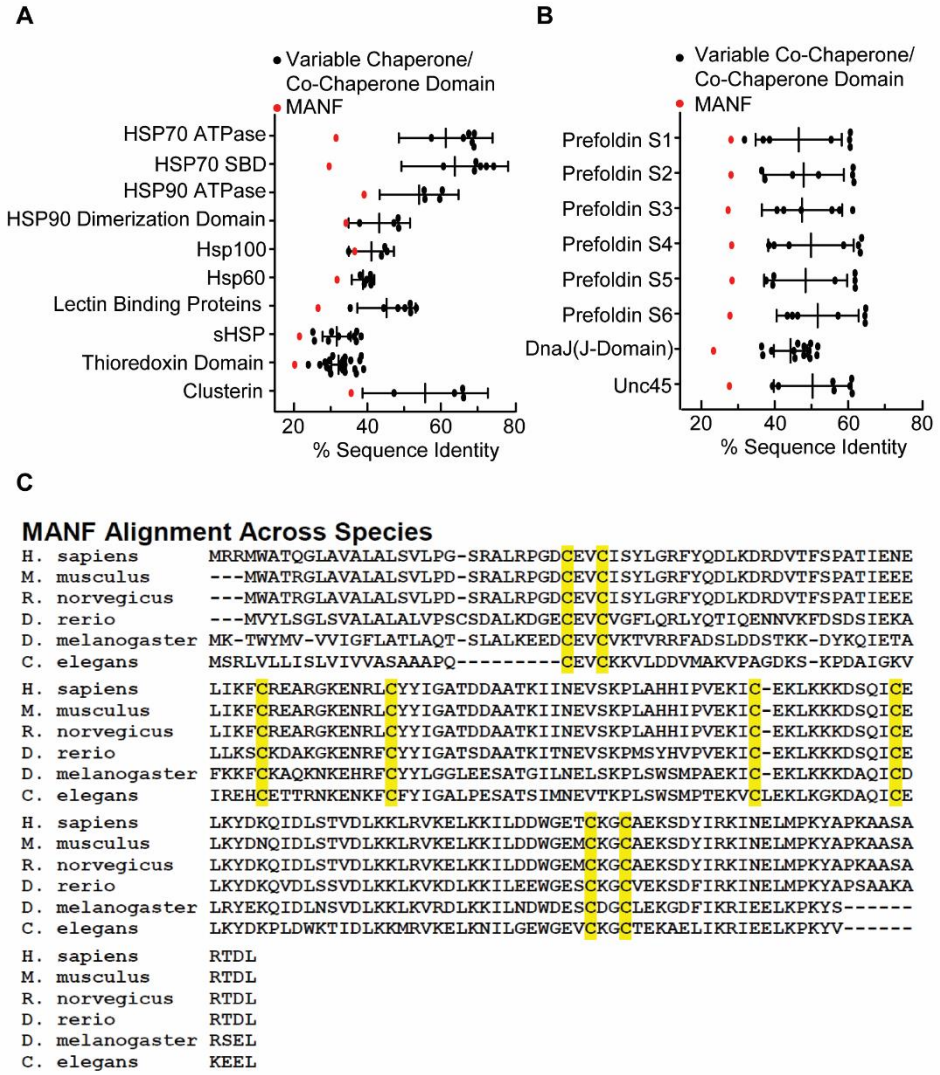

Figure 4.2: Sequence homology between MANF and known chaperone and co-chaperone orthologs or homologues and alignment of MANF across species. A and **B**, Clustal sequence identity analysis of MANF and various chaperones (A) and co-chaperones (B). Error bars, 95% confidence intervals. **C**, alignment of MANF sequences from different species. Highlighted in yellow are the positions of cysteine residues, the positions of which are conserved across the species shown.

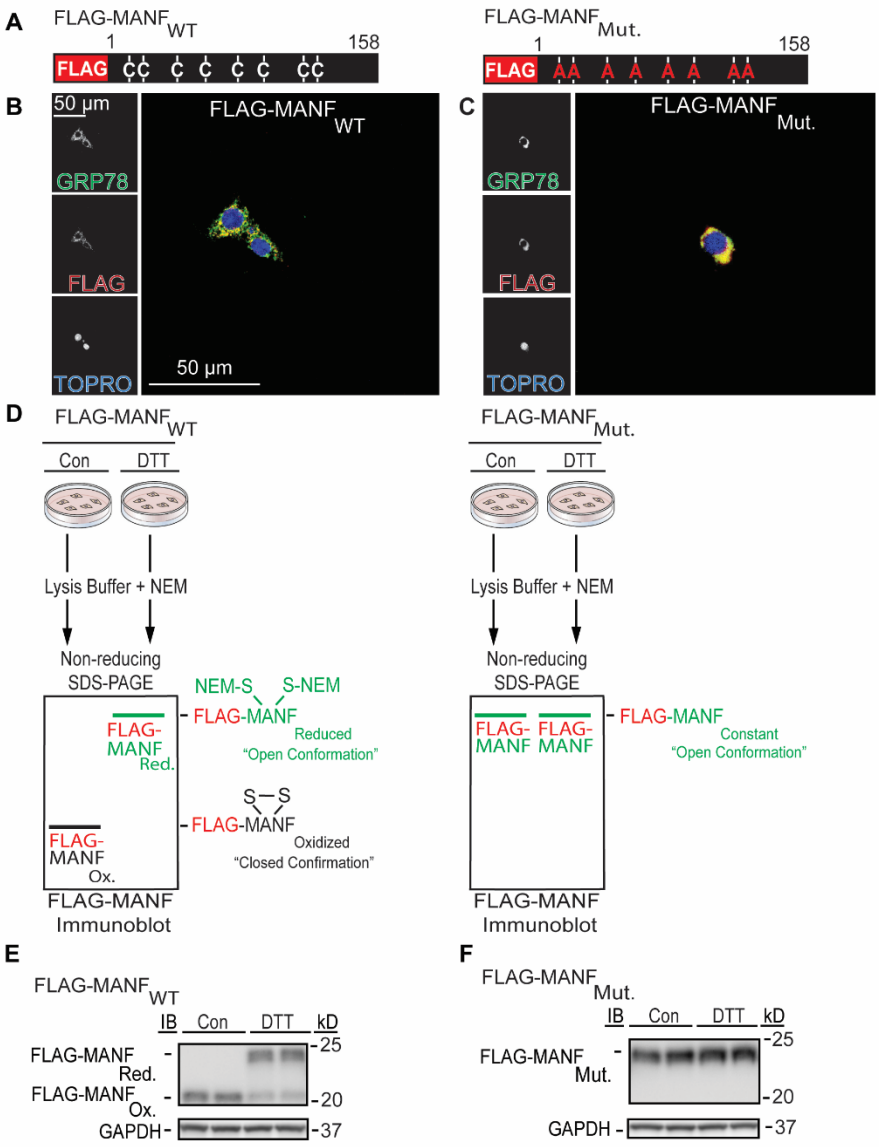

Figure 4.3: Immunocytofluorescence and non-reducing gel studies of FLAG-MANF$_{WT}$ and FLAG-MANF$_{Mut.}$ **A**, diagram of FLAG-MANF$_{WT}$ and FLAG-MANF$_{Mut.}$ constructs indicating cysteine-to-alanine mutations. **B** and **C**, immunocytofluorescence of FLAG-MANF. NRVMs were transfected with siManf targeted to the 3'-UTR of the Manf transcript, followed by infection with AdV-FLAG-MANF$_{WT}$ (**C**) or AdV-FLAG-MANF$_{Mut.}$ (**D**) and then treated with tunicamycin to induce GRP78 expression. NRVMs were then examined by immunocytofluorescence for GRP78 (green) and FLAG-MANF (red). Nuclei are indicated by TOPRO staining (blue). D, diagram of how non-reducing gel studies were performed on protein extracts from HeLa cells expressing FLAG-MANF$_{WT}$ or FLAG-MANF$_{Mut.}$ to assess how mutation of the cysteine residues of MANF affect its structure. **E**, **F** Non-reducing SDS-PAGE and FLAG-MANF immunoblots. HeLa cells expressing FLAG-MANF$_{WT}$ (**E**) or FLAG-MANF$_{Mut.}$ (**F**) were treated for 1 hour with vehicle or 2.5mM DTT in serum-free media followed by washing with 20mM NEM dissolved in PBS, lysis with lysis buffer containing 20mM NEM. Lysates were subjected to non-reducing SDS-PAGE and immunoblotting for FLAG-MANF and GAPDH.

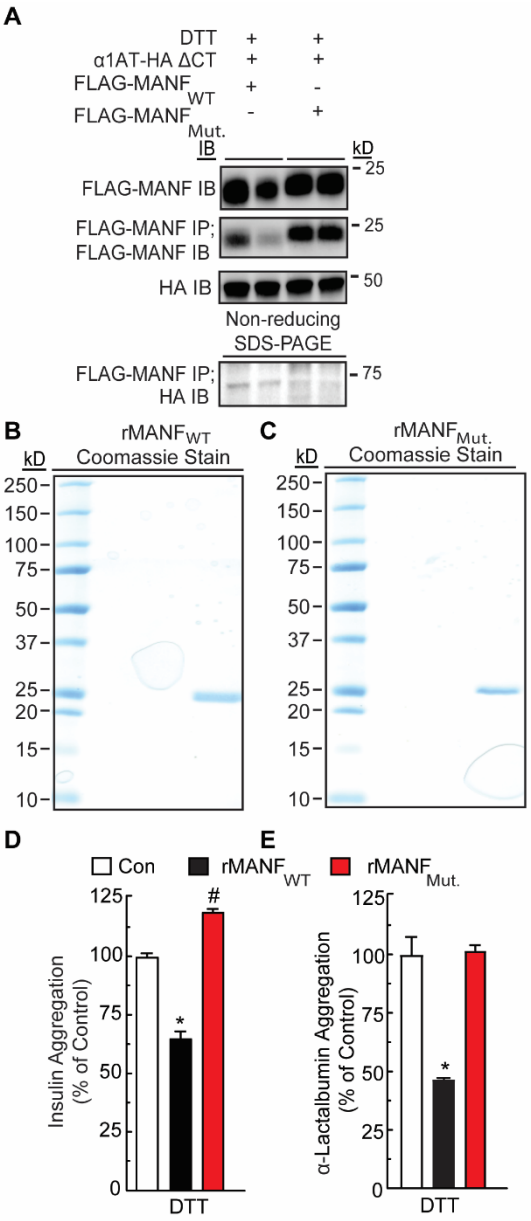

Figure 4.4: Effect of cysteine-to-alanine mutation on complex formation between FLAG-MANF and α1AT-HA ΔCT and rMANF chaperone activity. A, Duplicate HeLa cell cultures were co-transfected with plasmid constructs encoding FLAG-MANF$_{WT}$ or FLAG-MANF$_{Mut.}$ and α1AT-HA ΔCT and treated with DTT. The cell extracts were subjected to reducing SDS-PAGE followed by immunoblotting for α1AT-HA ΔCT (45 kDa) or FLAG-MANF (20 kDa). The cell extracts were also subjected to FLAG IP followed by nonreducing SDS-PAGE to maintain possible disulfide bonds between MANF and other proteins and then IB HA (bottom). (Note the FLAG-MANF/ α1AT-HA ΔCT complex shown at 65 kDa). **B**, **C** Coomassie Blue-stained gel of purified rMANF$_{WT}$ (**B**) and rMANF$_{Mut.}$, (**C**). **D**, effect of recombinant rMANF$_{WT}$ (23.4μM) or rMANF$_{Mut.}$ (23.4μM) on aggregation of insulin (113 μM). **E**, effect of rMANF$_{WT}$ (21μM) or rMANF$_{Mut.}$ (21μM) on aggregation of α-lactalbumin (14μM). * and #, statistically significant difference from all other groups by one-way ANOVA, $p \leq 0.05$, followed by Newman–Keuls post hoc analysis.

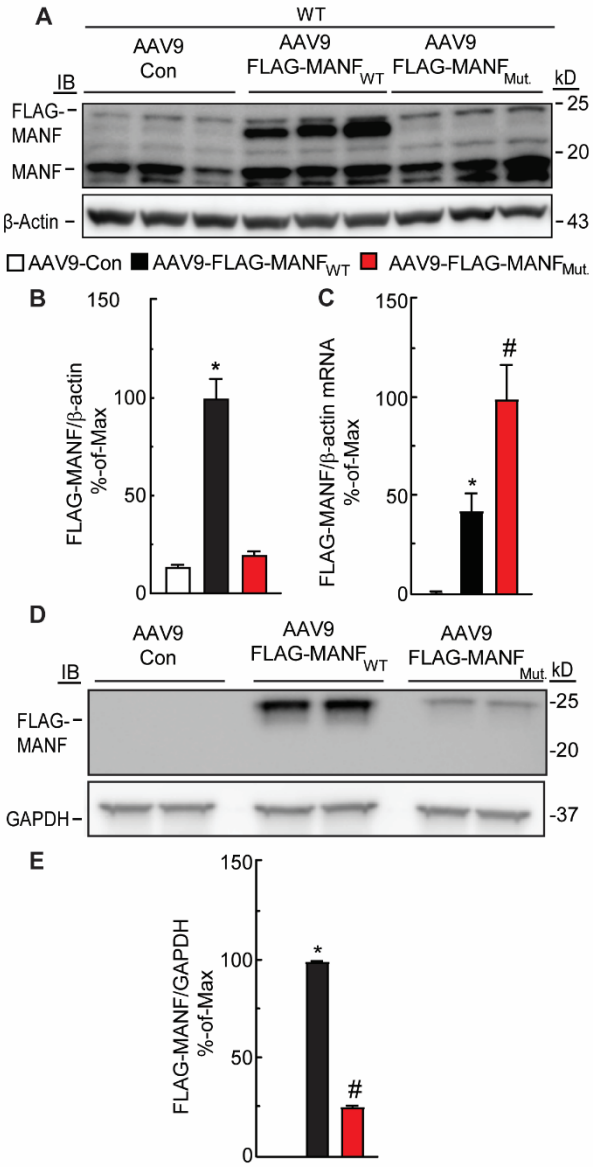

Figure 4.5: Expression of FLAG-MANF$_{WT}$ or FLAG-MANF$_{Mut.}$ in mouse hearts and in NRVM. AAV-9 FLAG-MANF$_{WT}$ or AAV-FLAG-MANF$_{Mut}$. was administered to WT mice by tail vein injection. Seven days later, male hearts were extracted and subjected to MANF and β-actin immunoblotting (**A**, **B**), or FLAG-MANF and β-actin qPCR (**C**). **B**, densitometry of immunoblots shown in **A**. Band intensities were normalized to those for β-actin and displayed as %-of-Max. **C**, FLAG-Manf mRNA levels were determined by RT-qPCR and displayed as %-of-Max. **D**, NRVMs were infected with AAV-9 FLAG-MANF$_{WT}$ or AAV-FLAG-MANF$_{Mut}$., and after 24 h protein extracts were immunoblotted for FLAG-MANF and GAPDH. **E**, densitometry of immunoblots shown in **D**. Band intensities were normalized to those for GAPDH and displayed as %-of-Max. * and #, statistically significant difference from all other groups by one-way ANOVA, $p \leq 0.05$, followed by Newman–Keuls post hoc analysis. Error bars, S.E.M.

conclusions are also supported by the observation that the cysteine residues are required for the chaperone activity of MANF and that they also mediate formation of intramolecular disulfide bonds with misfolded proteins.

One of the most studied ER chaperones is GRP78, also known as BiP [25, 26]. The Glembotski lab previously showed that Grp78 and MANF interact directly with each other in cardiac myocytes[34]. GRP78 plays a central role in ER protein folding in almost all cells in which it has been studied, including in cardiac myocytes. Whereas it has been known for some time that ER stress, and in particular, ischemia, induces *Grp78* in the heart[18, 35, 36], the importance of this chaperone in heart function has not been studied in depth until relatively recently, where Grp78 overexpression and deletion have demonstrated the adaptive and protective roles for Grp78 in mouse models of ischemic and hypertrophic heart disease[37, 38]. While these studies were in progress another study had shown that MANF interacts with Grp78 *in vitro* in a way that affects the chaperone activity of GRP78 in a manner predicted to improve ER proteostasis, *in vivo*[39]. In combination with that study, the results here demonstrate that MANF can improve ER protein folding by interacting with GRP78, and MANF can act as a chaperone itself, suggesting that there may be multiple ways that MANF improves ER protein folding and cardiac myocyte viability during reductive stresses, such as I/R and DTT. This is an unanticipated role for MANF, because the informatics analysis shown here indicated that, from a structural viewpoint, MANF does not share domains with other well-known chaperones, indicating that MANF may be a new type of chaperone. However, because MANF resides in the ER of cardiac myocytes, the chaperone function of MANF complements the roles of other ER chaperones with which MANF likely collaborates to maintain ER proteostasis. In conclusion, this dissertation extends our understanding of MANF function in an *in vivo* model of cardiac pathology, demonstrating that MANF plays an important role in ER protein folding within cardiac myocytes, where it protects myocytes from reductive stress (**Figure 4.6**). This protective function likely depends on the

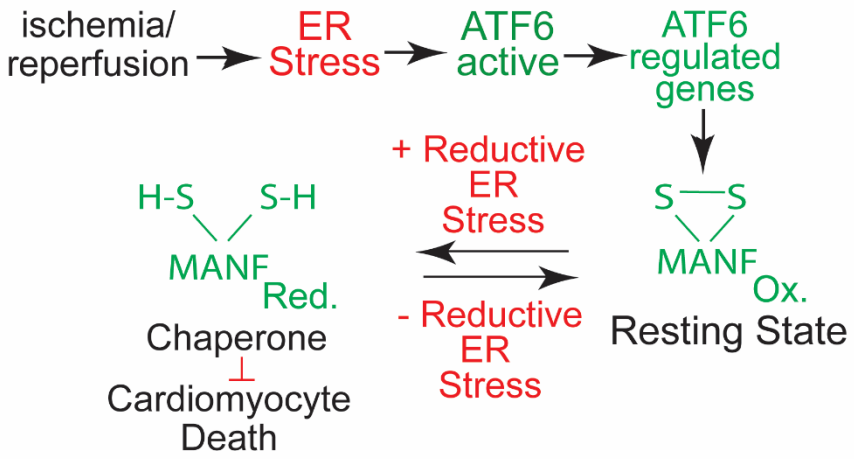

Figure 4.6. Conclusion Diagram: Ischemia/reperfusion in the heart results in activation of ATF6 and upregulation of MANF which at resting state possesses intermolecular disulfide bonds. During reductive stress, the cysteine residues of MANF are reduced and MANF becomes an active chaperone. The chaperone activity of MANF, which is dependent on its conserved cysteine residues, allows it to maintain ER protein folding thereby preventing myocyte death.

cysteine residues in MANF, which are required for expression in cardiac myocytes, its chaperone activity *in vitro* and for its ability to bind to misfolded proteins in the ER in cells, consistent with a role for MANF as an adaptive responder to reductive stress in the ER of cardiac myocytes during cardiac pathology.

References

1. Balchin, D., M. Hayer-Hartl, and F.U. Hartl, In vivo aspects of protein folding and quality control. Science, 2016. **353**(6294): p. aac4354.

2. Doroudgar, S. and C.C. Glembotski, The cardiokine story unfolds: ischemic stress-induced protein secretion in the heart. Trends Mol Med, 2011. **17**(4): p. 207-14.

3. Saibil, H., Chaperone machines for protein folding, unfolding and disaggregation. Nat Rev Mol Cell Biol, 2013. **14**(10): p. 630-42.

4. Moremen, K.W. and M. Molinari, N-linked glycan recognition and processing: the molecular basis of endoplasmic reticulum quality control. Curr Opin Struct Biol, 2006. **16**(5): p. 592-9.

5. Ushioda, R., J. Hoseki, K. Araki, G. Jansen, D.Y. Thomas, and K. Nagata, ERdj5 is required as a disulfide reductase for degradation of misfolded proteins in the ER. Science, 2008. **321**(5888): p. 569-72.

6. Ellgaard, L. and L.W. Ruddock, The human protein disulphide isomerase family: substrate interactions and functional properties. EMBO Rep, 2005. **6**(1): p. 28-32.

7. Christianson, J.C., T.A. Shaler, R.E. Tyler, and R.R. Kopito, OS-9 and GRP94 deliver mutant alpha1-antitrypsin to the Hrd1-SEL1L ubiquitin ligase complex for ERAD. Nat Cell Biol, 2008. **10**(3): p. 272-82.

8. Meusser, B., C. Hirsch, E. Jarosch, and T. Sommer, ERAD: the long road to destruction. Nat Cell Biol, 2005. **7**(8): p. 766-72.

9. Pobre, K.F.R., G.J. Poet, and L.M. Hendershot, The endoplasmic reticulum (ER) chaperone BiP is a master regulator of ER functions: Getting by with a little help from ERdj friends. J Biol Chem, 2019. **294**(6): p. 2098-2108.

10. Doroudgar, S., M. Volkers, D.J. Thuerauf, M. Khan, S. Mohsin, J.L. Respress, W. Wang, N. Gude, O.J. Muller, X.H. Wehrens, M.A. Sussman, and C.C. Glembotski, Hrd1 and ER-Associated Protein Degradation, ERAD, are Critical Elements of the Adaptive ER Stress Response in Cardiac Myocytes. Circ Res, 2015. **117**(6): p. 536-46.

11. Behnke, J., M.J. Mann, F.L. Scruggs, M.J. Feige, and L.M. Hendershot, Members of the Hsp70 Family Recognize Distinct Types of Sequences to Execute ER Quality Control. Mol Cell, 2016. **63**(5): p. 739-52.

12. Buchner, J., H. Grallert, and U. Jakob, Analysis of chaperone function using citrate synthase as nonnative substrate protein. Methods Enzymol, 1998. **290**: p. 323-38.

13. Thuerauf, D.J., H. Hoover, J. Meller, J. Hernandez, L. Su, C. Andrews, W.H. Dillmann, P.M. McDonough, and C.C. Glembotski, Sarco/endoplasmic reticulum calcium ATPase-2 expression is regulated by ATF6 during the endoplasmic reticulum stress response: intracellular signaling of calcium stress in a cardiac myocyte model system. J Biol Chem, 2001. **276**(51): p. 48309-17.

14. Belmont, P.J., W.J. Chen, M.N. San Pedro, D.J. Thuerauf, N. Gellings Lowe, N. Gude, B. Hilton, R. Wolkowicz, M.A. Sussman, and C.C. Glembotski, Roles for endoplasmic reticulum-associated degradation and the novel endoplasmic reticulum stress response gene Derlin-3 in the ischemic heart. Circ Res, 2010. **106**(2): p. 307-16.

15. Holmgren, A., Thioredoxin catalyzes the reduction of insulin disulfides by dithiothreitol and dihydrolipoamide. J Biol Chem, 1979. **254**(19): p. 9627-32.

16. Kubota, K., Y. Niinuma, M. Kaneko, Y. Okuma, M. Sugai, T. Omura, M. Uesugi, T. Uehara, T. Hosoi, and Y. Nomura, Suppressive effects of 4-phenylbutyrate on the aggregation of Pael receptors and endoplasmic reticulum stress. J Neurochem, 2006. **97**(5): p. 1259-68.

17. Blackwood, E.A., C. Hofmann, M. Santo Domingo, A.S. Bilal, A. Sarakki, W. Stauffer, A. Arrieta, D.J. Thuerauf, F.W. Kolkhorst, O.J. Muller, T. Jakobi, C. Dieterich, H.A. Katus, S. Doroudgar, and C.C. Glembotski, ATF6 Regulates Cardiac Hypertrophy by Transcriptional Induction of the mTORC1 Activator, Rheb. Circ Res, 2019. **124**(1): p. 79-93.

18. Jin, J.K., E.A. Blackwood, K. Azizi, D.J. Thuerauf, A.G. Fahem, C. Hofmann, R.J. Kaufman, S. Doroudgar, and C.C. Glembotski, ATF6 Decreases Myocardial Ischemia/Reperfusion Damage and Links ER Stress and Oxidative Stress Signaling Pathways in the Heart. Circ Res, 2017. **120**(5): p. 862-875.

19. Chaanine, A.H., M. Nonnenmacher, E. Kohlbrenner, D. Jin, J.C. Kovacic, F.G. Akar, R.J. Hajjar, and T. Weber, Effect of bortezomib on the efficacy of AAV9.SERCA2a treatment to preserve cardiac function in a rat pressure-overload model of heart failure. Gene Ther, 2014. **21**(4): p. 379-386.

20. Kozlov, G., C.L. Pocanschi, A. Rosenauer, S. Bastos-Aristizabal, A. Gorelik, D.B. Williams, and K. Gehring, Structural basis of carbohydrate recognition by calreticulin. J Biol Chem, 2010. **285**(49): p. 38612-20.

21. Lee, A.S., Glucose-regulated proteins in cancer: molecular mechanisms and therapeutic potential. Nat Rev Cancer, 2014. **14**(4): p. 263-76.

22. Lee, C.F., G.C. Melkani, and S.I. Bernstein, The UNC-45 myosin chaperone: from worms to flies to vertebrates. Int Rev Cell Mol Biol, 2014. **313**: p. 103-44.

23. Liu, Q. and W.A. Hendrickson, Insights into Hsp70 chaperone activity from a crystal structure of the yeast Hsp110 Sse1. Cell, 2007. **131**(1): p. 106-20.

24. Poon, S., S.B. Easterbrook-Smith, M.S. Rybchyn, J.A. Carver, and M.R. Wilson, Clusterin is an ATP-independent chaperone with very broad substrate specificity that stabilizes stressed proteins in a folding-competent state. Biochemistry, 2000. **39**(51): p. 15953-60.

25. Preissler, S., J.E. Chambers, A. Crespillo-Casado, E. Avezov, E. Miranda, J. Perez, L.M. Hendershot, H.P. Harding, and D. Ron, Physiological modulation of BiP activity by trans-protomer engagement of the interdomain linker. Elife, 2015. **4**: p. e08961.

26. Preissler, S., L. Rohland, Y. Yan, R. Chen, R.J. Read, and D. Ron, AMPylation targets the rate-limiting step of BiP's ATPase cycle for its functional inactivation. Elife, 2017. **6**.

27. Taylor, R.P. and I.J. Benjamin, Small heat shock proteins: a new classification scheme in mammals. J Mol Cell Cardiol, 2005. **38**(3): p. 433-44.

28. Vekich, J.A., P.J. Belmont, D.J. Thuerauf, and C.C. Glembotski, Protein disulfide isomerase-associated 6 is an ATF6-inducible ER stress response protein that protects cardiac myocytes from ischemia/reperfusion-mediated cell death. J Mol Cell Cardiol, 2012. **53**(2): p. 259-67.

29. Li, J., S. Zhang, and C. Wang, Only the reduced conformer of alpha-lactalbumin is inducible to aggregation by protein aggregates. J Biochem, 2001. **129**(5): p. 821-6.

30. Lodish, H.F. and N. Kong, The secretory pathway is normal in dithiothreitol-treated cells, but disulfide-bonded proteins are reduced and reversibly retained in the endoplasmic reticulum. J Biol Chem, 1993. **268**(27): p. 20598-605.

31. Lindahl, M., T. Danilova, E. Palm, P. Lindholm, V. Voikar, E. Hakonen, J. Ustinov, J.O. Andressoo, B.K. Harvey, T. Otonkoski, J. Rossi, and M. Saarma, MANF is indispensable for the proliferation and survival of pancreatic beta cells. Cell Rep, 2014. **7**(2): p. 366-375.

32. Ellgaard, L., C.S. Sevier, and N.J. Bulleid, How Are Proteins Reduced in the Endoplasmic Reticulum? Trends Biochem Sci, 2018. **43**(1): p. 32-43.

33. Poet, G.J., O.B. Oka, M. van Lith, Z. Cao, P.J. Robinson, M.A. Pringle, E.S. Arner, and N.J. Bulleid, Cytosolic thioredoxin reductase 1 is required for correct disulfide formation in the ER. EMBO J, 2017. **36**(5): p. 693-702.

34. Glembotski, C.C., D.J. Thuerauf, C. Huang, J.A. Vekich, R.A. Gottlieb, and S. Doroudgar, Mesencephalic astrocyte-derived neurotrophic factor protects the heart from ischemic damage and is selectively secreted upon sarco/endoplasmic reticulum calcium depletion. J Biol Chem, 2012. **287**(31): p. 25893-904.

35. Doroudgar, S., D.J. Thuerauf, M.C. Marcinko, P.J. Belmont, and C.C. Glembotski, Ischemia activates the ATF6 branch of the endoplasmic reticulum stress response. J Biol Chem, 2009. **284**(43): p. 29735-45.

36. Thuerauf, D.J., M. Marcinko, N. Gude, M. Rubio, M.A. Sussman, and C.C. Glembotski, Activation of the unfolded protein response in infarcted mouse heart and hypoxic cultured cardiac myocytes. Circ Res, 2006. **99**(3): p. 275-82.

37. Bi, X., G. Zhang, X. Wang, C. Nguyen, H.I. May, X. Li, A.A. Al-Hashimi, R.C. Austin, T.G. Gillette, G. Fu, Z.V. Wang, and J.A. Hill, Endoplasmic Reticulum Chaperone GRP78

Protects Heart From Ischemia/Reperfusion Injury Through Akt Activation. Circ Res, 2018. **122**(11): p. 1545-1554.

38. Zhang, G., X. Wang, X. Bi, C. Li, Y. Deng, A.A. Al-Hashimi, X. Luo, T.G. Gillette, R.C. Austin, Y. Wang, and Z.V. Wang, GRP78 (Glucose-Regulated Protein of 78 kDa) Promotes Cardiomyocyte Growth Through Activation of GATA4 (GATA-Binding Protein 4). Hypertension, 2019. **73**(2): p. 390-398.

39. Yan, Y., C. Rato, L. Rohland, S. Preissler, and D. Ron, MANF antagonizes nucleotide exchange by the endoplasmic reticulum chaperone BiP. Nat Commun, 2019. **10**(1): p. 541.